



UNIVERSITÀ DEGLI STUDI ROMA TRE
Dipartimento di Fisica "Edoardo Amaldi"
Dottorato di Ricerca in Fisica - XV Ciclo

Supersymmetric dark matter analysis with γ -rays

Andrea Lionetto

Coordinatore

prof. Filippo Ceradini

Tutore

dr. Francesco Fucito
dr. Aldo Morselli

Aprile 2003

Contents

Introduction	3
1 Dark Matter	5
1.1 Introduction	5
1.2 Theoretical motivations	8
1.3 Dark matter candidates	13
1.4 WIMP Relic Density	17
2 Supersymmetric theories	22
2.1 Introduction	22
2.2 Supersymmetry	24
2.3 Superfield formalism	27
2.4 Chiral superfields	29
2.5 Vector superfields	30
2.6 Supersymmetric lagrangians	31
2.7 Gauge invariance and supersymmetry	33
2.8 Supersymmetry breaking	37
2.9 The Minimal Supersymmetric Standard Model	40
3 Supersymmetry and RG	48
3.1 Introduction	48
3.2 RGE from Callan-Symanzik equations	49
3.3 Thresholds in RGE	52
3.4 β -functions in non abelian gauge theories	55
3.5 Renormalization group and supersymmetry	59
3.6 Minimal SUGRA models	66
3.7 Numerical RGE solutions for the MSSM	71
4 Supersymmetric Dark Matter	78
4.1 Introduction	78
4.2 Neutralino	79

4.3	Chargino	82
4.4	Neutralino annihilations	84
5	Indirect neutralino detection with cosmic γ-rays	92
5.1	Introduction	92
5.2	The EGRET data	93
5.3	The diffuse γ -ray background	94
5.4	γ -ray flux from WIMP annihilations	96
5.5	Fit of EGRET data	99
5.6	WIMP signal detection with GLAST	102
5.7	mSUGRA Neutralino detection with GLAST	107
5.8	GC Angular Extension as seen by GLAST	112
5.9	Optimal $\Delta\Omega$ for WIMP Signal Detection	114
5.10	Results	114
6	Conclusions	116
	Acknowledgments	118
A	Spinorial notation	119
B	Description of the algorithms	124
B.1	ISASUGRA	124
B.2	DarkSUSY	128
C	Fortran codes	132
C.1	SUGRGE subroutine	132

*To my father
an eternal golden braid*

Introduction

In this thesis we present the motivations to study supersymmetric dark matter through indirect detection with γ -rays. This is a part of a very interesting research area common to astrophysics, cosmology and fundamental particle physics. There are many experimental evidences and extremely compelling theoretical motivations for the existence of dark matter in the Universe. Our knowledge of the matter and energy content of the Universe has been greatly improving over the latest years. The picture emerging from recent data collected with a number of complementary techniques seems to be remarkably self-consistent, pointing at a flat Universe with about 70% of its present average energy density in a cosmological constant term and about 30% in non-relativistic matter. Recent measurements of the cosmic microwave background radiation indicate that the greater part of the non-relativistic matter is of a non luminous form. One of the major challenges in physics, today, is to understand the actual nature of this non luminous matter.

The plan of the thesis is the following: in chapter 1 we introduce the dark matter problem as it arises from the observational point of view and we setup the cosmological theoretical framework in which dark matter can be studied. We also review the possible dark matter candidates, and we try to single out the best motivated candidate. We see that weakly interacting massive particles are among the leading dark matter candidates: they would naturally appear as another of the thermal leftovers from the early Universe, and, at the same time, their existence is predicted in several classes of extensions of the Standard Model of particle physics.

In chapter 2 we just approach the fundamental particle physics side of the problem. We start describing supersymmetric theories as possible extensions of Standard Model. At the end we define the minimal supersymmetric extension of the Standard Model.

In chapter 3 we introduce the powerful tool of the renormalization group to show it is possible to obtain low energy predictions from a fundamental high energy theory. We also describe a particular underlying theory, called minimal supergravity, that allows to reduce the number of free parameters

and so to simplify the phenomenological analysis. At the end we describe the numerical procedure we have used to evolve, with renormalization group, these high energy parameters to the low energy scale.

In chapter 4 we describe in details the best motivated candidates in the context of R-parity conserving supersymmetric theories: the lightest neutralino. We show the possible relevant neutralino interactions that allows for an indirect detection.

Finally in the last chapter we analyze in details what can be learned of the dark matter properties from the already available data coming from γ -ray experiments and what we can expect from the upcoming experiments. In particular we concentrate our attention on the γ -rays coming from the Galactic Center that gives good chances to probe for supersymmetric dark matter.

Chapter 1

Dark Matter

1.1 Introduction

The dark matter problem is one of the most fascinating and intriguing issue of a research area that resides at the intersection of both astrophysics and fundamental particle physics.

Naively speaking, dark matter is a kind of a non luminous matter that is present in the Universe, whose actual nature has to be yet determined. The origin of the dark matter problem goes back to the early observations of the mass to light ratios of galaxies [1]. The argument used there can be formalized as follows. Given the numerical distribution of galaxies $n(L)$ with total luminosity L , one can compute the mean luminosity density of galaxies:

$$\mathcal{L} = \int n(L) L dL \quad (1.1)$$

which is experimental determined to be [2]:

$$\mathcal{L} = 2 \pm 0.2 \cdot 10^8 h L_{\odot} \text{ Mpc}^{-3} \quad (1.2)$$

where $L_{\odot} = 3.8 \cdot 10^{33} \text{ erg s}^{-1}$ is the solar luminosity and h is the present value of the Hubble constant H_0 parametrized in unit of $100 \text{ Km Mpc}^{-1} \text{ s}^{-1}$:

$$h = \frac{H_0}{100 \text{ Km Mpc}^{-1} \text{ s}^{-1}} \quad (1.3)$$

One can define a critical density $\rho_c = 3H^2/8\pi G_N$, in terms of which it is possible to define a critical mass-to-light ratio:

$$\left(\frac{M}{L}\right) = \frac{\rho_c}{\mathcal{L}} \sim 1390 h \frac{M_{\odot}}{L_{\odot}} \quad (1.4)$$

which, in turn, can be used to determine the cosmological matter density parameter (see the following section for details):

$$\Omega_m = \frac{\rho}{\rho_c} = \left(\frac{M}{L}\right) \left(\frac{M_\odot}{L_\odot}\right)^{-1} \quad (1.5)$$

The mass-to-light ratios are strongly dependent on the distance scale on which they are determined [3]. In the following table, we summarize the results on different distance scale, ranging from that of the solar neighborhood to the largest scale of clusters of galaxies:

Distance scale	M/L	Ω_m
Solar system	2 ± 1 (in solar unit)	0.001
Galaxies	$\sim 10h$	0.01
Small group of galaxies	$\sim 100h$	0.1
Clusters of galaxies	$\sim 500h$	0.3

It is well known that exists a strong limit on the amount of baryonic matter coming from the primordial cosmological nucleosynthesis. In fact the measured abundance of light elements (D, ^3He , ^4He and ^7Li) is in the range

$$0.011 \lesssim \Omega_B h^2 \lesssim 0.025 \quad (1.6)$$

where $h = 0.72 \pm 0.08$ is the present Hubble constant [20], expressed in units of $100 \text{ Km s}^{-1} \text{ Mpc}^{-1}$. The meaning of the Hubble constant will be described in more details in the following section. The mechanism of the primordial nucleosynthesis is very well explained in the context of the standard cosmological model. Thus, when we consider the scale of galaxies and larger in the previous table, the presence of dark matter is required to taking into account the discrepancy between Ω_m and Ω_B .

There are other observational evidences and theoretical motivations for considering the existence of the dark matter. From the observational point of view the most striking evidence comes from the rotation curves of the spiral galaxies. In fact, it is possible to determine the rotational velocity v_C (C stands for circular) of the neutral hydrogen clouds inside a spiral galaxy by measuring the 21-cm emission lines, shifted by the Doppler effect. The result, when expressed as a function of the distance r from the center of the galaxy, is that the velocity remains constant well beyond the point that corresponds to the fall-off to zero of the luminous disk. In the case of the NGC 6503 spiral galaxy this point is at $r \simeq 2.5 \text{ Kpc}$. This can be seen in figure 1.1. The experimental points clearly indicates that $v_C \sim \text{const.}$ for $r \gtrsim 2.5 \text{ Kpc}$. The sum of the contribution due to the observed disk and gas

cannot give a proper fit of these points. If we assume that Newton laws hold at the galactic scale¹ then we have:

$$\frac{v_C^2}{r} = \frac{M(r)}{r^2}$$

where $M(r)$ is the total mass contained inside a shell of radius r . Thus we can see that $r v_C \sim const.$ implies $M(r) \sim r$ that, in turn, implies that the matter density scales as:

$$\rho(r) \sim \frac{1}{r^2}$$

This is in contrast with the hypothesis that the bulk of the mass is luminous, because in this case $M(r) \sim const.$ and $v^2 \propto 1/r$ for $r \gtrsim 2.5$. Hence in order to fit the experimental data is necessary to introduce the contribution of a dark halo. In figure 1.1 this contribution is shown as a dot-dash curve.

Another compelling evidence comes from the larger scales of clusters of galaxies. In this case, the experimental data are available from strong gravitational lensing of a single background galaxy, of known red-shift, beyond a cluster of galaxies [7]. Using the cluster gravitational lensing, the existence of multiple images given by the same source at a known red-shift z allows to calibrate in an absolute way the total cluster mass deduced from the lens model. Hence having a physically motivated lens model, it is possible to relate the total cluster mass to the cosmological parameters that enter in a crucial way in the model definition. In this way it is possible to test the overall geometry of the Universe and hence to constrain the values of Ω_m and Ω_Λ , that are, respectively, the matter and cosmological constant contribution to the total density of the Universe, and will be described in detail in the following section. A different determination of Ω_m and Ω_Λ can be obtained by the study of the relation between the luminosity distance $d_L(z)$ and the red-shift z for a supernova sample at $z \lesssim 1$ and from measurements of the cosmic microwave background (CMB) [8].

The last resort to get an estimation of Ω_m on even larger scale is to study the distribution of peculiar velocities of galaxies and clusters. On these scales, there are measurements [9] that indicate a lower value for the overall matter density in the range:

$$\Omega_m \simeq 0.2 \div 0.5 \tag{1.7}$$

Again, this result is in good agreement with the other evidences coming from smaller scales.

¹this assumption is relaxed in the so called MOND scenarios in which the newtonian gravity is modified at the galactic scale

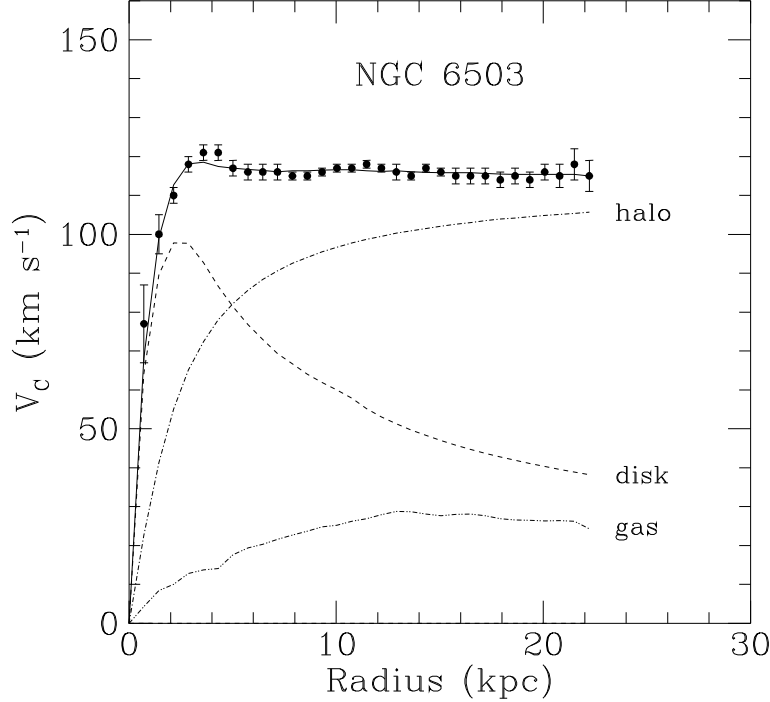


Figure 1.1: Rotation curve for the NGC 6503 spiral galaxy. The points are the measured circular rotation velocities as a function of distance from the galactic center. The dashed and dotted curves are the contribution due to the observed disk and gas, respectively, while the dot-dash curve is the contribution from the dark halo [6].

1.2 Theoretical motivations

From the point of view of the theory there are as many compelling reasons as from the experimental point of view, to consider the existence of the dark matter. Let us start by defining the theoretical framework: the cosmological standard model. We assume that the Universe can be described in terms of a Friedmann-Robertson-Walker (FRW) solution of the Einstein equations of General Relativity with a perfect fluid energy-momentum tensor. The metric of a FRW solution is a maximum spatially symmetric solution, that formally embodies the observed isotropy and homogeneity of the Universe, whose line element can be written as:

$$ds^2 = -dt^2 + a(t)^2 \left[\frac{dr^2}{1 - kr^2} + r^2 (d\theta^2 + \sin^2\theta d\phi^2) \right] \quad (1.8)$$

where $a(t)$ is the cosmological scale factor, k is the curvature constant of the 3-dimensional subspace. The values that k can assume, choosing the appropriate normalization, are $k = -1, 0, 1$, that correspond, respectively, to an open, spatially flat and closed Universe. The coordinates r , θ and ϕ constitute the so called *comoving reference frame*, in which a particle at rest remains at rest, with r , θ and ϕ constant. The time coordinate t is the proper time measured by an observer at rest in the comoving frame. What is actually changing is the metric that is not time independent due to the overall scale factor $a(t)$. Motion with respect to this privileged reference frame is usually addressed as peculiar motion. We can then introduce the *peculiar velocity* u^μ of a particle with respect to the comoving frame. The geodesic equation is given by:

$$\frac{du^\mu}{d\lambda} + \Gamma_{\nu\rho}^\mu u^\nu \frac{dx^\rho}{d\lambda} = 0 \quad (1.9)$$

where $v^\mu = dx^\mu/ds$ and λ is an affine parameter. We can express the four-velocity in terms of the ordinary three-velocity $v^i = dx^i/dt$ using the well known relation $u^\mu = (u^0, u^i) = (\gamma, \gamma v^i)$, where $\gamma = (1 - |\vec{v}|^2)^{-1/2}$ is the usual relativistic factor. If we choose $\lambda = s$ then the time component of the geodesic equation becomes:

$$\frac{du^0}{ds} + \Gamma_{\nu\rho}^0 u^\nu u^\rho = 0 \quad (1.10)$$

For the FRW metric (1.8) the only non vanishing component of $\Gamma_{\nu\rho}^0$ is:

$$\Gamma_{ij}^0 = \left(\frac{\dot{a}}{a}\right) \eta_{ij} \quad (1.11)$$

where η_{ij} is the spatial part of the flat Minkowski metric and the dot indicates a time derivative, *i.e.* $\dot{a} = da/dt$. Hence, substituting (1.11) into (1.10) we get:

$$\frac{du^0}{ds} + \left(\frac{\dot{a}}{a}\right) |\vec{u}|^2 = 0 \quad (1.12)$$

where $|\vec{u}|^2 = \eta_{ij} u^i u^j$ is the modulo of the spatial part of the four velocity. Since $u^0 du^0 = |\vec{u}| d|\vec{u}|$ the geodesic equation can be written as:

$$\frac{1}{u^0} \frac{d|\vec{u}|}{ds} + \frac{\dot{a}}{a} |\vec{u}| = 0 \quad (1.13)$$

At the end this equation can be further on reduced to the form:

$$\frac{\left|\frac{\dot{\vec{u}}}{|\vec{u}|}\right|}{|\vec{u}|} = -\frac{\dot{a}}{a} \quad (1.14)$$

which implies that $|\vec{u}| \propto a^{-1}$. Since $p^\mu = mu^\mu$ the magnitude of the three-momentum of a freely moving particle scales like the inverse of the scale factor a^{-1} . Hence a measurement of the peculiar velocities requires a difficult independent determination of both distance and velocity of the object, and so can be used to probe the mass distribution in the Universe.

The equation (1.8) is a solution of the Einstein equations of General Relativity (in unit with $c = 1$):

$$G_{\mu\nu} = R_{\mu\nu} - \frac{1}{2}R g_{\mu\nu} + \Lambda g_{\mu\nu} = -8\pi G_N T_{\mu\nu} \quad (1.15)$$

where $R_{\mu\nu}$ is the Riemann tensor, R is the Ricci scalar and $T_{\mu\nu}$ is the energy momentum tensor. In equation (1.15) we have introduced the Λ term, that is the (in)famous cosmological constant, whose nature is still controversial. Under the previously mentioned hypothesis of isotropy and homogeneity, that are consequences of the so called *cosmological principle*, the energy momentum tensor assumes a particularly simple solution:

$$T_{\mu\nu} = \text{diag}(\rho, p, p, p) \quad (1.16)$$

where ρ and p are respectively the density and the pressure associated to the matter content of the Universe, that is assumed to be a perfect fluid.

The expansion rate of the Universe can thus be determined once the Friedmann equation is written down:

$$H^2 = \frac{\dot{a}^2}{a^2} = \frac{8\pi G_N}{3}\rho - \frac{k}{a^2} + \frac{\Lambda}{3} \quad (1.17)$$

where we have introduced the Hubble parameter, that describes the evolution rate of the Universe:

$$H = \frac{\dot{a}}{a} \quad (1.18)$$

The Friedmann equation can be solved for $a(t)$ once ρ is assigned, so the evolution of the Universe is completely determined by the scale factor $a(t)$. This can be done using a local energy conservation law, that in the standard cosmological scenario is given by:

$$\frac{d}{da}(\rho a^3) = -3p \frac{d}{da} a^3 \quad (1.19)$$

where $p = p(\rho)$ is the pressure. Hence we have to supply an equation of state, too.

In the case of a perfect fluid composed only by radiation and matter, the equations of state are given by:

$$\begin{aligned} p &= \frac{1}{3}\rho && \text{radiation} \\ p &= 0 && \text{matter} \end{aligned} \tag{1.20}$$

Defining the critical density of the Universe ρ_c as:

$$H^2 = \frac{\dot{a}^2}{a^2} = \frac{8\pi G_N}{3}\rho_c \tag{1.21}$$

we are able to introduce an useful dimensionless parameter, the total density Ω :

$$\Omega = \frac{\rho}{\rho_c} \tag{1.22}$$

in terms of which we can rewrite the Friedmann equation (1.17) as:

$$(\Omega - 1)H^2 = \frac{k}{a^2} \tag{1.23}$$

where now the values of $k = -1, 0, 1$ correspond respectively to $\Omega < 1$, $\Omega = 1$ and $\Omega > 1$. Recalling that we have considered, in the Friedmann equation, the presence of a cosmological constant Λ , then the total density parameter would be the sum of two pieces $\Omega_{tot} \equiv \Omega = \Omega_m + \Omega_\Lambda$. The first contribution Ω_m is due to the matter density, associated to baryonic (from now on indicated by Ω_B) and non baryonic (more or less exotic) matter, while the second one $\Omega_\Lambda = \Lambda/3H^2$ is the contribution coming from the cosmological constant, whose presence is a long standing problem in cosmology [15].

A very interesting indication coming from the recent CMB measurements is the determination of the total density Ω_{tot} as well as the matter density Ω_m . Current experimental CMB anisotropy measurements coming from BOOMERanG give the following values [21]:

$$\begin{aligned} \Omega_{tot} &= 1.03 \pm 0.06 \\ \Omega_m h^2 &= 0.12 \pm 0.05 \\ \Omega_B h^2 &= 0.021^{+0.004}_{-0.003} \end{aligned} \tag{1.24}$$

Analogous measurements are available from the MAXIMA and DASI experiments. Their data are in substantial agreement with that of BOOMERanG [22][23]. More recently there has been an impressive improvement in the precision of the Ω determination coming from the WMAP satellite data [24]:

$$\begin{aligned} \Omega_{tot} &= 1.02 \pm 0.02 \\ \Omega_m h^2 &= 0.135^{+0.008}_{-0.009} \\ \Omega_B h^2 &= 0.0224 \pm 0.0009 \end{aligned} \tag{1.25}$$

These data seems to give a very strong evidence in favor of a flat Universe, and the discrepancy between the value of Ω_m and Ω_B suggest that a kind of non baryonic dark matter is necessary in order to explain the observations. From the theoretical point of view, the fact the Universe is flat, *i.e.* $|\Omega_{tot} - 1| \ll 1$, is naturally explained in the framework of the inflationary theories. This assertion does not mean, as sometimes erroneously stated, that inflation change the overall geometry of the Universe, but that locally the Universe is flat with a great precision [25].

A simple description of the typical inflationary mechanism can be obtained including an additional scalar field² ϕ , the so called inflaton field, in the standard cosmological scenario of equation (1.17), whose dynamics is specified by a suitable scalar potential $V(\phi)$. The inflaton field couples with gravity through a very peculiar stress-energy tensor $T_{\mu\nu}$ with an “exotic” equation of state:

$$p \propto -\rho$$

where p and ρ are the pressure and density associated to the scalar field ϕ .

Assuming the so called slow roll condition, with the first derivative term $\dot{\phi} \equiv \partial\phi/\partial t$ negligible, we obtain that the potential V must be essentially flat, in a wide region of ϕ values (see [25] for details). Under these constraints the equations (1.17) and (1.19) gives, for the cosmological scale factor, an exponential expansion law:

$$a(t) \propto e^{Ht} \tag{1.26}$$

that is very different form the typical power law solution of the standard model cosmology. The inflationary paradigm implies the existence of a period in the very early Universe in which the dynamics was dominated by the exponential expansion due to the presence of the scalar field. The standard FRW expansion is recovered when the scalar field ϕ enters in the region of the minimum of the potential $V(\phi)$. This phase is usually addressed as re-heating.

The inflation mechanism is able to solve a bunch of problems, starting from the so called flatness, or curvature problem. This problem arise because $\Omega = 1$ in standard cosmology is an unstable point in the evolution of the Universe, due to the fact that the curvature term k in the Friedmann equation (1.17) tends to dominate over the ρ term. In fact, since $\rho \propto a^{-3}$ or a^{-4} , the ρ term in the FRW solution falls to zero much more quickly than the k/a^2 term as the Universe expands. During the inflation period, instead, we have exactly the opposite situation and the k term is thus negligible implying that the point $\Omega = 1$ is now an attractor for the Universe evolution.

²whose origin has to be yet explained in terms of some fundamental theory.

Moreover inflation solves the horizon problem, because, naively speaking, our Universe is the result of the exponential expansion of a single causally connected region. Although the original formulation of inflation [26] was not able to make predictions about the initial spectrum of inhomogeneities, it is possible to adjust the inflation mechanism to give the right amplitude for the primordial fluctuations [27]. Finally it solves the magnetic monopole problem, that originate from the enormous production of this kind of particles in the Grand Unified Theory (GUT) phase of the Universe (referring to an underlying unifying theory at energy of about 10^{16} GeV).

During inflation the overall matter density, included that associated to the monopoles that could be present at that time, is diluted by the exponential expansion to a negligible value. Thus the overall density is completely dominated by the inflaton potential $V(\phi)$. Ordinary matter is created during the process of re-heating. Hence we have to suppose that the re-heating occurs not involving big enough temperatures to produce again monopoles.

We can try to summarize the scenario suggested by the CMB measurements and the inflationary theoretical framework that as been described. Firstly the prediction $\Omega_{tot} = 1$ is in a very good agreement with CMB anisotropy measurements. Moreover there are strong evidences that dark matter, at the end, must exist, since we cannot explain $\Omega_{tot} = 1$ only considering luminous objects. The most important indication, is that about 90% of this dark matter must be of a non baryonic nature.

So, from the previous discussion, we could consider the total matter density as a sum of terms due to several contributions:

$$\Omega_m = \Omega_B + \Omega_\chi \tag{1.27}$$

where Ω_B is the baryonic component and Ω_χ is the component associated to the dark matter.

1.3 Dark matter candidates

We have reviewed the present status of the dark matter problem, both from the theoretical and experimental point of view. The conclusion that arises is that there are strong indications of the presence of dark matter.

The first candidate to consider is something we already know to exist, that is a kind of baryonic matter that for some reason does not emit light. Because there is a stringent limit $\Omega_B h^2 \sim 0.021$ (from the experimental values in (1.24)), the baryonic matter cannot be the only dark matter component. This limit is in very good agreement with the primordial cosmological nucleosynthesis constraints given in (1.6). The main candidates of the baryonic

type are the so called massive compact halo objects, known as MACHOs. An example of these objects are the brown dwarfs, of typical mass of $0.08M_{\odot}$, that have not reached the nuclear fusion threshold. Although there are several arguments against a unique MACHOs composition of the dark matter (see for example [4]), big-bang nucleosynthesis constraints cannot exclude an halo who is entirely composed by MACHOs. Measurements of the galactic abundance of MACHOs, using gravitational microlensing, come from the MACHO and EROS experiments. The more recent results [29] shows that compact objects with a mass between $2 \cdot 10^{-7}M_{\odot}$ and $1M_{\odot}$ cannot account for more than 25% of the mass of a standard spherical, isothermal and isotropic galactic halo of $4 \cdot 10^{11}M_{\odot}$.

Another interesting possibility is that the galactic halo could be composed mainly by neutral hydrogen. It is usually assumed that this hydrogen is present in a gas form or even condensed in a kind of snow ball like state [4]. Aside from the question of how these objects were produced, their existence requires that their dimensions has to be sufficient in order to be gravitationally bounded. Under the simple assumption that this objects are electrostatically bounded, the average density of the condensed hydrogen is $\rho_ch = 0.07 \text{ g cm}^{-3}$ and the binding energy per molecule is about 1 eV. In order to survive, these kind of objects must be collisionless. This implies that the snow ball like states must have formed when the CMB temperature was about 9.5 K. At this temperature there is no equilibrium between the gaseous and condensed state, and the snow ball would sublimate.

One can also consider the possibility of an halo composed of hot hydrogen gas. It is possible to show, assuming that the gas is in thermal equilibrium, that the temperature is:

$$T_h \sim 1.3 \cdot 10^6 \text{ K} \quad (1.28)$$

The detection of hot gas is done by observing its X-ray emissions. Moreover, mapping these emissions, it is possible to obtain detailed profiles of the temperature and density of the hot gas. It can be seen that, in this case, the actual observations came in conflict with the theoretical expectation of an hot gas with temperature given by (1.28). At the end, there must be some cooling process of the gas in the halo, but this process necessarily imply star formation, *i.e.* luminous objects.

Other candidates, that can be considered in the baryonic matter category, are, for examples, black holes of mass near $100M_{\odot}$, white dwarfs and neutron stars. The black holes are by far the most intriguing candidates as sources of dark matter. One possibility is that there exist primordial black holes, which we can assume to be formed in the early history of the Universe, before nucleosynthesis took place. In this case they cannot be considered as

baryonic dark matter and the crucial property in order to have a significant portion of dark matter in the form of primordial black holes, is that the primordial fluctuations spectrum is not a simple scale-free power law. It can be estimated [17] the present contribution to the total density due to a primordial black hole of mass M :

$$\Omega_{PBH}(M) h^2 = 4.50 \cdot 10^7 \beta(M) \left(\frac{M_\odot}{M}\right)^{\frac{1}{2}} \quad (1.29)$$

where the probability $\beta(M)$ represents the fraction of energy density that is going to form a primordial black hole of mass M , computed at the time of formation of that black hole. The other possibility is that they formed at the end of the massive star gravitational collapse, and in this case there is no reason against a large population of massive black holes as the main baryonic dark matter component.

The previous list exhausts the baryonic dark matter candidates. So we are led to consider non baryonic component. At this stage there are two different possibilities, corresponding to two different cosmological scenarios, from the point of view of the structure formation: particles that can be classified as hot dark matter (HDM) and particles that can be classified as cold dark matter (CDM). The two terms, refer to the velocity of these kind of particles at the moment of the structure formation, in particular of the galaxy formation. Hot particles were highly relativistic, while the cold particles were non relativistic at that moment. These two scenarios lead to a very different primordial spectrum fluctuations [5]. The main implication of a scenario with hot dark matter is that it cannot cluster on galaxy scales, until it is cooled down to reach non relativistic speeds [30].

If we assume an hot dark matter scenario, we can consider essentially one candidate, that is a light neutrino. Recent analysis [10], assuming different theoretical framework, put a strong constraint on the lightest neutrino mass, that has to be of the order of 10^{-2} eV at 99% confidence level. This, in turn, puts an even harder constraint on the cosmological relic density of a Dirac neutrino. In fact the relic density is approximately $\Omega_\nu \sim (m_\nu/93 \text{ eV})$ and that of a Majorana neutrino is 1/2 of this quantity. Moreover, a free streaming relativistic neutrino suppresses the growth of the primordial fluctuations on scales below the horizon (Hubble scale $c/H(t)$), until they become non relativistic (see [11] for a recent review).

From the point of view of the relic abundance the observational evidences imply that the cosmological energy density of all the light weak interacting neutrinos is constrained in the range:

$$5 \cdot 10^{-5} \leq \Omega_\nu h^2 \leq 9 \cdot 10^{-2} \quad (1.30)$$

All these consideration, strongly imply that a light neutrino cannot be the dominant component of the dark matter. There is an important exception to this scenario when one introduce the possibility, absent in the Standard Model (unless one consider non renormalizable lepton number violating interactions), to consider a right handed neutrino. In this way one is able to generate, through the Higgs mechanism, in a way analogous to the other leptons, a Dirac or Majorana mass term. In fact, if we add a right handed state ν_R it is possible to generate a Dirac mass term for the neutrino:

$$m_\nu \bar{\nu}_R \nu_L$$

The corresponding mass parameter is given by:

$$m_\nu = \frac{Y_\nu v}{\sqrt{2}} \quad (1.31)$$

where Y_ν is the neutrino Yukawa coupling and v is the vacuum expectation value of the Higgs field. It is also possible to consider a Majorana mass term given by:

$$M \nu_R \nu_R$$

In the case $M \gg m_\nu$, the seesaw mechanism [18] produces two mass eigenstates given by:

$$m_{\nu_1} \simeq \frac{m_\nu^2}{M} \quad m_{\nu_2} \simeq M \quad (1.32)$$

where m_{ν_1} is a very light mass while m_{ν_2} is heavy. The neutrino state ν_1 could constitute an excellent dark matter candidate, but the viable mass range in order to obtain a consistent structure formation scenario, is quite restricted (see [19]).

Now we turn to the more interesting scenario of the cold dark matter. In this scenario we have to consider more or less exotic particles that have not yet been discovered. The main candidates could be divided into two categories: the axions and the weak interacting massive particles (WIMP). The axion boson (technically a pseudo Nambu-Goldstone boson [13]), let us indicate³ as a , arise as consequence of the Peccei-Quinn (PQ) solution of the strong CP problem in QCD (see [12] and references therein). Recent experimental constraints put for the axion mass the following limit:

$$m_a < 1 \text{ KeV}$$

and this imply that the early PQ proposal is not at all correct. Astrophysical limits are more stringent and rule out, for the axion mass, the interval:

$$0.4 \text{ eV} < m_a < 200 \text{ KeV}$$

³not to be confused with the scale factor $a(t)$

while an axion with mass $m_a > 200$ KeV is too heavy to be produced. If this type of particles have been produced in the QCD phase transition in the early Universe, then they could have the right cosmological density (of order of $\Omega_a \sim 1$). The experimental techniques that could probe a large portion of the axion parameter space rely on the interaction between axions and photons. The possible form of the interaction lagrangian is:

$$\mathcal{L}_{a\gamma\gamma} = -g_{a\gamma\gamma} \vec{E} \cdot \vec{B} a \quad (1.33)$$

where $g_{a\gamma\gamma}$ is the interaction coupling constant, that, in general, is weakly model dependent, \vec{E} and \vec{B} are the electric and magnetic fields, while a is the previously mentioned axion field. The coupling constant, in the interesting mass range, is very small, and so the expected lifetime is greater of the age of the Universe. The axions could be detected via resonant conversion of photons in a strong magnetic field [14].

We exhaust the list of cold dark matter candidates with the, by far, largest class of particles, the WIMP class. These are stable particles that usually appear in some extension of the Standard Model and that interact with ordinary matter mainly through weak interactions. One can consider different types of these candidates, like an heavy fourth generation Dirac or Majorana neutrinos or the neutralino and sneutrino in supersymmetric models. The most promising candidate is the neutralino, that will be described extensively in chapter 4. However it is possible to study some general properties of a WIMP without actually specifying its exact nature.

1.4 WIMP Relic Density

We now focus only on WIMP candidates and the first task to perform is to get an estimate of the relic cosmological abundance of these particles. It has been shown ([31] and reference therein) that if a stable particle χ exists, it could have the right cosmological abundance to be a good dark matter candidate. Here, we do not need to specify in details the nature of this particle. Such a particle exists in thermal equilibrium and in a great quantity in the early phase of the Universe expansion, when the temperature is:

$$T \gg m_\chi$$

where $T = T(t)$ is the temperature of the Universe at a given time t and m_χ is the WIMP mass. The equilibrium abundance is maintained through the annihilation of the particle with its own antiparticle $\bar{\chi}$ into a lighter couple of particle-antiparticle $l\bar{l}$.

The direct and indirect processes are:

$$\begin{aligned}\chi\bar{\chi} &\rightarrow l\bar{l} \\ \bar{l} &\rightarrow \chi\bar{\chi}\end{aligned}$$

In many case of interest χ is a Majorana particle, so it coincide with its own antiparticle $\chi = \bar{\chi}$. As the Universe cools down to a temperature:

$$T \ll m_\chi$$

the equilibrium abundance drops exponentially until the rate of the direct annihilation reaction, that is $\chi\bar{\chi} \rightarrow l\bar{l}$, falls below the expansion rate of the Universe H . At that point the interactions which maintains thermal equilibrium are not able to work anymore and so the relic abundance remains constant (this process is usually called freeze-in). It is rather clear that the result of the cosmological abundance calculation for a thermal relic is crucial to the arguments for WIMP dark matter.

Let us analyze a simple case where in addition to the known particles of the Standard Model there exists a new, yet undiscovered, stable WIMP of mass χ . In thermal equilibrium the number density of the χ particle is given by:

$$n_\chi^{eq} = \frac{g}{(2\pi)^3} \int f(p) d^3p \quad (1.34)$$

where g is the number of degrees of freedom of the particle and $f(p)$ is the Fermi-Dirac or Einstein-Bose distribution function. There are two limiting cases corresponding to the two regimes of high and low temperatures we have seen before:

$$\begin{aligned}n_\chi^{eq} &\propto T^3 && \text{for } T \gg m_\chi \\ n_\chi^{eq} &\sim g \left(\frac{m_\chi T}{2\pi}\right)^{3/2} \exp\left(\frac{-m_\chi}{T}\right) && \text{for } T \ll m_\chi\end{aligned} \quad (1.35)$$

where in the last case we can see the their density is Boltzmann suppressed. If the expansion of the Universe were so slow to maintain thermal equilibrium, the number of WIMPs today would be exponentially suppressed. In this case we would not have WIMPs at all. However we remind that the Universe is not static (recall the FRW solution (1.8)) and so the thermodynamic equilibrium cannot be ensured during the whole evolution. In fact, at high temperatures, *i.e.* $T \gg m_\chi$, the χ particles are present with a great abundance and the annihilation process into lighter particles, as well the inverse process, goes

on quickly. But when $T < m_\chi$ the number density n_χ^{eq} drops exponentially. The annihilation rate of the χ particles, is given by:

$$\Gamma = n_\chi \langle \sigma_{ann} v \rangle \quad (1.36)$$

where $\langle \sigma_{ann} v \rangle$ is the thermally averaged total annihilation cross section of $\chi\bar{\chi}$ into lighter particles times the relative velocity v . When Γ drops below the expansion rate:

$$\Gamma \lesssim H$$

there is a freeze-out condition for the WIMPs. In fact, the annihilation time scale given by Γ is less than the Hubble constant H , *i.e.* the time scale for the Universe expansion.

The simple scenario we have presented, can be quantitatively encoded into the Boltzmann equation, which describes the time evolution of the number density $n_\chi(t)$ of a generic WIMP:

$$\frac{dn_\chi}{dt} + 3Hn_\chi = - \langle \sigma_{ann} v \rangle \left[(n_\chi)^2 - (n_\chi^{eq})^2 \right] \quad (1.37)$$

where H and $a = a(t)$ are, respectively, the Hubble constant and the scale factor defined in section 1.2. The second term on the left-hand side (LHS) of this equation accounts for the expansion of the Universe, being proportional to H . If there are no interactions that change the WIMP number, the right-hand side (RHS) is zero, and we recover the previous result where $n_\chi \propto a^{-3}$ (in this regime there are roughly as many χ particles as photons and $a \propto T^{-1}$ in the radiation dominated era). The two terms in brackets on the RHS of equation account for annihilation and creation of WIMPs in the direct and indirect channel. At the equilibrium we clearly have that this term is zero. The equation (1.37) describes both Dirac particles as well as Majorana particles which are self annihilating, because, in this case, $\chi = \bar{\chi}$. However the two cases are distinct, because for Majorana particles, the annihilation rate is:

$$\frac{n_\chi^2}{2} \langle \sigma_{ann} v \rangle$$

In each annihilation two particles are involved, and so this cancels the factor 2 in the annihilation rate. For Dirac particles which have no particle-antiparticle asymmetry, $n_\chi = n_{\bar{\chi}}$, the Boltzmann equation (1.37) still holds. In this case the total number of particles plus antiparticle is now $2n_\chi$. In the case of particle-antiparticle asymmetry, the relic abundance is generally given by this asymmetry [28]. A typical example is given by the relic proton density that is essentially fixed by the proton-antiproton asymmetry, *i.e.* the baryon number of the Universe.

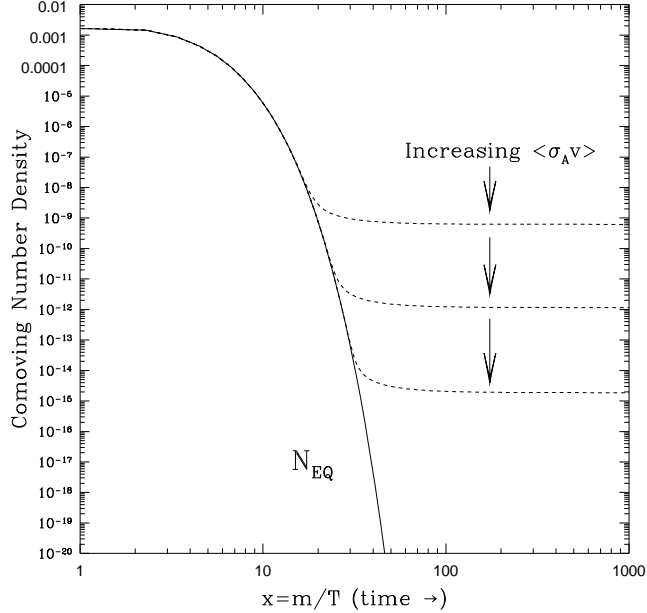


Figure 1.2: Comoving number density of a WIMP as a function of $x = m_\chi/T$. The dashed curve are the actual abundances for different thermal averaged annihilation cross sections while the solid curve is the equilibrium abundance [30].

There is no known closed form solution for the Boltzmann equation, but it is possible to write down an approximate solution for the case in which $\langle\sigma_{ann} v\rangle$ is weakly energy dependent. In this case the WIMP relic abundance is given by [31]:

$$\Omega_\chi h^2 = \frac{m_\chi n_\chi}{\rho_c} \sim \left(\frac{3 \cdot 10^{-27} \text{ cm}^3 \text{ s}^{-1}}{\langle\sigma_{ann} v\rangle} \right) \quad (1.38)$$

There is no dependence from the WIMP mass, modulo logarithmic corrections, and it is inversely proportional to the annihilation cross section.

We can show some examples of numerical solution of the Boltzmann equation in figure 1.2. The number density functions per comoving volume are denoted with dashed lines. They are functions of $x \equiv m_\chi/T$, that increase with cosmic time. For comparison there is also the equilibrium solution, denoted with a solid line. The relation (1.38) shows that, if a stable new particle exist with a weak scale interaction, *i.e.* with an annihilation cross section of the order of:

$$\langle\sigma_{ann} v\rangle \sim 10^{-25} \text{ cm}^3 \text{ s}^{-1} \quad (1.39)$$

then it will account for the right order of magnitude for the relic abundance. This is a quite interesting result because there is no a priori reason for a weak scale interaction to have something in common with the relic abundance, that is a cosmological parameter. Hence the most motivated candidate for the dark matter is a stable particle associated with new physics at the electroweak scale.

Chapter 2

Supersymmetric theories

2.1 Introduction

We have seen in the previous chapter that the most motivated candidate for the cold dark matter, that seems to be the only scenario compatible with our current understanding of the structure formation, is a kind of WIMP particle. This candidate has to be found in some new theoretical extension of the Standard Model (SM) of the fundamental interactions based on the gauge group $SU(3) \otimes SU(2) \otimes U(1)$. The SM describes in an accurately way, up to the energy currently reached in the experiments $E \sim 1$ TeV, the electroweak interactions of the Glashow-Weinberg-Salam model and even the QCD section of the strong hadron interactions. However the SM has some undesirable features, at least from an “aesthetic” point of view. In fact, it is quite disappointing that the SM depends on a great number of free parameters, like the three coupling constants, the two Higgs potential parameters, the fermion masses, the angles and phases associated to the Cabibbo-Kobayashi-Maskawa (CKM) matrix. Moreover, the SM does not include the gravitational interactions and does not lead to the coupling unification at high energies. Moreover it is overly sensitive to radiative corrections. This problem is common to all gauge theories with a spontaneous broken symmetry. In fact the radiative corrections to the mass of the scalar particle, like the Higgs one, quadratically diverge due to fermion loops. The classical Higgs scalar potential is:

$$V = m_H^2 |H|^2 + \lambda |H|^4 \quad (2.1)$$

where m_H^2 is the Higgs boson mass squared parameter and λ is the coupling constant. The SM requires a non-vanishing vacuum expectation value (VEV) for H at the minimum of the potential. This can be achieved if $m_H^2 < 0$, resulting in $\langle H \rangle = \sqrt{-m_H^2/2\lambda}$. Since we know experimentally that $\langle H \rangle = 174$ GeV, it follows that $m_H^2 \sim -(100 \text{ GeV})^2$.

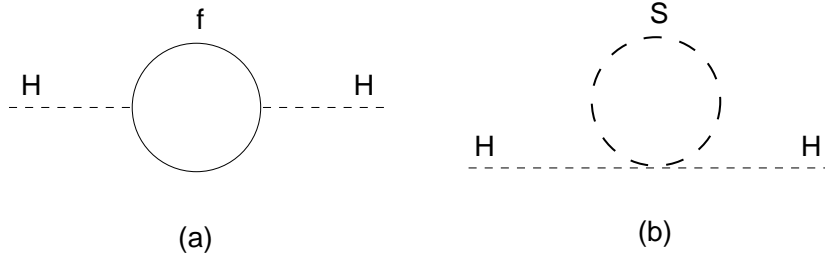


Figure 2.1: Quantum corrections to the Higgs mass due to: (a) fermion loop, (b) scalar loop

The Higgs boson mass squared receive quantum corrections and so can be written as:

$$m_H^2 = m_{bare}^2 + \delta m^2 \quad (2.2)$$

where the correction δm , coming from the loop (a) in figure 2.1 is:

$$\delta m^2 \sim \alpha^2 \int_0^\Lambda \frac{d^4 k}{(\not{k} - m_f)(\not{k} + \not{p} - m_f)} \sim \mathcal{O}(\alpha^2) \Lambda^2 \quad (2.3)$$

where α is the coupling constant, m_f is the fermion mass, p is the scalar particle momentum and Λ is the cutoff energy scale of our theory, beyond which the theory is not valid anymore. For the SM, $\Lambda = M_{GUT}$, *i.e.* the unification scale. From equation (2.3) we can see that the scalar particle masses are of the order $\alpha\Lambda$, so it is necessary that m_{bare} in the relation (2.2) be of the same order of $\alpha\Lambda$. This requires an extremely precise fine tuning, that seems very unnatural. In fact this kind of problem is known as the naturalness problem. At the same time the SM does not explain why $m_H \ll \alpha\Lambda$, and this is known as the hierarchy problem. All these facts seems to indicate that the SM is a low energy theory approximation of a more fundamental theory.

Supersymmetry seems to be able to solve in a simple and natural way (from a theoretical point of view) both problems. This enhanced symmetry establishes a perfect balance between bosonic and fermionic degrees of freedom. So supersymmetric partners of the ordinary SM particle possess the same quantum numbers and the same mass, but have different spins. In this way the naturalness problem is immediately solved, because to every fermionic loop is associated a bosonic loop, in which the particle that flows in the loop has the same mass and couplings of the fermionic one. Due to the different statistic of fermions and bosons, the two contributions have opposite signs and so the quadratic divergences is cancelled:

$$\delta m_H^2 = \delta m_b^2 - \delta m_f^2 = 0 \quad (2.4)$$

A supersymmetric theory has the very important property of being free from quadratic divergences. But, supersymmetry can only be an approximate symmetry of the underlying theory of fundamental interactions since it must be broken at the energy scales that are currently probed by our experiments. In fact, to agree with experiments, the superparticles belonging to the same supersymmetry multiplet must have higher mass. In this case (2.4) is not exact and the Higgs boson receives a radiative contribution of the order of the supersymmetric mass scale Λ_{SUSY} :

$$\delta m_H^2 \sim \Lambda_{SUSY}^2 \quad (2.5)$$

In order to solve the hierarchy problem δm_H must be of the same order of the mass m_H and this, in turn, implies that the supersymmetry scale is of the order:

$$\Lambda_{SUSY} \sim \mathcal{O}(1 \text{ TeV}) \quad (2.6)$$

To summarize, we can say that supersymmetry is able to solve, at the same time, the naturalness and the hierarchy problem, and that this solution essentially sets the scale to which supersymmetry appear. Moreover it is possible to find inside the supersymmetric theories massive stable particle that are the natural candidates as WIMP constituents of the dark matter.

In the following sections we will introduce supersymmetry and his important properties. We will introduce the necessary mathematical ingredients, and define the minimal supersymmetric extension of the SM, indicated as MSSM, that constitutes our theoretical framework in which to describe the neutralino as a natural supersymmetric candidate for the dark matter.

2.2 Supersymmetry

In this section we define formally the concept of supersymmetry, a transformation that turns a bosonic state into a fermionic state. Let us recall that, in ordinary gauge theories, like the SM, fermions and bosons belong to different representations of the gauge group, and only the gauge vector boson interactions are completely determined by the local gauge invariance of the theory. So we could introduce a symmetry that links in some way the different representations of the gauge group. Formally [33] we can define the action of an operator Q as the generator of this symmetry:

$$Q|Boson\rangle = |Fermion\rangle \quad Q|Fermion\rangle = |Boson\rangle \quad (2.7)$$

and this operator must be an anticommuting spinor, due to the different statistic. Let us sketch a simple argument that demonstrate this statement.

Because fermions and bosons behave differently under rotations, the operator Q cannot be invariant under such rotations. We can, for example, apply the unitary operator U which, in the Hilbert space, represents a rotation in the configuration space of 2π around some axis. Then from the formal definition of equation (2.7) we get that:

$$\begin{aligned} UQ|Boson\rangle &= UQU^{-1}U|Boson\rangle = U|Fermion\rangle \\ UQ|Fermion\rangle &= UQU^{-1}U|Fermion\rangle = U|Boson\rangle \end{aligned} \quad (2.8)$$

since the fermionic states pick up a minus sign when rotated through 2π , while the bosonic state do not, we have:

$$U|Fermion\rangle = -|Fermion\rangle \quad U|Boson\rangle = |Boson\rangle \quad (2.9)$$

Now, since fermionic and bosonic states form a basis in the Hilbert space, we get:

$$UQU^{-1} = -Q \quad (2.10)$$

which implies that the rotated supersymmetry generator picks up a minus sign, just as a fermionic state does. Extending this analysis to an arbitrary Lorentz transformation shows precisely that Q is a spinor (anticommuting) operator. The result of a Lorentz transformation followed by a supersymmetry transformation is different from that when the order of the transformations is reversed. Let us see how to derive the algebra of these symmetry transformation. Firstly we require the theory¹ to be invariant with respect to Poincare transformations, whose generators are the translation generator, the momentum P_μ , and the Lorentz generators $M_{\mu\nu}$. Moreover the theory can possess a group of internal symmetry G , whose generators can be indicated with t_i . The Poincare group and internal group generators satisfy the following algebra:

$$\begin{aligned} [P_\mu, P_\nu] &= 0 \\ [P_\mu, M_{\rho\sigma}] &= i(g_{\mu\rho}P_\sigma - g_{\mu\sigma}P_\rho) \\ [M_{\mu\nu}, M_{\rho\sigma}] &= i(g_{\mu\sigma}M_{\nu\rho} + g_{\nu\rho}M_{\mu\sigma} - g_{\mu\rho}M_{\nu\sigma} - g_{\nu\sigma}M_{\mu\rho}) \\ [t_i, t_j] &= if_{ij}^k t_k \end{aligned} \quad (2.11)$$

Coleman and Mandula [32] have shown, that under some general assumption, like the existence of a non trivial S-matrix and the existence of a unique vacuum state with a finite energy gap between it and the lowest particle state, any group of bosonic symmetries of the S-matrix in a relativistic field theory

¹we consider only theories in $D = 4$ space-time dimensions

is the direct product of the Poincare group with an internal symmetry group. This symmetry group, moreover, must be the direct product of a compact semi-simple group with $U(1)$ factors.

This important result imply that the Poincare group and internal symmetry group operators must commute with each other:

$$\begin{aligned} [P_\mu, t_i] &= 0 \\ [M_{\mu\nu}, t_i] &= 0 \end{aligned} \tag{2.12}$$

and as a consequence we have the two following relations:

$$[W^2, t_i] = 0 \tag{2.13}$$

$$[P^2, t_i] = 0 \tag{2.14}$$

where $P^2 = P_\mu P^\mu$ is the mass square operator and $W^2 = W_\mu W^\mu$ is the generalized spin operator, with W^μ the Pauli-Lubanski vector, defined as:

$$W^\mu = -\frac{1}{2}\epsilon^{\mu\nu\rho\sigma} P_\nu M_{\rho\sigma}$$

Equation (2.17) implies that every particle belonging to an irreducible representation of the internal gauge symmetry group must have the same spin, while equation (2.18) implies that they must have the same mass. This is what usually happens in gauge theories, where the fact that particles in the same multiplet have different masses is due to a symmetry breaking mechanism. The Coleman and Mandula theorem prohibits the existence, in an invariant Poincare theory, of bosonic operators that transforms fields of different statistic into each other. As we have previously seen, this is possible if we introduce fermionic operators. In this case the concept of Lie group must be enlarged in order to taking into account fermionic generators[34]. The results is the so called superalgebras or graded Lie Algebras. If next to the bosonic operators, let us indicate by B_i , we introduce fermionic operators F_α (with the right spinor index α), we can write the commutation relations for a superalgebra, that involves both commutators and anticommutators:

$$\begin{aligned} \{F_\alpha, F_\beta\} &= r_{\alpha\beta}{}^i B_i \\ [B_i, B_j] &= ic_{ij}{}^k B_k \\ [F_\alpha, B_i] &= s_{\alpha i}{}^\beta F_\beta \end{aligned} \tag{2.15}$$

where $r_{\alpha\beta}{}^i$, $c_{ij}{}^k$ and $s_{\alpha i}{}^\beta$ are the structure constants of the algebra. The simplest realization of this algebra is $N = 1$ supersymmetry, obtained implementing the Poincare invariance and transformations generated by two

spinorial operators Q_α and $\bar{Q}_{\dot{\beta}}$ (see the appendix A for the two component Van Der Warden notation). The index N counts the number of fermionic charges. The commutation relations are given by the equations (2.11) and by the following relations:

$$\begin{aligned}
\{Q_\alpha, Q_\beta\} &= \{\bar{Q}_{\dot{\alpha}}, \bar{Q}_{\dot{\beta}}\} = 0 \\
\{Q_\alpha, \bar{Q}_{\dot{\beta}}\} &= 2\sigma_{\alpha\dot{\beta}}^\mu P_\mu \\
[Q_\alpha, P_\mu] &= [\bar{Q}_{\dot{\alpha}}, P_\mu] = 0 \\
[Q_\alpha, M_{\mu\nu}] &= \frac{1}{2}(\sigma_{\mu\nu})_\alpha^\beta Q_\beta \\
[\bar{Q}_{\dot{\alpha}}, M_{\mu\nu}] &= -\frac{1}{2}\bar{Q}_{\dot{\beta}}(\bar{\sigma}_{\mu\nu})^{\dot{\beta}}_{\dot{\alpha}}
\end{aligned} \tag{2.16}$$

where the spinorial operators Q_α and $\bar{Q}_{\dot{\beta}}$ belong, respectively, to the representations $(1/2, 0)$ and $(0, 1/2)$ of the Lorentz group. They transform as left-handed spinor for Q_α , and a right-handed spinor for $\bar{Q}_{\dot{\beta}}$. When they are applied onto a field of spin j , they transform it in a field of spin $j \pm 1/2$.

Two important consequences of the supersymmetry algebra (2.16) are the following relations that substitute the previously derived relations (2.17) and (2.18):

$$[W^2, Q_\alpha] \neq 0 \tag{2.17}$$

$$[P^2, Q_\alpha] = 0 \tag{2.18}$$

that shows that the elements of the same multiplet have different spins. They belong to what is called supermultiplet. However particles in the same supermultiplet must have the same mass. Because there are no experimental evidences of this kind of supermultiplets, supersymmetry must be broken at some energy scale.

It is possible to construct supersymmetric theories with a higher number of generators N . Consistent renormalizable extended supersymmetric theories can be built for $N \leq 4$ [36]. If we consider also supergravity, consistent theories can be built for $N \leq 8$ [57]. In the following discussion we will concentrate on $N = 1$ theories.

2.3 Superfield formalism

We have defined an $N = 1$ supersymmetric theory as the theory that is invariant under the transformations (2.16). In order to describe in a simple way this invariance, it is useful to introduce a mathematical tool that enlarges

the usual $D = 4$ space-time introducing fermionic coordinates: this is called the superspace [35]. In the $N = 1$ case, superspace is built by introducing two anticommuting coordinates, let us call θ^α and $\bar{\theta}^{\dot{\alpha}}$, that satisfy the following relations:

$$\{\theta^\alpha, \theta^\beta\} = \{\bar{\theta}^{\dot{\alpha}}, Q_\beta\} = [P_\mu, \theta^\alpha] = 0 \quad (2.19)$$

These coordinates commute with ordinary space-time translations. The two coordinates θ^α and $\bar{\theta}^{\dot{\alpha}}$ are Weyl spinor that corresponds to two inequivalent representations of the group $SL(2, \mathbb{C})$. Superspace is defined by the following set of coordinates:

$$(x^\mu, \theta^\alpha, \bar{\theta}^{\dot{\alpha}})$$

where the x^μ 's are the ordinary space-time, bosonic, coordinates. More technically, ordinary space-time can be defined as the coset space of the Poincare group (whose transformations has been defined in the equation (2.11)) over the Lorentz group, and so in similar way we can define global flat superspace as the coset space of the super-Poincare group (defined in the equation (2.16)) plus the ordinary Poincare transformations (2.11) over the Lorentz group.

A generic supersymmetry transformation is defined in superspace as follows:

$$h(x^\mu, \theta^\alpha, \bar{\theta}^{\dot{\alpha}}) = e^{i(-x^\mu P_\mu + \theta^\alpha Q_\alpha + \bar{\theta}^{\dot{\alpha}} \bar{Q}_{\dot{\alpha}})} \quad (2.20)$$

that is a convenient parameterization of the coset space, relative to some origin [35]. The application of two successive transformations $h(x, \theta, \bar{\theta}) h(y, \zeta, \bar{\zeta})$ on superspace has the net effect of a translation:

$$(x^\mu, \theta, \bar{\theta}) \rightarrow (x^\mu + y^\mu + i\theta\sigma^\mu\bar{\zeta} - i\zeta\sigma^\mu\bar{\theta}, \theta + \zeta, \bar{\theta} + \bar{\zeta}) \quad (2.21)$$

where we have not written the spinorial indices. From this finite transformation it is possible to obtain the differential form of the generators Q_α and $\bar{Q}_{\dot{\alpha}}$:

$$\begin{aligned} Q_\alpha &= \frac{\partial}{\partial\theta^\alpha} - i\sigma_{\alpha\beta}^\mu \bar{\theta}^{\dot{\alpha}} \partial_\mu \\ \bar{Q}_{\dot{\alpha}} &= -\frac{\partial}{\partial\bar{\theta}^{\dot{\alpha}}} + i\theta^\beta \sigma_{\beta\dot{\alpha}}^\mu \partial_\mu \end{aligned} \quad (2.22)$$

recalling that $P_\mu = -i\partial_\mu$. It is possible to shown that the differential operators (2.22) are associated to the left multiplications acting on the superspace coordinates. We could consider, as well, the differential operators acting from the right:

$$\begin{aligned} D_\alpha &= \frac{\partial}{\partial\theta^\alpha} + i\sigma_{\alpha\beta}^\mu \bar{\theta}^{\dot{\alpha}} \partial_\mu \\ \bar{D}_{\dot{\alpha}} &= -\frac{\partial}{\partial\bar{\theta}^{\dot{\alpha}}} - i\theta^\beta \sigma_{\beta\dot{\alpha}}^\mu \partial_\mu \end{aligned} \quad (2.23)$$

that satisfies the following anticommutation relations:

$$\begin{aligned}\{D_\alpha, \bar{D}_{\dot{\alpha}}\} &= -2i\sigma_{\alpha\dot{\alpha}}^\mu \partial_\mu \\ \{D_\alpha, D_\beta\} &= \{\bar{D}_{\dot{\alpha}}, \bar{D}_{\dot{\beta}}\} = 0\end{aligned}\tag{2.24}$$

while D_α and Q_α anticommute.

At this stage we are able to introduce the superfield concept, that is a function of the superspace coordinates $(x, \theta, \bar{\theta})$ that realizes a representation of the supersymmetry algebra. The superfield components can be retrieved as a power series in θ and $\bar{\theta}$. This series has a finite number of terms, because all the powers higher than θ^2 and $\bar{\theta}^2$ are identically zero, due to the anticommutation relations. The more general form in which a superfield can be written is:

$$\begin{aligned}F(x, \theta, \bar{\theta}) &= f(x) + \theta\phi(x) + \bar{\theta}\bar{\chi}(x) + \\ &\quad + \theta\theta m(x) + \bar{\theta}\bar{\theta}n(x) + \theta\sigma^\mu\bar{\theta}v_\mu(x) + \\ &\quad + \theta\theta\bar{\theta}\bar{\lambda}(x) + \bar{\theta}\bar{\theta}\theta\psi(x) + \theta\theta\bar{\theta}\bar{\theta}d(x)\end{aligned}\tag{2.25}$$

From the algebra (2.16) it is possible to derive the mass dimensions of the operator Q , that is $[Q] = 1/2$, and so $[\theta] = -1/2$. The field components of the superfield have then increasing dimension from $[f]$ to $[d] - 2$, while the mass dimension of the superfield coincides with the dimension of lowest component f . The fields ϕ , χ , λ and ψ have a spinorial index and so they are fermionic fields, while the remaining fields f , m , n , v_μ and d are bosonic fields. We know that the physical fields have dimensions 1 if they are bosonic and 3/2 if they are fermionic. So it is possible to build two different kinds of supermultiplets: the chiral and the vector supermultiplets. In the former the fermionic component has the right mass dimension while in the latter the vector component v_μ has the right bosonic mass dimension. All the other fields in the supermultiplet are auxiliary fields that can be eliminated using the equations of motion.

The superfield representation given by (2.25) is the more general possible and it is reducible. So in order to reduce the representation we can impose some constraints on the superfield. From these constraints we will be able to build the chiral and the vector superfields.

2.4 Chiral superfields

The constraint that has to be imposed in order to define a chiral superfield is:

$$\bar{D}_{\dot{\alpha}}\Phi = 0\tag{2.26}$$

To deduce the form of the chiral superfield Φ it is convenient to introduce a new variable:

$$y^\mu = x^\mu + i\theta\sigma^\mu\bar{\theta} \quad (2.27)$$

and it is quite straightforward to show that the variable y satisfies:

$$\bar{D}_{\dot{\alpha}}(y^\mu) = \bar{D}_{\dot{\alpha}}(x^\mu + i\theta\sigma^\mu\bar{\theta}) = 0 \quad (2.28)$$

Every functions of the variable y and θ satisfies (2.26), too. The most general solution of this type can be written as:

$$\Phi = A(y) + \sqrt{2}\theta\psi(y) + \theta\theta F(y) \quad (2.29)$$

where the lowest component $A(y)$ is a bosonic scalar field, $\psi(y)$ is a fermionic field and $F(y)$ is the auxiliary field component. The superfield Φ is called left-handed chiral superfield, because in model building it is used to contain fermions of left-handed chirality. It is obviously possible to consider right-handed chiral superfields, defined by the equation:

$$D_\alpha\Phi^\dagger = 0 \quad (2.30)$$

where Φ^\dagger can be naturally expressed as a function of $(y^+)^\mu = x^\mu - i\theta\sigma^\mu\bar{\theta}$ and $\bar{\theta}$. The expansion series in $\bar{\theta}$ power is, in this case, given by:

$$\Phi^\dagger = A^*(y^+) + \sqrt{2}\bar{\theta}\bar{\psi}(y^+) + \bar{\theta}\bar{\theta}F^*(y^+) \quad (2.31)$$

2.5 Vector superfields

In order to define the vector superfield we must recall that, in every gauge theory, the vector boson fields are real fields. To define a vector superfield V we then impose the reality condition:

$$V^\dagger = V \quad (2.32)$$

and this condition reduces the number of components to seven, five bosonic and 2 fermionic [35]. To further reduce the number of components in the vector field, we can use the so called Wess-Zumino (WZ) gauge. A vector superfield in this gauge is given by:

$$V = -\theta\sigma^\mu\bar{\theta}v_\mu(x) + i\theta\theta\bar{\theta}\bar{\lambda}(x) - i\bar{\theta}\bar{\theta}\theta\lambda(x) + \frac{1}{2}\theta\theta\bar{\theta}\bar{\theta}D(x) \quad (2.33)$$

and it describes a bosonic vector field v_μ and a fermionic spinorial field λ_α . There are two interesting relations satisfied by a vector superfield:

$$\begin{aligned} V^2 &= -\frac{1}{2}\theta\theta\bar{\theta}\bar{\theta}v_\mu v^\mu \\ V^3 &= 0 \end{aligned} \quad (2.34)$$

due to the anticommutativity properties of θ and $\bar{\theta}$.

2.6 Supersymmetric lagrangians

A convenient way to obtain an invariant supersymmetric action is based on the property that the highest component of a supermultiplet transforms as a total space-time derivative [35][36][37]. The integral over the whole volume vanishes identically, if we impose that the fields are zero along the boundary of the integration region. The common way to build an invariant action is thus to consider only the highest components of superfields and product of superfields. For chiral superfields the highest components is that proportional to $\theta\theta$, called F-term, while for the vector superfields the highest components is that proportional to $\theta\theta\bar{\theta}\bar{\theta}$, called D-term. Now we have to introduce the Berezin integration [35] for anticommuting variables as:

$$\int d\theta = 0, \quad \int \theta d\theta = 1 \quad (2.35)$$

and all the properties of this peculiar type of integration can be summarized saying that the Berezin integration is equivalent to the differentiation:

$$\int d\theta_\alpha f(\theta) = \frac{\partial}{\partial\theta^\alpha} f(\theta) \quad (2.36)$$

and so:

$$\int d\theta_\alpha = \frac{\partial}{\partial\theta^\alpha} \quad (2.37)$$

The invariant action can be explicitly written as:

$$\begin{aligned} S &= \int d^4x \left(\int d^2\theta \mathcal{L}_F + \int d^2\theta d^2\bar{\theta} \mathcal{L}_D \right) \\ &= \int d^4x (\mathcal{L}_F|_{\theta\theta} + \mathcal{L}_D|_{\theta\theta\bar{\theta}\bar{\theta}}) \end{aligned} \quad (2.38)$$

where we have introduced the symbol $|...$ to denote the projection over the corresponding θ and $\bar{\theta}$ terms, and where \mathcal{L}_F and \mathcal{L}_D are respectively the lagrangian density associated to chiral superfields and to vector superfields. The chiral superfield lagrangian density is made out of chiral superfields. The product of chiral superfields is again a superfield, while the product of a right-handed chiral superfield Φ^\dagger with a left-handed superfield Φ , behaves like a vector superfield. If we want to obtain a renormalizable theory we have to use in the lagrangian operators with mass dimension $d \leq 4$ [61]. This implies to have products of no more three chiral superfields, because the mass dimension of a chiral superfield is equal to that of his lowest component, *i.e.* $d = 1$.

The most general renormalizable lagrangian that contains only chiral superfields Φ_i , with the index $i = 1, \dots, N$ running on the number of superfields, is thus [35]:

$$\mathcal{L}_\Phi = \Phi_i^\dagger \Phi_i \Big|_{\theta\theta\bar{\theta}\bar{\theta}} + \left[\left(\lambda_i \Phi_i + \frac{1}{2} m_{ij} \Phi_i \Phi_j + \frac{1}{3} g_{ijk} \Phi_i \Phi_j \Phi_k \right) \Big|_{\theta\theta} + h.c. \right] \quad (2.39)$$

where m_{ij} and g_{ijk} are the coupling constants, totally symmetric under the exchange of their indices. The term $\Phi_i^\dagger \Phi_i \Big|_{\theta\theta\bar{\theta}\bar{\theta}}$ is the kinetic term, while the remaining terms describe the couplings and the interactions between the fields. This can be observed more clearly if we write the lagrangian in terms of component fields [38]:

$$\begin{aligned} \mathcal{L}_\Phi = & i\partial_\mu \bar{\psi}_i \sigma^\mu \psi_i + A_i^* \square A_i + F_i^* F_i + \\ & + \left[m_{ij} \left(A_i F_j - \frac{1}{2} \psi_i \psi_j \right) + g_{ijk} (A_i A_j F_k - \psi_i \psi_j A_k) + \lambda_i F_i + h.c. \right] \end{aligned} \quad (2.40)$$

From (2.41) we see that the auxiliary fields F_i do not have a kinetic term. Their equations of motion are purely algebraic and so can be used to eliminate the fields F_i from the lagrangian. This generates the cubic and quartic interaction terms for the scalar fields A_i :

$$\begin{aligned} \mathcal{L}_\Phi = & i\partial_\mu \bar{\psi}_i \sigma^\mu \psi_i + A_i^* \square A_i - \frac{1}{2} m_{ij} \psi_i \psi_j \\ & - \frac{1}{2} m_{ij}^* \bar{\psi}_i \bar{\psi}_j - g_{ijk} \psi_i \psi_j A_k - g_{ijk}^* \bar{\psi}_i \bar{\psi}_j A_k^* - \mathcal{V}(A_i, A_j^*) \end{aligned} \quad (2.41)$$

where we have introduced the scalar potential $\mathcal{V}(A_i, A_j^*)$ that is equal to:

$$\mathcal{V}(A_i, A_j^*) = F_i^* F_i = |\lambda_k + m_{ik} A_i + g_{ijk} A_i A_j|^2 \quad (2.42)$$

where F_i^* and F_i are given in terms of the solutions of their equations of motion:

$$\begin{aligned} F_k &= -\lambda_k^* - m_{ik}^* A_i^* - g_{ijk}^* A_i^* A_j^* \\ F_k^* &= -\lambda_k - m_{ik} A_i - g_{ijk} A_i A_j \end{aligned} \quad (2.43)$$

The scalar potential \mathcal{V} is automatically bounded from below as a consequence of the supersymmetry. The points for which $F_i = 0$ are absolute minima of the potentials.

Once we have written the lagrangian for the chiral superfields we can build the lagrangian part involving vector superfields. The most straightforward

method is to write down the right kinetic terms for a vector field v_μ starting from a superfield V , defining a superfield that contains, as a component, a field strength for the vector field $f_{\mu\nu} = \partial_\mu v_\nu - \partial_\nu v_\mu$. This can be achieved introducing two spinorial quantities:

$$\begin{aligned} W_\alpha &= -\frac{1}{4}\bar{D}\bar{D}D_\alpha V \\ \bar{W}_{\dot{\alpha}} &= -\frac{1}{4}DD\bar{D}_{\dot{\alpha}}V \end{aligned} \tag{2.44}$$

where the superfield V can be thought as the supersymmetric generalization of the Yang-Mills potential. The superfields W_α and $\bar{W}_{\dot{\alpha}}$ are, respective, left-handed and right-handed chiral superfields. Chirality follows immediately:

$$\begin{aligned} \bar{D}_{\dot{\beta}}W_\alpha &= 0 \\ D_\beta\bar{W}_{\dot{\alpha}} &= 0 \end{aligned} \tag{2.45}$$

The lagrangian that describes the kinetic term for a vector superfield is given by:

$$\mathcal{L}_V = \frac{1}{4} W^\alpha W_\alpha|_{\theta\theta} + \bar{W}_{\dot{\alpha}}\bar{W}^{\dot{\alpha}}|_{\bar{\theta}\bar{\theta}} \tag{2.46}$$

that, using the Wess-Zumino gauge can be written, in terms of field components, as:

$$\mathcal{L}_V = -\frac{1}{4}v^{\mu\nu}v_{\mu\nu} - i\lambda\sigma^\mu\partial_\mu\bar{\lambda} + \frac{1}{2}D^2 \tag{2.47}$$

where we can recognize the two kinetic terms for the vector field v_μ (involving the field-strength $v_{\mu\nu}$) and for the fermionic field λ . Again the auxiliary field D has no dynamics and so it is possible to eliminate it through the equations of motion. In the case of the free theory, we simply have $D = 0$. In the next section we will see how, in the more general case of an interacting gauge theory, one is able to generate the quartic interaction terms for the scalar fields.

2.7 Gauge invariance and supersymmetry

We have seen in the previous section how to build a theory, involving scalar, fermionic and vector fields, invariant under supersymmetry transformations. We have also seen that the superfield formalism allows us to write the theory in a compact and very elegant way. The next step consists in requiring also gauge invariance. In order to perform this task, it is necessary to extend the

notion of gauge transformations to superfields. This can be realized as in the analogous non supersymmetric case: once the gauge transformations for the scalar and fermionic fields are defined, we introduce a vector field, that belongs to a vector supermultiplet, which has the right transformation properties under gauge transformations and the right couplings with matter fields in order to guarantee the invariance of the total lagrangian [39][40][41][42].

To see how the gauge invariance works let us start with a simple abelian case in which the gauge group is $U(1)$. The transformation changes a chiral superfield by a phase:

$$\begin{aligned}\Phi &\rightarrow \Phi' = e^{-ig\Lambda}\Phi \\ \Phi^\dagger &\rightarrow \Phi'^\dagger = e^{ig\Lambda^\dagger}\Phi^\dagger\end{aligned}\tag{2.48}$$

where g is the $U(1)$ charge associated to the superfield Φ and Λ is the transformation parameter. Requiring Φ' to be still a chiral superfield, it is easy to see [35] that Λ must be a left-handed chiral superfield (so $\bar{D}_{\dot{\alpha}}\Lambda = 0$). In the case of global invariance under $U(1)$ transformations the superfield Λ does not depend on space-time coordinates and so the chiral part of the lagrangian (2.39) contains only a term that is not invariant under global $U(1)$ transformations:

$$\lambda_i \Phi_i$$

We will not consider this term anymore. When we employ a local version of the transformations (2.48) with $\Lambda = \Lambda(x)$, we can see that even the kinetic term $\Phi_i^\dagger \Phi_i \Big|_{\theta\theta\bar{\theta}\bar{\theta}}$ is not invariant. The way to restore gauge invariance is by introducing a vector superfield V that transforms as follows:

$$V \rightarrow V' = V + i(\Lambda - \Lambda^\dagger)\tag{2.49}$$

and to redefine the kinetic term of the chiral superfields, with a minimal coupling prescription, as:

$$\Phi_i^\dagger \Phi_i \rightarrow \Phi_i^\dagger e^{gV} \Phi_i\tag{2.50}$$

Analyzing the vector superfield transformations (2.49) in terms of component fields, we see that they encode the correct gauge transformation for the vector field v_μ :

$$\begin{aligned}v_\mu &\rightarrow v'_\mu = v_\mu - i\partial_\mu(a - a^*) \\ \lambda &\rightarrow \lambda' = \lambda \\ D &\rightarrow D' = D\end{aligned}\tag{2.51}$$

where a is the scalar component of the gauge supermultiplet Λ . The fields λ and D are gauge invariant.

The new transformation (2.50) is able to generate the usual minimal coupling between matter and gauge fields. The lagrangian invariant under both supersymmetry and gauge transformations can thus be written as:

$$\begin{aligned}\mathcal{L} &= \frac{1}{4} W^\alpha W_\alpha|_{\theta\theta} + \bar{W}_{\dot{\alpha}} \bar{W}^{\dot{\alpha}}|_{\bar{\theta}\bar{\theta}} + \Phi_i^\dagger e^{gV} \Phi_i \Big|_{\theta\theta\bar{\theta}\bar{\theta}} + \mathcal{L}_{SP} \\ \mathcal{L}_{SP} &= \left(\frac{1}{2} m_{ij} \Phi_i \Phi_j + \frac{1}{3} g_{ijk} \Phi_i \Phi_j \Phi_k \right) \Big|_{\theta\theta} + h.c.\end{aligned}\quad (2.52)$$

where the term \mathcal{L}_{SP} is the so called superpotential term and must contain only gauge invariant combinations of chiral superfields. At first sight the lagrangian (2.52) looks badly non renormalizable, due to the presence of the kinetic term for the chiral superfields. But we have the gauge freedom to evaluate it in the WZ gauge, where $V^3 = 0$. Thus, the kinetic term for the chiral superfields, written in terms of field components, assume the form:

$$\begin{aligned}\Phi_i^\dagger e^{gV} \Phi_i \Big|_{\theta\theta\bar{\theta}\bar{\theta}} &= FF^* + A \square A^* + i \partial_\mu \bar{\psi} \bar{\sigma}^\mu \psi + \\ &+ g v^\mu \left(\frac{1}{2} \bar{\psi} \bar{\sigma}_\mu \psi + \frac{i}{2} A^* \partial_\mu A - \frac{i}{2} \partial_\mu A^* A \right) + \\ &- \frac{i}{\sqrt{2}} g (A \bar{\lambda} \bar{\psi} - A^* \lambda \psi) + \frac{1}{2} \left(g D - \frac{1}{2} g^2 v_\mu v^\mu \right) A^* A\end{aligned}\quad (2.53)$$

where we have neglected the flavor indices. We see that in the WZ gauge the lagrangian contains no terms with mass dimension higher than four.

The generalization to non abelian compact groups is only a little more complex, but we can use the same formalism that we have developed before. We define the same transformation rule for the chiral superfield as in the equation (2.50), but now the parameter Λ is a matrix:

$$\Lambda_{ij} = T_{ij}^a \Lambda_a \quad (2.54)$$

where the matrices T^a are the hermitian generators of the gauge group in the representation defined by the chiral superfield Φ . In the adjoint representation of the gauge group the matrices T^a satisfy the usual commutation relation:

$$[T^a, T^b] = i t^{abc} T^c \quad (2.55)$$

where t^{abc} are the completely antisymmetric structure constants and we have chosen an appropriate normalization for our hermitian generators. We must introduce as many vector superfields V_a as generators in the gauge group. The generalization of equation (2.49) to the non abelian case leads to:

$$e^{gV} \rightarrow e^{gV'} = e^{-ig\Lambda^\dagger} e^{gV} e^{ig\Lambda} \quad (2.56)$$

with Λ and V given by:

$$\begin{aligned}\Lambda_{ij} &= T_{ij}^a \Lambda_a \\ V_{ij} &= T_{ij}^a V_a\end{aligned}\tag{2.57}$$

and where the minimal coupling is always defined as in (2.50). The supersymmetric field-strength W^α may be readily generalized to the non abelian case:

$$W_\alpha = -\frac{1}{4} \bar{D} \bar{D} e^{-gV} D_\alpha e^{gV}\tag{2.58}$$

where the vector superfields are matrices as in (2.57), but with the generators in the adjoint representation of the gauge group. It is quite easy to verify that:

$$W_\alpha \rightarrow W'_\alpha = e^{-i\Lambda} W_\alpha e^{i\Lambda}\tag{2.59}$$

under non abelian gauge transformations. The most general renormalizable lagrangian invariant under both supersymmetry and gauge transformations is still given by equation (2.52).

It is important to observe that every chiral superfield Φ that appears in the lagrangian (2.52) and that contains the matter fields of the theory, besides belonging to a chiral representation of the supersymmetry transformations, belongs to a representation of the gauge group. Usually this representation is the fundamental one. In the same way, the vector superfield belongs to a real representation of the supersymmetry transformations and to the adjoint representation of the gauge group.

The superpotential defined in the equation (2.52) can contain, in general, an arbitrary gauge invariant product of two or three chiral superfields. In such a way it is possible to introduce, in the superpotential, terms that violate the conservation of some global quantum number, as the baryonic or leptonic number. To avoid the appearance of such terms, we can constraint the form of the superpotential introducing some new global symmetries in the lagrangian. The supersymmetry transformations, in particular, allow to introduce a general class of global continuous symmetries, called R-symmetries [43][44].

The most simple situation is when we consider a discrete subgroup of these symmetries, the so called R-parity transformations [45]. This transformation introduce a new quantum number defined as follows:

$$\begin{aligned}R &= +1 && \text{for ordinary particles} \\ R &= -1 && \text{for supersymmetric particles}\end{aligned}\tag{2.60}$$

Sometimes it can be useful to recast R-parity in terms of the baryonic number B and the leptonic number L :

$$R = (-1)^{3(B-L)+2S}\tag{2.61}$$

where S is the particle spin. The introduction of this new quantum number R , besides preventing the violation of B and L , has an important phenomenological consequence, especially from the point of view of the search of a candidate for the dark matter: supersymmetric particles can be produced only in couple from ordinary particles and they cannot decay in a state containing only ordinary particles. This last property implies that the lightest supersymmetric particle (LSP) is stable and thus can be a good candidate for the dark matter.

2.8 Supersymmetry breaking

Any supersymmetric theory, in order to have phenomenological consequences, must necessarily exhibit a supersymmetry breaking at some energy scale to take into account the observational evidence that none of the superpartners of the ordinary particles has been yet discovered. Yet we want the theory free of quadratic divergences. There are two main mechanisms to realize supersymmetry breaking: spontaneous supersymmetry breaking and soft supersymmetry breaking.

The spontaneous breaking of ordinary gauge symmetry is well understood, but supersymmetry imposes additional conditions which need a more careful analysis. These constraints rest on the property that the hamiltonian of the supersymmetry generators Q_α and $\bar{Q}_{\dot{\alpha}}$ is [35]:

$$H = \frac{1}{4} (\bar{Q}_1 Q_1 + Q_1 \bar{Q}_1 + \bar{Q}_2 Q_2 + Q_2 \bar{Q}_2) \quad (2.62)$$

that is a direct consequence of the supersymmetry algebra (2.16). The equation (2.62) tells us that:

$$\langle \Psi | H | \Psi \rangle \geq 0$$

for every state $|\Psi\rangle$. Moreover, it tells us that state with vanishing energy density are supersymmetric ground states of the theory. Such states are ground states because the expectation value of H positive semidefinite. They are supersymmetric states because $E_{vac} = \langle 0 | H | 0 \rangle = 0$ implying that that the vacuum state is invariant:

$$Q_\alpha |0\rangle = \bar{Q}_{\dot{\alpha}} |0\rangle = 0 \quad (2.63)$$

Ground states with $E_{vac} = 0$ preserve supersymmetry, while those with $E_{vac} > 0$ break it spontaneously. The situation is sketched in figure (2.2).

Let us see briefly two examples of models that exhibit spontaneous supersymmetry breaking. The first one is a model that has been proposed

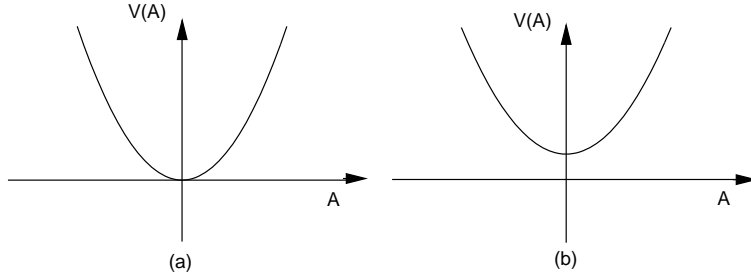


Figure 2.2: Ground state of a theory that: (a) preserves supersymmetry $E_{vac} = 0$, (b) breaks supersymmetry spontaneously $E_{vac} > 0$

by O’Raifeartaigh [46], constructed from chiral superfields and in which the ground state breaks supersymmetry. We know that the scalar potential is given by the equation (2.42) with the auxiliary field F_k^* that satisfies the equation of motion (2.43):

$$F_k^* = -\lambda_k - m_{ik}A_i - g_{ijk}A_iA_j \quad (2.64)$$

Every vacuum expectation value of $\langle A_i \rangle = a_i$ for which $F_k = 0$ defines the supersymmetric minima of the scalar potential. To break supersymmetry we must choose special values for the parameters λ_k , m_{ik} and g_{ijk} , that appear in the equation of motion for F_k^* , in such a way that the equation:

$$\lambda_k + m_{ik}a_i + g_{ijk}a_i a_j = 0 \quad (2.65)$$

has no solutions in the VEVs a_i . In order to have no solutions and so to break supersymmetry [35][46], it is necessary to introduce three chiral superfields, with the simplest model given by the following superpotential term:

$$\mathcal{L}_{SP} = \lambda\Phi_1 + m\Phi_2\Phi_3 + g\Phi_1\Phi_2\Phi_3 + h.c. \quad (2.66)$$

The second model has been proposed by Fayet and Iliopoulos [47]. They have shown how to break supersymmetry spontaneously in gauge theories with abelian gauge groups. The key point is that the $\theta\theta\bar{\theta}\bar{\theta}$ component of a vector superfield is both supersymmetric and gauge invariant. If a term $2\kappa V$ is added to an abelian theory, it leads to spontaneously supersymmetry breaking.

Let us write the lagrangian:

$$\begin{aligned} \mathcal{L} = & \frac{1}{4} (W^\alpha W_\alpha + \bar{W}_{\dot{\alpha}} \bar{W}^{\dot{\alpha}}) + \Phi_1^\dagger e^{qV} \Phi_1 + \Phi_2^\dagger e^{-qV} \Phi_2 + \\ & + m (\Phi_1 \Phi_2 + \Phi_1^\dagger \Phi_2^\dagger) + 2\kappa V \end{aligned} \quad (2.67)$$

where κ is a constant parameter with mass dimension $d = 2$ and q is the charge associated to the abelian group. In this model the scalar potential is then given by:

$$\mathcal{V} = \frac{1}{2}D^2 + F_1F_1^* + F_2F_2^* \quad (2.68)$$

where D, F_1 and F_2 are solutions of the equations of motion:

$$\begin{aligned} D + \kappa + \frac{q}{2}(A_1^*A_1 - A_2^*A_2) &= 0 \\ F_1 + mA_2^* &= 0 \\ F_2 + mA_1^* &= 0 \end{aligned} \quad (2.69)$$

It can be shown that there is no solutions, in terms of the scalar fields A_1 and A_2 , that makes the scalar potential vanish $\mathcal{V} = 0$. In this way supersymmetry is spontaneously broken.

However, in the general case, it is very difficult to build models with spontaneously broken supersymmetry in which the superpartners of the ordinary particles acquire sufficiently high masses. One possible solution may be given by theories with dynamical supersymmetry breaking (for a review see for example [48] and [49]), but we will not discuss these kind of theories here. Instead, we will see that supersymmetry breaking can be realized simply adding to the supersymmetric lagrangian (2.52) suitable terms that explicitly break supersymmetry, yet leaving the theory linearly divergent. These terms are called soft supersymmetry breaking terms and their general classification can be found in [50].

It can be shown that the only possible soft terms are general combination of mass dimension $d = 2$ built by the scalar fields components, A_i and F_i , of a chiral superfield:

$$\mathcal{L}_{break} = \mu^2 (A^2 + F^2) \quad (2.70)$$

We have omitted the internal symmetry labels and use the symbolic notation $A^2 = c_{ij}A_iA_j$, and so on. This term accounts for a common mass term for the spin-0 fields of a scalar multiplet. It is possible to write another term of the same type:

$$\mathcal{L}_{break} = \mu^2 (A^2 - F^2) \quad (2.71)$$

which gives opposite contribution to the masses of A and F fields. Moreover it is possible to introduce two other terms involving operators with mass dimension $d = 3$. The first one is an F-term:

$$\mathcal{L}_{break} = \mu\bar{\lambda}\lambda \quad (2.72)$$

that gives a mass term for the gaugino λ that appears in the vector multiplet. The second and last term that can be considered is an explicit non

supersymmetric interaction term:

$$\mathcal{L}_{break} = \gamma (A^3 - 3AB^2) \tag{2.73}$$

that describes a trilinear coupling, with γ as coupling constant, between scalar fields. This list essentially exhausts all cases of soft supersymmetry breaking. The important result is that mass terms for the matter fermions of the type:

$$\mathcal{L}_{break} = \mu \bar{\psi} \psi \tag{2.74}$$

can not be generated because they induce quadratic divergences for all members of a scalar multiplet.

2.9 The Minimal Supersymmetric Standard Model

We have discussed the general formulation of a theory both invariant under $N = 1$ supersymmetry and arbitrary gauge transformations. The lagrangian that describes such a theory has been written in the equation (2.52) plus the soft supersymmetry breaking terms described in the previous section. We know that the physics below 1 TeV is well described by the SM of the electroweak and strong interactions, based on the gauge group $SU(3) \otimes SU(2) \otimes U(1)$. Therefore now we want to formulate the minimal supersymmetric extension of the SM, the MSSM [36][37][51].

In the SM the matter fields are described by fermions with given chirality and by the Higgs boson field (responsible for the mass generation mechanism). The interactions between fields are mediated by the gauge vector bosons. It is possible to insert these fields inside a supersymmetric formalism in accordance with the following scheme:

SM field	MSSM supermultiplet
fermion	chiral
gauge vector boson	vector
Higgs boson	chiral

The fermions belong to the fundamental representation of the gauge group, while the gauge vector bosons belong to the adjoint representation. So it is not possible to put together fermions and vectors, inside the same supermultiplet. Moreover, it is not even possible to insert the Higgs bosons in the same chiral multiplet of the standard fermions because this does not allow to obtain the right fermionic mass spectrum [45]. The crucial observation here is that in the SM left-handed fermions transform differently under

the gauge group than the right-handed fermions. So they must be accommodated in different chiral supermultiplet. To every standard particle we must associate a supersymmetric partner.

The names for the scalar partners of the quarks and leptons are constructed adding the prefix “s”, which is short for scalar. Thus generically they are called squarks and sleptons (short for “scalar quark” and “scalar lepton”). The left-handed and right-handed pieces of the quarks and leptons are separate two-component Weyl fermions with different gauge transformation properties in the SM, so each must have its own complex scalar partner. The symbols for the squarks and sleptons² are the same as for the corresponding fermion, but with a tilde used to denote the superpartner of a SM particle. For example, the superpartners of the left-handed and right-handed parts of the electron Dirac field are called left- and right-handed selectrons, and are denoted \tilde{e}_L and \tilde{e}_R . It is important to keep in mind that left-handed or right-handed here does not refer to the helicity of the selectrons (they are scalar particles) but to that of their superpartners. A similar nomenclature applies for smuons and staus: $\tilde{\mu}_L, \tilde{\mu}_R, \tilde{\tau}_L, \tilde{\tau}_R$. In the SM the neutrinos are always left-handed, so the sneutrinos are denoted generically by $\tilde{\nu}$, with a possible subscript indicating which lepton flavor they carry: $\tilde{\nu}_e, \tilde{\nu}_\mu, \tilde{\nu}_\tau$. Finally, a complete list of the squarks is \tilde{q}_L, \tilde{q}_R with $q = u, d, s, c, b, t$. The gauge interactions of each of these squark and slepton fields are the same as those of the corresponding SM fermion; for instance, a left-handed squark like \tilde{u}_L will couple to the W boson while \tilde{u}_R will not. It seems clear that the Higgs scalar boson must reside in a chiral supermultiplet, since it has spin 0. Actually, it turns out that one chiral supermultiplet is not enough. One way to see this is to note that if there were only one Higgs chiral supermultiplet, the electroweak gauge symmetry would suffer a triangle gauge anomaly, and would be inconsistent as a quantum theory. This is because the conditions for cancellation of gauge anomalies include

$$Tr[Y^3] = Tr[T_3^2 Y] = 0,$$

where T_3 and Y are the third component of weak isospin and the weak hypercharge, respectively, in a normalization where the ordinary electric charge is $Q_{EM} = T_3 + Y$. The traces run over all of the left-handed Weyl fermionic degrees of freedom in the theory. In the SM, these conditions are already satisfied, somewhat miraculously, by the known quarks and leptons. Now, a fermionic partner of a Higgs chiral supermultiplet must be a weak isodoublet with weak hypercharge $Y = 1/2$ or $Y = -1/2$. In either case alone, such a fermion will make a non-zero contribution to the traces and spoil the anomaly

²from now on we will essentially use the notation of [38]

cancellation. This can be avoided if there are two Higgs supermultiplets, one with each of $Y = \pm 1/2$. In that case the total contribution to the anomaly traces from the two fermionic members of the Higgs chiral supermultiplets will vanish.

We will call the $SU(2)$ doublet complex scalar fields corresponding to these two cases H_u and H_d respectively. The weak isospin components of H_u with $T_3 = (+1/2, -1/2)$ have electric charges 1, 0 respectively, and are denoted (H_u^+, H_u^0) . Similarly, the $SU(2)$ doublet complex scalar H_d has $T_3 = (+1/2, -1/2)$ components (H_d^0, H_d^-) . The neutral scalar that corresponds to the physical SM Higgs boson is in a linear combination of H_u^0 and H_d^0 . The generic nomenclature for a spin-1/2 superpartner is to add the suffix “-ino” to the name of the SM particle, so the fermionic partners of the Higgs scalars are called higgsinos. They are denoted by \tilde{H}_u, \tilde{H}_d for the $SU(2)$ doublet left-handed Weyl spinor fields, with weak isospin components $\tilde{H}_u^+, \tilde{H}_u^0$ and $\tilde{H}_d^0, \tilde{H}_d^-$.

This exhausts the classification of the chiral supermultiplets of the MSSM. The matter content of the theory can be summarized in table 2.1, which gives the transformation properties of the SM fields with respect to the gauge group.

Supermultiplet	spin 0	spin 1/2	$SU(3) \otimes SU(2) \otimes U(1)$
Q_i	$(\tilde{u}_L \tilde{d}_L)$	$(u_L d_L)$	$(\mathbf{3}, \mathbf{2}, 1/6)$
\bar{u}_i	\tilde{u}_R^*	u_R^\dagger	$(\bar{\mathbf{3}}, \mathbf{1}, -2/3)$
\bar{d}_i	\tilde{d}_R^*	d_R^\dagger	$(\bar{\mathbf{3}}, \mathbf{1}, 1/3)$
L_i	$(\tilde{\nu} \tilde{e}_L)$	(νe_L)	$(\mathbf{1}, \mathbf{2}, -1/2)$
\bar{e}_i	\tilde{e}_R^*	e_R^\dagger	$(\mathbf{1}, \mathbf{1}, 1)$
H_u	$(H_u^+ H_u^0)$	$(\tilde{H}_u^+ \tilde{H}_u^0)$	$(\mathbf{1}, \mathbf{2}, 1/2)$
H_d	$(H_d^0 H_d^-)$	$(\tilde{H}_d^0 \tilde{H}_d^-)$	$(\mathbf{1}, \mathbf{2}, -1/2)$

Table 2.1: MSSM chiral supermultiplets

In the first row of table 2.1 we have put the chiral superfields that contain the component fields indicated in the other rows, $i = 1, 2, 3$ is a family index. We have followed the standard convention that all chiral supermultiplets are defined in terms of left handed Weyl spinors, so that in the table there are the conjugates of the right handed quarks and leptons.

The chiral superfield Q , neglecting now the family indices and the gauge indices, stands for an $SU(2)$ doublet chiral supermultiplet, can be written,

in terms of component fields, as:

$$Q = \tilde{q}_L + \sqrt{2}\theta q_L + \theta^2 F^{(q)} \quad (2.75)$$

where $q = u$ for the weak isospin component $T_3 = +1/2$, $q = d$ for the weak isospin component $T_3 = -1/2$ and $F^{(q)}$ is the associated auxiliary field. The superfield \bar{u} , instead, stands for the $SU(2)$ singlet supermultiplet:

$$\bar{u} = \tilde{u}_R^* + \sqrt{2}\theta u_R^\dagger + \theta^2 F^{(\bar{u})} \quad (2.76)$$

where the bar we have used to denote fields, is a part of the field name and does not denote any type of conjugation.

The vector bosons of the SM clearly must reside in gauge supermultiplets. The fermionic superpartners are referred as gauginos. The $SU(3)$ color gauge interactions of QCD are mediated by the gluon g , denoted as \tilde{g} . The electroweak gauge symmetry $SU(2) \otimes U(1)$ possesses as gauge bosons W^+ , W^0 , W^- and B^0 . The corresponding spin 1/2 superpartners \tilde{W}^+ , \tilde{W}^0 , \tilde{W}^- and \tilde{B}^0 are called, respectively, winos and bino. After electroweak symmetry breaking, the W^0 and B^0 gauge eigenstates mix to give mass eigenstates Z^0 and γ . The corresponding gaugino mixtures of \tilde{W}^0 and \tilde{B}^0 , denoted by \tilde{Z}^0 and $\tilde{\gamma}$, are called, respectively, zino and photino: if supersymmetry were unbroken, they would be mass eigenstates with masses m_Z and 0. In the table 2.2, we have summarized the gauge supermultiplets of the MSSM.

Fields	spin 1/2	spin 1	$SU(3) \otimes SU(2) \otimes U(1)$
gluino, gluon	\tilde{g}	g	$(\mathbf{8}, \mathbf{1}, 0)$
winos, W bosons	$\tilde{W}^\pm \tilde{W}^0$	$W^\pm W^0$	$(\mathbf{1}, \mathbf{3}, 0)$
bino, B boson	\tilde{B}^0	B^0	$(\mathbf{1}, \mathbf{1}, 0)$

Table 2.2: MSSM gauge supermultiplets

The chiral and gauge supermultiplets appearing in tables 2.1 and 2.2 completely describe the particle content of the MSSM. We have already seen that in a renormalizable supersymmetric theory, the interactions and masses of all particles are determined just by their gauge transformation properties, that in the case of the MSSM are given by the $SU(3) \otimes SU(2) \otimes U(1)$ gauge group, and by the superpotential W , that appear in the most general $N = 1$ supersymmetric lagrangian that we have written in the equation (2.52).

The superpotential W is a function of chiral superfields only, and so it determines every non gauge interactions of the theory:

$$W = \frac{1}{2}m_{ij}\Phi_i\Phi_j + \frac{1}{2}y_{ijk}\Phi_i\Phi_j\Phi_k \quad (2.77)$$

Here we have slightly changed the notation to stress that the superpotential determines not only the scalar interactions but the fermion masses and Yukawa couplings as well. Thus, once the supermultiplet content of theory is given, the form of the superpotential is constrained by gauge invariance, and so only a subset of the couplings m_{ij} and y_{ijk} are allowed to be non zero. For example the entries of the mass matrix m_{ij} can only be non zero for i and j such that the superfields Φ_i and Φ_j transform under the gauge group in representations that are conjugate of each other³. Likewise, the Yukawa couplings y_{ijk} can only be non zero when Φ_i , Φ_j and Φ_k transform in representations which can combine to form a singlet.

The superpotential for the MSSM is given by:

$$W_{MSSM} = \mu H_u H_d + (y_u \bar{u} Q H_u - y_d \bar{d} Q H_d - y_e \bar{e} L H_d) \quad (2.78)$$

where the fields that appear in this equation are the chiral superfields defined in table 2.1 and where we have suppressed all the gauge and family indices. The dimensionless Yukawa couplings y_u , y_d and y_e are 3×3 matrices in family space. The first term in equation (2.78) is the so called “ μ term”, and it is the only allowed mass term. It is the supersymmetric analogue of the Higgs mass term, and it essentially unique because terms like $H_u^* H_u$ or $H_d^* H_d$ are forbidden in the superpotential (2.78), which is an analytic function of chiral superfields. It can be written in terms of an $SU(2)$ doublet as:

$$\mu H_u H_d = \mu \epsilon^{\alpha\beta} (H_u)_\alpha (H_d)_\beta \quad (2.79)$$

where $\epsilon^{\alpha\beta}$ is the $SU(2)$ metric. In an analogous way, the second term, that is a Yukawa type term can be written as:

$$y_u \bar{u} Q H_u = \epsilon^{\alpha\beta} \bar{u}_a^i (y_u)_i^j Q_{j\alpha}^a (H_u)_\beta \quad (2.80)$$

where now we have explicitly written the family indices $i = 1, 2, 3$ and the $SU(3)$ gauge indices $a = 1, 2, 3$ of the fundamental representation $\mathbf{3}$.

The Yukawa matrices determine the masses and CKM mixing angles of the ordinary quarks and leptons, after the neutral scalar components of H_u and H_d get VEVs. Since the top quark t , the bottom quark b and the τ

³in fact we will see that in the MSSM there is only one possible term of this type

lepton are the heaviest fermions in the SM, it is often useful to make an approximation that only the (3, 3) family components of y_u , y_d and y_e are important:

$$y_u \sim \begin{pmatrix} 0 & 0 & 0 \\ 0 & 0 & 0 \\ 0 & 0 & y_t \end{pmatrix} \quad y_d \sim \begin{pmatrix} 0 & 0 & 0 \\ 0 & 0 & 0 \\ 0 & 0 & y_b \end{pmatrix} \quad y_e \sim \begin{pmatrix} 0 & 0 & 0 \\ 0 & 0 & 0 \\ 0 & 0 & y_\tau \end{pmatrix} \quad (2.81)$$

In this limit, only the third family and Higgs fields contribute to the MSSM superpotential. However, it is useful to remember that the dimensionless interactions determined by the superpotential (2.78) are often not the most important ones from the phenomenological point of view. In fact the Yukawa couplings are very small, except for those of the third family. Instead, the decay and production processes of superpartners in the MSSM are typically dominated by the supersymmetric interactions of gauge coupling strength. The couplings of the SM gauge bosons to the MSSM particles are completely determined by the gauge invariance of the kinetic terms in the lagrangian [37].

There are also various scalar quartic interactions in the MSSM which are uniquely determined by gauge invariance and supersymmetry. They are dictated by the scalar potential defined in the equation (2.42). The dimensionful terms in the supersymmetric part of the MSSM lagrangian are all dependent on μ , that appears in the generalization of the Higgs mass term of the MSSM superpotential (2.78). We find that μ gives the higgsino mass terms in the MSSM lagrangian:

$$\mathcal{L} \supset -\mu \left(\tilde{H}_u^+ \tilde{H}_d^- - \tilde{H}_u^0 \tilde{H}_d^0 \right) + c.c. \quad (2.82)$$

as well as Higgs mass square terms in the scalar potential

$$-\mathcal{L} \supset \mathcal{V} \supset |\mu|^2 (|H_u^0|^2 + |H_u^+|^2 + |H_d^0|^2 + |H_d^-|^2) \quad (2.83)$$

where \mathcal{V} is the scalar potential of equation (2.42). Since the Higgs part of the scalar potential is positive definite, we cannot understand electroweak symmetry breaking without including soft supersymmetry breaking terms for the Higgs scalars, which can be negative. So to complete the description of the MSSM, we need to specify the soft supersymmetry breaking, of the type allowed that we have found in section (2.8). The soft breaking lagrangian can thus be written as [38]:

$$\mathcal{L}_{soft}^{MSSM} = -\frac{1}{2} \left(M_3 \tilde{g}\tilde{g} + M_2 \tilde{W}\tilde{W} + M_1 \tilde{B}\tilde{B} \right) + c.c$$

$$\begin{aligned}
& - \left(\tilde{u} a_u \tilde{Q} H_u - \tilde{d} a_d \tilde{Q} H_d - \tilde{e} a_e \tilde{L} H_d \right) + c.c. \\
& - \tilde{Q}^\dagger m_Q^2 \tilde{Q} - \tilde{L}^\dagger m_L^2 \tilde{L} - \tilde{u} m_u^2 \tilde{u}^\dagger - \tilde{d} m_d^2 \tilde{d}^\dagger - \tilde{e} m_e^2 \tilde{e}^\dagger \\
& - m_{H_u}^2 H_u^* H_u - m_{H_d}^2 H_d^* H_d - (b H_u H_d + c.c.) \tag{2.84}
\end{aligned}$$

where M_1 , M_2 and M_3 are the bino, wino and gluino mass terms and we have suppressed all the gauge indices. The second line of equation (2.84) contains the trilinear scalar couplings. Each of a_u , a_d and a_e is a complex 3×3 matrix in family space, with mass dimension $d = 1$. These matrices are in one-to-one correspondence with the Yukawa coupling matrices that appear in the superpotential (2.78). The third line of the equation (2.84) contains the squark and slepton squared mass terms. Each of m_Q^2 , m_L^2 , m_u^2 , m_d^2 and m_e^2 is a 3×3 matrix in family space⁴ which in general can have complex entries. Since the lagrangian must be real, these matrices are hermitian. Finally the last line of equation (2.84) contains the supersymmetry breaking contributions to the Higgs potential: $m_{H_u}^2$, $m_{H_d}^2$ and b (usually indicated in the literature as $B\mu$) are the only squared mass terms that can occur in the MSSM.

To summarize this discussion about the soft supersymmetry breaking, we must show the order of magnitude of all these terms:

$$M_1, M_2, M_3, a_u, a_d, a_e \sim m_{soft} \tag{2.85}$$

$$m_Q^2, m_L^2, m_u^2, m_d^2, m_e^2, m_{H_u}^2, m_{H_d}^2, b \sim m_{soft}^2 \tag{2.86}$$

where m_{soft} is the characteristic mass scale of supersymmetry breaking which is of the order ~ 1 TeV, in order to continue to solve the hierarchy problem [37]. The soft breaking lagrangian (2.84) has the most general form which is compatible with gauge invariance and with R-parity, defined in (2.61), conservation.

In contrast to the supersymmetry preserving part of the lagrangian (2.52), the soft lagrangian (2.84) introduces many new parameters which were not present in the ordinary SM. A careful count (see [52]) reveals that in the MSSM lagrangian there are 105 new parameters, respect to the ordinary SM, that cannot be rotated away by redefining the phases and flavor basis for the quark and lepton supermultiplets. Thus, in principle, supersymmetry breaking introduces a huge arbitrariness in the lagrangian.

But we can reduce some of this arbitrariness because most of the new parameters can be constrained by the request that there is no flavor mixing or CP violation of the type which is already restricted by experiments [53]. All these dangerous effects can be evaded assuming the the supersymmetry

⁴to avoid an heavy notation we have neglected the tilde over the name of the scalar fields, like, for example Q .

breaking is “universal”. This means that the squark and slepton masses are flavor blind, so they should be each proportional to the the 3×3 identity matrix in family space:

$$\begin{aligned} (m_Q^2)_i^j &= m_Q^2 \mathbf{1}_{3 \times 3} & (m_{\bar{u}}^2)_i^j &= m_{\bar{u}}^2 \mathbf{1}_{3 \times 3} & (m_d^2)_i^j &= m_d^2 \mathbf{1}_{3 \times 3} \\ (m_L^2)_i^j &= m_L^2 \mathbf{1}_{3 \times 3} & (m_{\bar{e}}^2)_i^j &= m_{\bar{e}}^2 \mathbf{1}_{3 \times 3} \end{aligned} \quad (2.87)$$

where $i, j = 1, 2, 3$ are the family indices. In this way all squark and slepton mixing angles are rendered trivial, because squarks and sleptons with the same electroweak quantum numbers will be degenerate in mass and can be rotated into each other. In such limit, supersymmetric contributions to flavor changing processes will therefore be very small.

Moreover, one can make the further assumption that the trilinear scalar couplings are each proportional to the corresponding Yukawa couplings:

$$a_u = A_{u0} y_u \quad a_d = A_{d0} y_d \quad a_e = A_{e0} y_e \quad (2.88)$$

This ensures that only the squarks and sleptons of the third family can have large trilinear couplings. Finally, one can avoid disastrously large CP violating effects assuming that the soft parameters do not introduce new complex phases, *i.e.*:

$$\arg(M_1), \arg(M_2), \arg(M_3), \arg(A_{u0}), \arg(A_{d0}), \arg(A_{e0}) = 0, \pi \quad (2.89)$$

The only CP violating phase in the theory will be the ordinary CKM phase found in the ordinary Yukawa couplings. The relations (2.87), (2.88) and (2.89) make up the so called assumption of soft breaking universality.

The origin of the supersymmetry breaking terms and the soft breaking universality relations seems to require an underlying theory that must explain, at the end, the peculiar scale $m_{soft} \sim 1$ TeV. Moreover it remains to explain the origin of the μ -term in the Higgs sector of the scalar potential that appears in the equation (2.83). In fact, we expect that μ should be roughly of the order of 10^2 or 10^3 GeV, in order to allow an Higgs VEV of order of 174 GeV without a fine tuning between $|\mu|^2$ and the negative mass squared terms in the last line of the soft lagrangian (2.84). The MSSM scalar potential seems to depend on two types of dimensionful parameters which are conceptually quite distinct, namely the supersymmetry respecting mass μ and the supersymmetry breaking soft mass term m_{soft} . The so called μ problem refers to the fact that this two unrelated parameters are of the same order of magnitude. Several different solutions of the μ problem has been proposed [54][55][56]. However, from the phenomenological point of view we will treat μ as an independent parameter without asking his origin.

Chapter 3

Supersymmetry and RG

3.1 Introduction

In the previous chapter we have shown how to build a supersymmetric theory and, in particular a minimal supersymmetric extension of the SM, with the same ordinary particle content. We have seen that the crucial feature that allows the MSSM to have a phenomenological predictive power is the presence of the soft supersymmetry breaking terms $\mathcal{L}_{soft}^{MSSM}$. We have put these terms by hand into the full lagrangian. This is quite an ad hoc procedure and it determines an huge increase of the number of free parameters that define the theory. In order to understand the origin of the soft breaking terms we must consider an underlying theory, for which the MSSM is only a low energy limit. This underlying theory is usually defined at some very high energy scale, such as the unification scale $M_{GUT} \sim 10^{16}$ GeV. The number of parameters that define this theory, given at the input high energy scale, are much less of that of the MSSM. This allows for a great simplification of all the analysis that we can perform in this theoretical framework.

If we use the high energy lagrangian to compute masses and cross sections for experiments at the common electroweak energy scale, the results will involve large logarithms corrections coming from the loop diagrams. To avoid this problem we can use a very powerful tool in quantum field theory: the renormalization group (RG). Using the RG we can conveniently resum the large logarithms, by treating the couplings and masses that appear in the lagrangian as running parameters, *i.e.* functions of the energy scale. Therefore the universality relations (2.87), (2.88) and (2.89) have to be treated as boundary conditions on the running soft parameters defined at the high energy scale, which is very far removed from direct experimental probes. The RG allows to evolve all of the soft parameters, the superpotential parameters

and the gauge couplings down to the electroweak scale or comparable scales where the experiments can be performed.

In this chapter we review the RG concepts, starting from the ordinary non supersymmetric field theories and ending with the supersymmetric case. In particular we will study the evolution of the soft breaking parameters and we will choose a particular model for the origin of these terms.

3.2 RGE from Callan-Symanzik equations

In this first section we want to describe how to derive the renormalization group equations (RGE) starting from the so called Callan-Symanzik equations. This is a very interesting and useful approach in order to obtain, for example, the β -functions of an arbitrary theory. We start with applying this method to a simple gauge theory: the abelian case $U(1)$.

It is well known that in any model of particle physics, if radiative corrections, that is corrections beyond the leading tree level order, are to be taken into account, some renormalization procedure must be implemented. Let us start with a lagrangian written in terms of bare parameters (bare masses and couplings) and bare fields. The bare mass m_b and coupling e_b are replaced by the renormalized parameters m and e , and the associated counterterms, δ_m and δ_e with:

$$m_b = m + \delta m \quad e_b = e + \delta e$$

while the bare fields are equal to the renormalized fields multiplied by a wave function renormalization factor:

$$\psi_b = Z^{1/2}\psi$$

The value of the counterterms has to be specified at some energy scale, that is usually called renormalization scale. In general, it is convenient to evaluate the renormalization conditions at $p^2 = -M^2$, in term of an arbitrary renormalization mass scale M . Let's consider the renormalized n -point Green function expressed as a function of the mass scale M and of the coupling constant¹ g :

$$G^{(n)} = G^{(n)}(x_1, \dots, x_n; M, g)$$

The Callan-Symanzik equation (from now on CS) for a massless theory with a dimensionless coupling can be written as:

$$\left[M \frac{\partial}{\partial M} + \beta \frac{\partial}{\partial g} + n\gamma \right] G^{(n)}(x_1, \dots, x_n; M, g) = 0 \quad (3.1)$$

¹to simplify the analysis we consider a theory with only one coupling constant. The generalization to the case of more than one coupling is straightforward: there is a γ term for each field and a β term for each coupling

where the parameters β and γ are the same for every n and must be independent from the space-time coordinates x_i . We refer to them, respectively, as the β -function and the so called anomalous dimension. Moreover, because the $G^{(n)}$ is a renormalized Green function, β and γ cannot depend from the cut-off, and from dimensional analysis they cannot depend from the mass scale M . Hence, the only possible dependence is from the coupling constant g . A consequence of the CS equation is that β and γ are two universal functions of the theory, related to the shift in the coupling constant and field strength, that compensates the shift in the renormalization scale M :

$$\begin{aligned}\beta &= \beta(g) \\ \gamma &= \gamma(g)\end{aligned}\tag{3.2}$$

The CS equation (3.1) generalizes without difficulty to other massless theories with dimensionless couplings. In theories with multiple fields and couplings, there is a γ term for each field and a β term for each coupling. Let us see what is the result of applying the CS equation in the case of QED defined in the zero electron mass limit by using the same renormalization scale $p^2 = -M^2$. Then the renormalized Green's functions satisfy the following CS equation:

$$\left[M \frac{\partial}{\partial M} + \beta(e) \frac{\partial}{\partial e} + n\gamma_2(e) + m\gamma_3(e) \right] G^{(n,m)}(x_1, \dots, x_n; M, e) = 0 \tag{3.3}$$

where e is the usual QED coupling constant, n and m are, respectively, the number of electron and photon fields in the Green's function $G^{(n,m)}$ and γ_2 and γ_3 are the anomalous dimensions associated to the electron and photon fields. It is a well known result that the photon propagator can be written, in the t'Hooft-Feynman gauge, as:

$$D^{\mu\nu}(q) = D(q) \left(g^{\mu\nu} - \frac{q^\mu q^\nu}{q^2} \right) + \frac{-i q^\mu q^\nu}{q^2} \tag{3.4}$$

where the last term does not contribute to gauge invariant observables. Hence, we can concentrate on the first term, projected onto the transverse component. In this way, it is easy to check that (3.4) indeed satisfy the CS equation (3.1). At leading order, we have to compute the γ_2 and γ_3 functions associated, respectively, to the two counterterms δ_2 and δ_3 :

$$\gamma_2 = \frac{1}{2} M \frac{\partial}{\partial M} \delta_2, \quad \gamma_3 = \frac{1}{2} M \frac{\partial}{\partial M} \delta_3$$

where δ_2 and δ_3 are associated to the diagrams shown in figure 3.1.

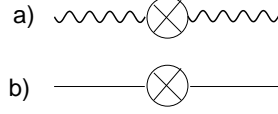


Figure 3.1: Counterterms for: a) photon propagator $-i (g^{\mu\nu} q^2 - q^\mu q^\nu) \delta_3$, b) fermionic propagator $i (\not{p} \delta_2 - \delta_m)$.

In an analogous way, we can consider the 3-points connected Green function $\langle \bar{\psi}(p_1) \psi(p_2) A_\mu(q) \rangle$ projected onto the transverse component, that at leading order is:

$$\langle \bar{\psi}(p_1) \psi(p_2) A_\mu(q) \rangle = \frac{i}{\not{p}_1} (-ie\gamma^\mu) \frac{i}{\not{p}_2} \frac{-i}{q^2} \left(g^{\mu\nu} - \frac{q^\mu q^\nu}{q^2} \right)$$

By applying the CS equations (3.3), we find that the β -function for the QED coupling constant can be written, as a function of the lagrangian counterterms, as:

$$\beta(e) = M \frac{\partial}{\partial M} \left(-\delta_g + \frac{1}{2} g \sum \delta_{Z_i} \right) \quad (3.5)$$

In QED we have the following relations for the counterterms:

$$\begin{aligned} \delta_{Z_1} &= \delta_1 = Z_1 - 1 = \delta_g \\ \delta_{Z_2} &= \delta_2 = Z_2 - 1 \\ \delta_{Z_3} &= \delta_3 = Z_3 - 1 \end{aligned}$$

so that the β -function for the QED coupling become:

$$\begin{aligned} \beta(e) &= M \frac{\partial}{\partial M} \left[-\delta_1 + \frac{e}{2} (2\delta_2 + \delta_3) \right] \\ &= M \frac{\partial}{\partial M} \left(-\delta_1 + e\delta_2 + \frac{e}{2}\delta_3 \right) \end{aligned} \quad (3.6)$$

The counterterms can be evaluated with dimensional regularization and using the renormalization conditions for massless fermions (we are interested only to the gauge coupling constant), for the euclidean momentum $p^2 = -M^2$. We have:

$$\begin{aligned} e^{-1} \delta_1 = \delta_2 &= -\frac{e^2}{(4\pi)^2} \frac{\Gamma(2-d/2)}{(M^2)^{2-d/2}} + (\text{finite terms}) \\ \delta_3 &= -\frac{4}{3} \frac{e^2}{(4\pi)^2} \frac{\Gamma(2-d/2)}{(M^2)^{2-d/2}} + (\text{finite terms}) \end{aligned} \quad (3.7)$$

while for the anomalous dimensions, we obtain:

$$\gamma_2(e) = \frac{e^2}{16\pi^2} \quad \gamma_3(e) = \frac{e^2}{12\pi^2} \quad (3.8)$$

where $d = 4 - \epsilon$ and Γ is the Euler function.

Putting the counterterms relations (3.7) into the expression for the β -function (3.6), we obtain the well known result for the β -function of the QED coupling constant:

$$\beta(e) = \frac{e^3}{12\pi^2} \quad (3.9)$$

We want to recall that this result is obtained using the Feynman gauge and this is crucial in the computation of δ_2 , because it is the counterterm associated to the fermion propagator. On the other hand, the QED vacuum polarization, and therefore γ_3 and β are gauge invariant.

Starting from the CS equations we can obtain the differential equation that describes the flow of a modified coupling constant, that is function of the renormalization scale $p^2 = -M^2$ at which is evaluated. We can formally refer to it as the so called running coupling constant:

$$\bar{g} = \bar{g}(p; g)$$

The rate of changing of this function as a function of M is dictated exactly by the β -function, that solves the following equation, together with the boundary conditions:

$$\frac{d}{d \log(p/M)} \bar{g}(p; g) = \beta(\bar{g}), \quad \bar{g}(p; g) = g \quad (3.10)$$

This equation is called the *renormalization group equation* (RGE).

3.3 Thresholds in RGE

We have seen in the previous section that the dependence of the β -function from the explicit renormalization scale M is through the counterterms. The analysis has been done restricting to quantum field theories in the massless limit. It is not difficult to generalize this formalism to theories with mass terms and other operators, whose coefficients have positive mass dimension. But in this case the renormalization scheme has to be carefully taken into account, because of the presence of new mass scales. In fact, using a mass independent subtraction scheme, there is no decoupling of the massive particles, and the Appelquist-Carazzone theorem cannot be applied [58]. This

is quite obvious because the particle contribution to the β -function does not depend from the particle mass. So if we wish to use a mass independent renormalization scheme, such as the MS (Minimal Subtraction) or \overline{MS} (Modified Minimal Subtraction), in order to obtain, at every energy scale, the effective theory, we must put *by hand* in our equations the particle content of the theory at that energy, removing the heaviest particles. At the end we want to replace the full theory with a succession of effective theories.

Let us see the meaning of the last quite fuzzy assertion in a simple case. We concentrate on the one loop contribution of a fermion of mass m to the QED coupling constant β -function. We have already obtained the result (3.9) using the CS equation.

If we evaluate the amplitude using dimensional regularization (so that the Ward identities are satisfied), we have:

$$i \frac{e^2}{2\pi^2} (q_\mu q_\nu - q^2 g_{\mu\nu}) \left[\frac{1}{6\epsilon} - \frac{\gamma}{6} - \int_0^1 dx x(1-x) \log \left(\frac{m^2 - q^2 x(1-x)}{4\pi\mu^2} \right) \right] \quad (3.11)$$

where q is the external momentum, m is the fermion mass, γ is the Euler-Mascheroni constant and μ is the scale parameter that appears in the dimensional regularization. We can see that the amplitude is of the form:

$$(q_\mu q_\nu - q^2 g_{\mu\nu}) \Pi^{\mu\nu} (q^2)$$

Now we have to renormalize the amplitude. Let us choose firstly a mass dependent renormalization scheme, imposing an arbitrary cut-off M . In order to cancel the divergent part we must subtract the amplitude computed for an external euclidean momentum $q^2 = -M^2$, obtaining:

$$i \frac{e^2}{2\pi^2} (q_\mu q_\nu - q^2 g_{\mu\nu}) \left[\int_0^1 dx x(1-x) \log \left(\frac{m^2 - q^2 x(1-x)}{m^2 + M^2 x(1-x)} \right) \right] \quad (3.12)$$

We can obtain the fermionic contribution to the β -function applying the operator $(e/2)M\partial/\partial M$ on the coefficient of $(q_\mu q_\nu - q^2 g_{\mu\nu})$. The result shows an actual dependence from the renormalization scale M :

$$\beta(e; m^2/M^2) = \frac{e^3}{2\pi^2} \int_0^1 dx x(1-x) \frac{M^2 x(1-x)}{m^2 + M^2 x(1-x)} \quad (3.13)$$

We can consider two different regimes: in the case $m \ll M$, *i.e.* the fermion mass flowing in the loop is much smaller than the renormalization scale, the β -function simplifies to:

$$\beta(e; m^2/M^2) \sim \frac{e^3}{2\pi^2} \int_0^1 dx x(1-x) = \frac{e^3}{12\pi^2}$$

that is the result already obtained in (3.9). In the other case, $M \ll m$, the renormalization scale becomes lower than the fermionic mass m , and the fermionic contribution to the β -function goes to zero as:

$$\beta(e; m^2/M^2) \sim \frac{e^3}{2\pi^2} \int_0^1 dx x(1-x) \frac{M^2 x(1-x)}{m^2} = \frac{e^3}{60\pi^2} \frac{M^2}{m^2}$$

The effect of the presence of a threshold, as can be seen in figure 3.2, is thus to “smooth” the β -function that interpolates the two limiting cases. So a mass dependent renormalization prescription has the property of a manifest decoupling of the heavy particles.

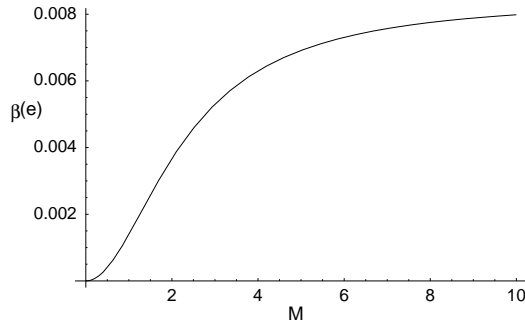


Figure 3.2: β -function (arbitrary rescaled) for the QED coupling, in a presence of a fermion of mass m , as a function of the renormalization scale M

Now we try to evaluate the fermionic contribution to the β -function in a mass independent renormalization scheme, such as the \overline{MS} . In this scheme the recipe is simply to subtract the $1/\epsilon$ pole and to redefine $4\pi\mu^2 \exp(-\gamma) \rightarrow \mu^2$, having:

$$-i \frac{e^2}{2\pi^2} (q_\mu q_\nu - q^2 g_{\mu\nu}) \left[\int_0^1 dx x(1-x) \log \left(\frac{m^2 - q^2 x(1-x)}{\mu^2} \right) \right] \quad (3.14)$$

We can obtain the β -function in the same way we have previously seen, by applying the operator $(e/2)\mu\partial/\partial\mu$ on the coefficient of $(q_\mu q_\nu - q^2 g_{\mu\nu})$. The result is:

$$\beta(e) = \frac{e^3}{2\pi^2} \int_0^1 dx x(1-x) = \frac{e^3}{12\pi^2} \quad (3.15)$$

that is, as we expected, independent from the fermion mass m and from the renormalization scale μ . In this case the fermionic contribution to the β -function doesn't vanish when $m \gg \mu$, and so there is no decoupling of the

heavy particle. There is another difficulty with the \overline{MS} scheme. The finite part of the loop diagram for $q \rightarrow 0$ is:

$$-i \frac{e^2}{2\pi^2} (q_\mu q_\nu - q^2 g_{\mu\nu}) \left[\int_0^1 dx x(1-x) \log \left(\frac{m^2}{\mu^2} \right) \right]$$

and we can see explicitly that when $\mu \ll m$ there is a logarithmic divergence and so the perturbation theory breaks down. This behavior is a consequence of the fact that the coupling constant used in the low energy limit is not the “correct” one, because it was obtained with the “wrong” β -function. The two problems, namely the logarithmic corrections and the inconsistency of the perturbation theory, can be simultaneously resolved integrating out the heavy particle: there is one effective theory that includes the fermion for $m < \mu$ and one that doesn’t include the fermion for $m > \mu$. The effects of the heavy particle in the low energy theory are reproduced considering, in the lagrangian, operators with higher dimension, which are suppressed by inverse powers of the heavy particle mass. The matching condition for the two theories at the scale m is determined by the equality of the elements of the S matrix for the light particle scattering, computed both in the low energy theory without the heavy particle and in the high energy theory with the heavy particle. In other words the heavy particle decoupling, in any mass independent regularization scheme such as the \overline{MS} , must be implemented by hand integrating out the heavy particle for $\mu < m$. One possible choice is to use a step θ function that can mimic in a rough way the behavior of figure 3.2. The β -function, in this case, can be simply written as:

$$\beta(e) = \begin{cases} e^3/12\pi^2 & \text{for } \mu > m \\ 0 & \text{for } \mu < m \end{cases}$$

3.4 β -functions in non abelian gauge theories

In this section we extend the results previously obtained for an abelian gauge theory, such as QED, to a non abelian gauge theory. This result is important because it can be immediately applied to the SM, with the gauge group $SU(3) \otimes SU(2) \otimes U(1)$, and to every supersymmetric extension of the SM with the same gauge group, such as the minimal one, *i.e.* the Minimal Supersymmetric SM (MSSM). The method we used is straightforward, but there is another, more abstract, approach: the Wilson method, based on the idea of integrating out the massive degrees of freedom. The results are the same and the two approaches are completely equivalent (see for example any standard textbook [61]).

Let us consider a theory with only one gauge coupling constant g and with n_f fermion species, that transforms in a representation r of a gauge group G . As usual in gauge theory r coincide with the fundamental representation. The generators of the group, or more properly the generators of the associated Lie algebra, t_a , satisfies the identity:

$$[t^a, t^b] = i f^{abc} t^c$$

where f_{abc} is the structure constant of the group. There are two other useful relations that will be used later:

$$\begin{aligned} \text{tr} [t^a t^b] &= C(r) \delta^{ab} \\ f^{acd} f^{bcd} &= C_2(G) \delta^{ab} \end{aligned} \quad (3.16)$$

where $C(r)$ is the index of the representation r and $C_2(G)$ is the second casimir operator in the adjoint representation.

At leading order, that is at 1-loop order, we have for the β -function a generalization of the equation (3.6):

$$\beta(g) = gM \frac{\partial}{\partial M} \left(-\delta_1 + \delta_2 + \frac{1}{2} \delta_3 \right) \quad (3.17)$$

where we have used the conventions of figure 3.3 for the counterterms δ_1, δ_2 and δ_3 .

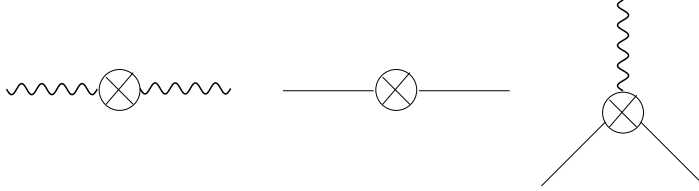


Figure 3.3: QED counterterms

From left to right, the first diagram is equal to $-i(k^2 g^{\mu\nu} - k^\mu k^\nu) \delta^{ab} \delta_3$, the second one is equal to $i \not{p} \delta_2$ and the last one is equal to $igt^a \gamma^\mu \delta_1$. In QED, using the Ward identity $g^{-1} \delta_1 = \delta_2$, we find that the β -function depends only from δ_3 . In the non abelian case, instead, there is a contribution from every terms. So, in order to cancel the divergences that appear in the 1-loop pure gauge amplitude, δ_3 must be of the form:

$$\delta_3 = \frac{g^2}{(4\pi)^2} \frac{\Gamma(2-d/2)}{(M^2)^{2-d/2}} \left[\frac{5}{3} C_2(G) - \frac{4}{3} n_f C(r) \right] \quad (3.18)$$

where M is the renormalization scale. Depending on the renormalization scheme used, there can be finite contributions to δ_3 , δ_2 and δ_1 , but the β -function contribution is scheme independent, because only the divergent parts have an explicit dependence from M . If we use dimensional regularization, the logarithmic divergences take the form:

$$\frac{\Gamma(2 - d/2)}{(\Delta)^{2-d/2}}$$

where Δ is an arbitrary combination of momentum invariants. We have seen that one possible choice is $\Delta = M^2$.

The next step consists in computing the δ_2 and δ_1 counterterms, that are necessary in order to cancel the divergences coming from the diagrams that involve fermions. At 1-loop order in a non abelian gauge theory, we have to consider three such diagrams, as can be seen in figure 3.4.

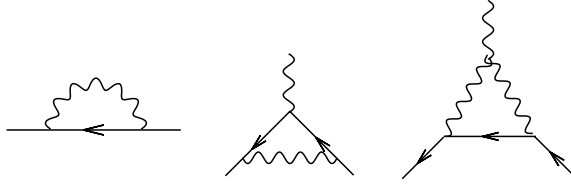


Figure 3.4: Fermionic counterterms

The δ_2 counterterm cancels the divergence in the first diagram, that is the fermionic self energy contribution. At the renormalization scale M we have:

$$\delta_2 = -\frac{g^2}{(4\pi)^2} \frac{\Gamma(2 - d/2)}{(M^2)^{2-d/2}} \cdot C_2(r) \quad (3.19)$$

where $C_2(r)$ is the quadratic casimir operator of the representation r . The δ_1 counterterm cancels the divergences associated to the second and to the third diagram of figure 3.4. The result can be written as:

$$\delta_1 = -\frac{g^2}{(4\pi)^2} \frac{\Gamma(2 - d/2)}{(M^2)^{2-d/2}} \cdot [C_2(r) + C_2(G)] \quad (3.20)$$

and we can see that, unlike the abelian case, $\delta_1 \neq \delta_2$, because δ_1 has an extra term proportional to $C_2(G)$ (the gauge bosons are “colored”). The β -function is obtained summing the three contributions coming from the counterterms, remembering that the only dependence from M is in the logarithmic term,

that in dimensional regularization assumes the form:

$$\frac{\Gamma(2 - d/2)}{(M^2)^{2-d/2}} \sim \frac{2}{\epsilon} - \log(M^2) - \gamma$$

At the end we obtain:

$$M \frac{\partial}{\partial M} \left(\frac{\Gamma(2 - d/2)}{(M^2)^{2-d/2}} \right) \sim M \frac{\partial}{\partial M} \left(\frac{2}{\epsilon} - \log(M^2) - \gamma \right) = M \frac{\partial}{\partial M} \log(M^2) = 2$$

and so:

$$\begin{aligned} \beta(g) &= (-2) \frac{g^3}{(4\pi)^2} \left[(C_2(r) + C_2(G)) - C_2(r) + \frac{1}{2} \left(\frac{5}{3} C_2(G) - \frac{4}{3} n_f C(r) \right) \right] \\ &= -\frac{g^3}{(4\pi)^2} \left[\frac{11}{3} C_2(G) - \frac{4}{3} n_f C(r) \right] \end{aligned} \quad (3.21)$$

The previous calculation, that is a well known result, has been performed starting from the divergences of the fermion vertices (associated to the δ_3 counterterm) and from the divergences of the field strength (associated to the counterterms δ_1 and δ_2). The same result for the β -function could be obtained starting from the divergences of the gauge bosons vertex. This is a common feature in every gauge theory.

The equation (3.21) refers only to a single coupling constant associated with the gauge group G . We can immediately extend this result, as was noted in section 3.2, in the case of the direct product of gauge groups $G = G_1 \otimes \dots \otimes G_n$ with n coupling constants $g_1 \dots g_n$. We simply obtain, for every g_i associated to the corresponding subgroup G_i , a β -function of the same form of (3.21) with $G \rightarrow G_i$ and considering the appropriate representation for the n_f fermions coming from the transformation properties under the gauge group G_i .

In the SM case we must consider the representation of $SU(3) \otimes SU(2) \otimes U(1)$. So, let us consider the general case of $SU(N)$. It is possible to shown that for the fundamental representation, that could be labelled by N , we have:

$$C(N) = \frac{1}{2}, \quad C_2(N) = \frac{N^2 - 1}{2N} \quad (3.22)$$

while for the quadratic casimir of the adjoint representation, we obtain:

$$C_2(G) = C(G) = N \quad (3.23)$$

and so the β -function, for a theory with n_f fermions in the fundamental representation and n_s real scalars², that transforms in a representation r' , can be written as:

$$\beta(g) = -\frac{g^3}{(4\pi)^2} \left[\frac{11}{3}N - \frac{2}{3}n_f - \frac{1}{6}n_s C(r') \right] \quad (3.24)$$

We are now able to write down the 1-loop β -functions for the SM gauge couplings:

$$\beta(g_i) = \frac{1}{(4\pi)^2} b_i g_i^3 \quad (3.25)$$

and the corresponding 1-loop RG equations:

$$\frac{d}{dt} g_i = \frac{1}{(4\pi)^2} b_i g_i^3 \quad (3.26)$$

with $t = \log(M/M_0)$ (M_0 is some convenient renormalization scale where the boundary conditions are defined) and where we have introduced the constant coefficients b_i that are determined only by the particle content of the theory. The index $i = 1, 2, 3$ runs over the gauge couplings g_1, g_2, g_3 . The g_1 and g_2 couplings can be written, in terms of the conventional electroweak gauge couplings g and g' (with $e = g \sin \theta_W = g' \cos \theta_W$), as:

$$g_1 = \sqrt{\frac{5}{3}} g', \quad g_2 = g$$

Introducing the number of generations of matter multiplets $N_{fam} = 2n_f$ and the number of Higgs doublets $N_{Higgs} = n_s$, it's quite easy to see that the SM coefficients are:

$$b_i^{SM} = \left(\frac{44}{10}, \frac{-19}{6}, -7 \right) \quad (3.27)$$

where we have used $N_{fam} = 3$ and $N_{Higgs} = 1$.

One important consequence of this result is that the SM cannot ensure the unification of the coupling constant at some very high energy scale.

3.5 Renormalization group and supersymmetry

Many calculations beyond the three level involves mass independent regularization scheme such as the dimensional regularization, usually called *DREG*

²In the SM there is at least a scalar: the Higgs boson

or known as 'naive dimensional reduction', that is an elegant and convenient way to deal with the infinities that arise in quantum field theory [74], in which the number of space-time dimensions is analytically continued to $d = 4 - \epsilon$. It is very well adapted to gauge theories because it preserves gauge invariance, but it is not so well suited for supersymmetric theories, because the supersymmetric transformations holds in general only for fixed values of the space-time dimensions d . In fact it introduces a mismatch between the off shell numbers of gauge boson degrees of freedom and the gaugino degrees of freedom. This mismatch is of order ϵ , but if we consider an n -loop calculation, it introduce an error of order $1/\epsilon^n$. So it becomes clear the importance to choose a regularization and renormalization scheme that do not explicitly violate supersymmetry.

The solution consist in modifying the procedure of dimensional regularization, in which the continuation from 4 to d space-time dimensions is performed with compactification, or stated otherwise via dimensional reduction. In this method, that is called *DRED*, the momentum integrals are d dimensional, while the number of field components remain unchanged and so supersymmetry still holds. There exist a set of transformations that are able to relate β -functions of a particular theory calculated with the *DRED* scheme to the β -functions of the same theory computed using the *DREG* scheme.

The notation usually employed makes use of greek indices $\mu, \nu \dots$ to denote the $d = 4$ space-time, while latin indices $i, j \dots$ denote the $d = 4 - \epsilon$ space-time, with corresponding metric tensors $g_{\mu\nu}$ and g_{ij} . It's useful to introduce the hatted quantities like $\hat{g}_{\mu\nu}$ and $\hat{\gamma}^\mu$, that are equal respectively to g_{ij} and γ^i in the subspace $d = 4 - \epsilon$ while the other components are zero. The momentum p_μ is defined only in the subspace $d = 4 - \epsilon$, so there is no need to use the hat notation.

There are interesting relations between the dimensional reduced quantities and the four dimensional one:

$$\begin{aligned}
\not{p} &= p_\mu \gamma^\mu = p_\mu \hat{\gamma}^\mu \\
g_{\mu\nu} g^{\mu\nu} &= 4 \\
\hat{g}_{ij} \hat{g}^{ij} &= d \\
\hat{g}^{\mu\nu} g_\nu^\lambda &= \hat{g}^{\mu\lambda} \\
\hat{g}^{\mu\nu} \gamma_\nu &= \hat{\gamma}^\mu
\end{aligned} \tag{3.28}$$

Having introduced this notation we are able to see how *DRED* works in the case of a non supersymmetric (so without elementary scalars) Yang-Mills theory with a set of fields $W_\mu^a(x)$ transforming in the adjoint representation of

a gauge group G , and with a multiplet of spin $1/2$ fields $\psi^\alpha(x)$ transforming in a representation r of the same semi-simple gauge group G . If in particular ψ is Majorana, then r has to be a real representation, since the Majorana condition is not preserved by a unitary transformation. The gauge fixed bare lagrangian can be written as:

$$\mathcal{L}_B = -\frac{1}{4}G_{\mu\nu}^2 - \frac{1}{2}(\partial^\mu W_\mu)^2 + C^{a*}\partial^\mu D_\mu^{ab}C^b + i\bar{\psi}^p\gamma^\mu D_\mu^{pq}\psi^q \quad (3.29)$$

where:

$$\begin{aligned} G_{\mu\nu}^a &= \partial_\mu W_\nu^a - \partial_\nu W_\mu^a + gf^{abc}W_\mu^bW_\nu^c \\ D_\mu^{ab} &= \delta^{ab}\partial_\mu - gf^{abc}W_\mu^c \\ D_\mu^{pq} &= \delta^{pq}\partial_\mu - ig(T^a)^{pq}W_\mu^a \end{aligned} \quad (3.30)$$

where f^{abc} are the totally antisymmetric structure constants of the semi-simple gauge group G , T^a are the group generators that acts on the fermionic representation r and where we have introduced the standard landau gauge fixing and ghost terms. We have explicitly written the two covariant derivatives that act on different representations of the gauge group G .

Following the dimensional reduced notation we can perform the following decomposition, in order to see the consequences of the DRED procedure:

$$W_\mu^a(x^j) = \{W_i^a(x^j), W_\sigma^a(x^j)\} \quad (3.31)$$

where:

$$\delta_i^i = \delta_j^j = d \quad \delta_{\sigma\sigma} = \epsilon$$

and it can be shown that we can separate the lagrangian as follows:

$$\mathcal{L}_B = \mathcal{L}_B^d + \mathcal{L}_B^\epsilon$$

with:

$$\mathcal{L}_B^d = -\frac{1}{4}G_{ij}^2 - \frac{1}{2}(\partial^i W_i)^2 + C^{a*}\partial^i D_i^{ab}C^b + i\bar{\psi}^\alpha\gamma^i D_i^{\alpha\beta}\psi^\beta \quad (3.32)$$

$$\mathcal{L}_B^\epsilon = \frac{1}{2}(D_i^{ab}W_\sigma^b)^2 - g\bar{\psi}\gamma_\sigma R^a\psi W_\sigma^a - \frac{1}{4}g^2 f^{abc}f^{ade}W_\sigma^bW_{\sigma'}^cW_\sigma^dW_{\sigma'}^e \quad (3.33)$$

In the conventional dimensional regularization *DREG* we keep only the equation (3.32), while in the *DRED* procedure we keep both the equations (3.32) and (3.33), that together are able to satisfy the supersymmetric Ward identities, at least at 1-loop level. The lagrangian (3.33) is precisely

what is required to restore the supersymmetric Ward identities at 1-loop in supersymmetric theories. If we consider only the previous non supersymmetric case we see that the *DRED* method gives rise to some ambiguity with gauge transformations. In fact, it can be seen that each term in (3.33), satisfies the dimensional reduced form of the gauge transformations:

$$\begin{aligned}\delta W_i^a &= \partial_i \Lambda^a + g f^{abc} W_i^b \Lambda^c \\ \delta W_\sigma^a &= g f^{abc} W_\sigma^b \Lambda^c \\ \delta \psi^p &= ig (T^a)^{pq} \psi^q \Lambda^a\end{aligned}\tag{3.34}$$

where the W_σ have the same transformation properties of the scalar fields, and so they are called ϵ -scalars. The gauge invariance alone is not able, because of the existence of the set of transformations (3.34), to guarantee that, for example, the vertex $\bar{\psi}\psi W_\sigma$ has the same renormalization properties of the vertex $\bar{\psi}\psi W_i$.

However in the case of supersymmetric theories, that interests to us, these difficulties do not arise: if ψ is in the adjoint representation, then \mathcal{L}_B is supersymmetric. In this case, there is a relation between W_σ and W_i , that is not broken by the dimensional reduction. Thus the vertices $\bar{\psi}\psi W_\sigma$ and $\bar{\psi}\psi W_i$, that are both equal to g at tree level, remain equal under renormalization.

In complete analogy with the non supersymmetric case, analyzed in section 3.4, all the running couplings of a supersymmetric theory must be renormalized using *DRED* with modified minimal subtraction, that we denote as \overline{DR} , rather than the usual *DREG* with modified minimal subtraction, *i.e.* \overline{MS} . However, it is possible to work consistently in the \overline{MS} scheme, as long as one is going to use a “dictionary” that permits to translate all the \overline{DR} couplings and masses into the \overline{MS} counterparts [59]. The two schemes differs only by a small offset:

$$\frac{1}{\alpha_i^{\overline{DR}}} = \frac{1}{\alpha_i^{\overline{MS}}} - \frac{C_i}{12\pi}\tag{3.35}$$

where $\alpha_i = g_i^2/4\pi$ and the $C_i = C_2(G)$ is the quadratic Casimir operator of the group G . For example, for a non abelian group like $SU(N)$ we have $C_i = N$, while for an abelian one, like $U(1)$ we have $C_i \equiv 0$, so the electromagnetic coupling α_1 remains the same.

The complete set of renormalization group equations for the MSSM, at 2-loop level, in the \overline{DR} scheme, are given in [60].

Some of the main properties of the RG equations for a theory like the MSSM, that is a theory with softly broken supersymmetry, can be studied even at one loop level.

One of the most important additional feature that comes with supersymmetry, is, by far, the unification of the coupling constants. This, for

example, took place in the MSSM. In fact, in the minimal extension of the SM, there are fermions that live in the adjoint representation of the gauge group, as well scalars that live in the fundamental representation, as can be seen by the tables 2.1 and 2.2 of the previous chapter, that together modify the coefficients (3.27) as:

$$b_i^{MSSM} = \left(\frac{33}{5}, 1, -3 \right) \quad (3.36)$$

where we have used the general β -function (3.24), valid for the gauge couplings, with $n_f = N_{fam}/2 = 3$ and $n_s = N_{Higgs} = 2$.

These new set of coefficients ensure that there is an effective unification at energy scale of about $M_U \sim 10^{15} \text{ GeV}$. This could be a strong hint for the existence of supersymmetry, but this is not an exclusive prediction, because is shared with, for example, the grand unified theories (GUT) based on larger gauge groups than the SM (like $SU(5)$).

The complete one loop RG equations for the MSSM couplings, including the Yukawa, could be written as:

$$\begin{aligned} \frac{d}{dt} g_i &= \frac{1}{(4\pi)^2} b_i^{MSSM} g_i^3 \\ \frac{d}{dt} Y_U &= -Y_L \left(\frac{16}{3} g_3 + 3g_2 + \frac{13}{15} g_1 - 6Y_U - Y_D \right) \\ \frac{d}{dt} Y_D &= -Y_D \left(\frac{16}{3} g_3 + 3g_2 + \frac{7}{15} g_1 - Y_U - 6Y_D - Y_L \right) \\ \frac{d}{dt} Y_L &= -Y_L \left(3g_2 + \frac{9}{5} g_1 - 3Y_D - 4Y_L \right) \end{aligned} \quad (3.37)$$

In the MSSM the supersymmetry is softly broken, so we are led to consider the RGE for the soft terms, in particular for the gaugino masses. A very nice feature of the renormalization of the softly broken supersymmetric theories is that it is completely defined by the unbroken theory [62][63]. This means, in particular, that the non-renormalization theorems and the cancellation of quadratic divergences still holds.

From this point of view, it is very convenient to use the supergraph technique, that can be extended immediately to softly broken theories by using the so called ‘‘spurion’’ external superfields [50][75][76]. The introduction of this superfield allows us to rewrite soft breaking terms inside of the superfields formalism. The key point, in this approach, is that a softly broken supersymmetric gauge theory can be considered as a rigid supersymmetric theory embedded into an external space-time independent superfield, so that all couplings and masses become external superfields.

Let us see how this procedure works in the case of a softly broken $N = 1$ supersymmetric pure Yang-Mills theory with a simple gauge group. The lagrangian of the rigid theory is given by:

$$\mathcal{L}_{rigid} = \int d^2\theta Tr(W^\alpha W_\alpha) + \int d^2\bar{\theta} Tr(\bar{W}^{\dot{\alpha}} \bar{W}_{\dot{\alpha}}) \quad (3.38)$$

with the field strength chiral superfield W^α (recalling the equation (2.58)) given by:

$$W_\alpha = -\frac{1}{4} \bar{D} \bar{D} e^{-gV} D_\alpha e^{gV} \quad (3.39)$$

where $V_{ij} = T_{ij}^a V_a$ and T^a are the group generators. To perform the soft supersymmetry breaking we can introduce a gaugino mass term. We write the only term that is allowed by the gauge invariance (see section 2.8 of chapter 2 for details):

$$-\mathcal{L}_{soft} = \frac{m_a}{2} \lambda \lambda + \frac{m_a}{2} \bar{\lambda} \bar{\lambda} \quad (3.40)$$

where λ is the gaugino field. Now in order to rewrite this terms in the superfields language we introduce an external spurion superfield:

$$\eta = \theta^2 \quad \bar{\eta} = \bar{\theta}^2 \quad (3.41)$$

In terms of which the total lagrangian of the theory can be written as:

$$\begin{aligned} \mathcal{L}_{tot} &= \mathcal{L}_{rigid} + \mathcal{L}_{soft} \quad (3.42) \\ &= \int d^2\theta (1 - 2\mu\eta) Tr(W^\alpha W_\alpha) + \int d^2\bar{\theta} (1 - 2\mu\bar{\eta}) Tr(\bar{W}^{\dot{\alpha}} \bar{W}_{\dot{\alpha}}) \\ &= \int d^2\theta (1 - 2\mu\theta^2) Tr(W^\alpha W_\alpha) + \int d^2\bar{\theta} (1 - 2\mu\bar{\theta}^2) Tr(\bar{W}^{\dot{\alpha}} \bar{W}_{\dot{\alpha}}) \end{aligned}$$

In terms of field components, the interaction with the superfield η produces a gaugino mass $m_a = \mu$, while the other gauge fields remain massless. In fact, looking carefully to the soft breaking piece of the lagrangian:

$$- \int d^2\theta (2\mu\theta^2) Tr(W^\alpha W_\alpha)$$

we see that now, due to the presence of the extra θ^2 , we must select the lowest component of the product $W^\alpha W_\alpha$, that is precisely the component $\lambda^\alpha \lambda_\alpha$.

The next step, in order to obtain the complete $N = 1$ supersymmetric lagrangian with soft breaking terms, is to add a set of chiral matter superfields Φ_i to the pure supersymmetric Yang-Mills theory (3.38):

$$\mathcal{L} = \int d^2\theta d^2\bar{\theta} \bar{\Phi}^i (e^V)_i^j \Phi_j + \int d^2\theta \mathcal{W} + \int d^2\bar{\theta} \bar{\mathcal{W}} \quad (3.43)$$

where the superpotential is of the form:

$$\mathcal{W} = \frac{1}{6}\lambda^{ijk}\Phi_i\Phi_j\Phi_k + \frac{1}{2}M^{ij}\Phi_i\Phi_j \quad (3.44)$$

while the soft breaking terms are of the type:

$$\mathcal{L}_{soft} = -\Phi^i (m^2)_i^k \eta \bar{\eta} (e^V)_k^i \Phi_j - A^{ijk} \eta \Phi_i \Phi_j \Phi_k - \frac{1}{2} B^{ij} \eta \Phi_i \Phi_j \quad (3.45)$$

written in terms of the previously introduced spurion superfield η .

Having introduced this formalism, we can perform the renormalization procedure of a softly broken theory following a simple recipe: one starts with the renormalization constants of a rigid theory, computed using some massless scheme such as the \overline{DR} , substitutes instead of the couplings of the rigid theory (gauge and Yukawa) their modified expressions, which depend by the spurion field η , and finally expand over this variable. This procedure gives the renormalization constants for the soft terms, that, upon differentiating with respect the renormalization scale, gives at the end the corresponding renormalization group equations.

In the case of the MSSM, considering the couplings:

$$\alpha_i = \frac{g_i^2}{(4\pi)} \quad (3.46)$$

instead of the g_i couplings, we can write down the modified couplings, including the Yukawa, as:

$$\begin{aligned} \tilde{\alpha} &= \alpha_i (1 + M_i \eta + \overline{M}_i \bar{\eta} + (M_i \overline{M}_i + \Sigma_{\alpha_i}) \eta \bar{\eta}) \\ \tilde{Y}_k &= Y_k (1 - A_k \eta - \overline{A}_k \bar{\eta} + (A_k \overline{A}_k + \Sigma_k) \eta \bar{\eta}) \end{aligned} \quad (3.47)$$

where M_i are the gaugino masses, A_k are the trilinear scalar couplings, Σ_k are a particular combination of soft squark and slepton masses entering in the expression of the Yukawa vertex and the Σ_{α_i} are related to the mass of the soft supersymmetric ghost terms \tilde{m}_{ghost}^2 . At one loop order $\tilde{m}_{ghost}^2 = 0$ and $\Sigma_{\alpha_i} \equiv 0$.

Performing the procedure previously described, we are able to obtain the RGE for the soft terms. The following equations are for the gaugino masses, the trilinear scalar couplings A_k and the sfermion masses \tilde{m}_Q^2 :

$$\begin{aligned} \frac{d}{dt} M_i &= (4\pi) b_i^{MSSM} \alpha_i M_i = b_i^{MSSM} g_i^2 M_i \\ \frac{d}{dt} A_U &= \frac{16}{3} \alpha_3 M_3 + 3\alpha_2 M_2 + \frac{13}{15} \alpha_1 M_1 + 6Y_U A_U + Y_D A_D \end{aligned}$$

$$\begin{aligned}
\frac{d}{dt}A_D &= \frac{16}{3}\alpha_3 M_3 + 3\alpha_2 M_2 + \frac{7}{15}\alpha_1 M_1 + 6Y_D A_D + Y_U A_U + Y_L A_L, \\
\frac{d}{dt}A_L &= 3\alpha_2 M_2 + \frac{9}{5}\alpha_1 M_1 + 3Y_D A_D + 4Y_L A_L, \\
\frac{d}{dt}\tilde{m}_Q^2 &= - \left[\left(\frac{16}{3}\alpha_3 M_3^2 + 3\alpha_2 M_2^2 + \frac{1}{15}\alpha_1 M_1^2 \right) - Y_U(\tilde{m}_Q^2 + \tilde{m}_U^2 + m_{H_2}^2 + A_U^2) \right. \\
&\quad \left. - Y_D(\tilde{m}_Q^2 + \tilde{m}_D^2 + m_{H_1}^2 + A_D^2) \right] \tag{3.48}
\end{aligned}$$

The complete RGE for all the MSSM soft terms, up to three loop level, can be found in [64].

3.6 Minimal SUGRA models

We have previously seen (in chapter 2) that the MSSM soft terms can be put by hand in the full lagrangian of the theory. We have also seen that a possible explanation for the origin of these terms is through an underlying more fundamental theory, in which the supersymmetry breaking is realized spontaneously (in a dynamical way or not). The models described in the section 2.8 of the previous chapter do not give rise to an acceptable solution. So supersymmetry breaking cannot be generated by any of the fields that belong to the supermultiplets of the MSSM [36].

There are several difficulties in realizing the supersymmetry breaking, at tree level, in a phenomenologically viable way, working only with renormalizable terms in the lagrangian. The first problem is to give masses to the MSSM gauginos, because supersymmetry does not allow scalar-gaugino-gaugino couplings which could turn into gaugino mass terms when the scalar gets a VEV. The second problem comes in for the sum rule which governs the tree level³ squared masses of scalars and chiral fermions in theories with spontaneous supersymmetry breaking [36]:

$$Tr(M_{real\ scalars}^2) = 2Tr(M_{chiral\ fermions}^2) \tag{3.49}$$

where $M_{real\ scalars}$ and $M_{chiral\ fermions}$ are the mass matrices for fields in the same supermultiplet. Because we already know that the masses of all of the MSSM chiral fermions are small (except for the t quark and the higgsinos), it is difficult to explain why we have no observational evidences for light squarks or sleptons.

³in general the sum rule is not valid if we consider radiative corrections

For the reasons we have listed, we can expect that the MSSM soft terms arise indirectly via radiative processes rather than from tree level renormalizable couplings. We can construct models in which supersymmetry breaking occurs in an “hidden sector” (whose nature is not at all well defined) of particles which have no (or only very small) direct couplings to the “visible sector” of chiral supermultiplets of the MSSM. However the two sectors must interact in some way and this interaction must communicate the supersymmetry breaking. In this scenario, the sum rule (3.49) need not hold for the visible sector fields, so that we can obtain a supersymmetric viable mass spectrum. Moreover, if the interactions are flavor blind, then the MSSM soft terms may automatically satisfy the universality conditions (2.87), (2.88) and (2.89).

We concentrate on models for which the flavor blind interaction are gravitational. The situation is sketched in figure 3.5.

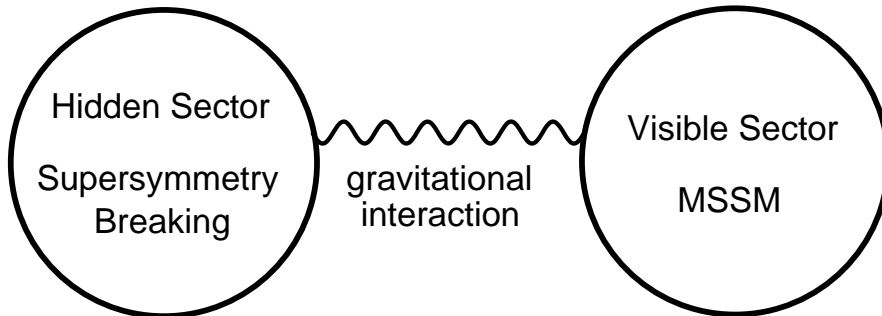


Figure 3.5: Model with hidden sector that communicate the supersymmetry breaking, through gravitational interaction, to the visible sector where the MSSM lives.

The key property of these kind of models is that the hidden sector of the theory communicates with the MSSM in the visible sector only (or dominantly) through gravitational interactions, and so the underlying theory is supergravity (SUGRA) [57]. From the point of view of the low energy field theory, this means that the supergravity lagrangian contains non renormalizable pieces which communicate with the two sectors and which are suppressed by inverse powers of the Planck mass M_{Pl} . In the following description we want only give a setup of the model and we suggest, for a more in depth discussion, the references [36][70][71][72].

The non renormalizable lagrangian will include the terms:

$$\mathcal{L}_{NR} = -\frac{1}{M_{Pl}} F_X \sum_a \frac{1}{2} f_a \lambda^a \lambda^a + c.c.$$

$$\begin{aligned}
& -\frac{1}{M_{Pl}^2} F_X F_X^* k_j^i \phi_i \phi^{*j} \\
& -\frac{1}{M_{Pl}} F_X \left(y^{ijk} \phi_i \phi_j \phi_k + \frac{1}{2} m^{ij} \phi_i \phi_j \right)
\end{aligned} \tag{3.50}$$

where F_X is the auxiliary field for a chiral supermultiplet X in the hidden sector, and ϕ_i and λ^a are the scalar and gaugino fields of the MSSM. The dimensionless parameters (f_a , k_j^i , y^{ijk} and m^{ij}) that appear in \mathcal{L}_{NR} are to be determined by the underlying supergravity theory. The non renormalizable terms (3.50) are not supersymmetric but it can be shown [36] that they are part of a supersymmetric lagrangian that contains other terms that can be safely ignored. Now if we assume that the auxiliary field F_X gets, due to some not specified mechanism, a VEV of order:

$$\langle F_X \rangle \sim 10^{10} \text{ GeV}$$

then the non renormalizable lagrangian (3.50) will give exactly the soft breaking lagrangian $\mathcal{L}_{soft}^{MSSM}$, that we have formally written in the equation (2.84) with:

$$m_{soft} \sim 1 \text{ TeV}$$

In general computing the parameters f_a , k_j^i , y^{ijk} and m^{ij} is a very difficult task to perform, but a dramatic simplification occurs if one assumes a minimal form for the normalization of kinetic terms and gauge interactions in the full, non renormalizable, lagrangian [36]. In this case we find that $f_a = f$ is common to all the gauginos, $k_j^i = k \delta_j^i$ is common to all scalars, while the other couplings are all proportional to the corresponding part in the superpotential:

$$y^{ijk} = c_1 y^{ijk} \quad m^{ij} = c_2 m^{ij}$$

with universal dimensionless constants c_1 and c_2 . The result is that the soft breaking lagrangian $\mathcal{L}_{soft}^{MSSM}$ can be written in terms of only four parameters, that have to be specified at the high energy scale of the SUGRA theory (typically the unification scale M_{GUT} or even the Planck scale M_{Pl}):

$$m_{1/2} = f \frac{\langle F_X \rangle}{M_{Pl}} \quad m_0^2 = k \frac{|\langle F_X \rangle|^2}{M_{Pl}^2} \quad A_0 = c_1 \frac{\langle F_X \rangle}{M_{Pl}} \quad B_0 = c_2 \frac{\langle F_X \rangle}{M_{Pl}} \tag{3.51}$$

The soft breaking parameters can thus be written in terms of these high scale input parameters, as follows:

$$M_1 = M_2 = M_3 = m_{1/2}$$

$$\begin{aligned}
m_Q^2 &= m_u^2 = m_d^2 = m_L^2 = m_e^2 = m_0^2 \mathbf{1}_{3 \times 3} \\
m_{H_u}^2 &= m_{H_d}^2 = m_0^2 \\
a_i &= A_0 y_i \quad i = t, b, \tau \\
b &= B_0 \mu
\end{aligned} \tag{3.52}$$

where we have assumed the third family approximation for the Yukawa couplings. These relations are stronger realization of the universality conditions and they have to be thought as boundary conditions at the high energy scale, when we RG evolve the parameters down to the electroweak scale. The entire MSSM spectrum is given in terms of only these five parameters⁴: m_0 , $m_{1/2}$, A_0 , B_0 and the Higgs mass parameter μ . The framework that we have described is referred to as the minimal supergravity (mSUGRA) or supergravity inspired scenario for the soft terms. In these type of models the electroweak symmetry breaking (EWSB) is actually driven purely by quantum corrections. This mechanism is therefore known as radiative electroweak symmetry breaking [73]. Let us see what are the physical Higgs degrees of freedom after the electroweak symmetry breaking. We already know that in the MSSM there are two complex Higgs scalar fields and each one is an $SU(2)$ doublet. Thus, there are eight real degrees of freedom. When the electroweak symmetry is broken, three of them are the Nambu-Goldstone bosons G^0 and G^\pm , which become the longitudinal modes of the Z^0 and W^\pm massive vector bosons. The remaining five Higgs scalar mass eigenstates consist of one CP odd neutral scalar A^0 , two charged scalar H^+ and its charged conjugate H^- , together with two CP neutral scalars h^0 and H^0 . It is possible to write down the conditions that allow a right electroweak symmetry breaking:

$$\begin{aligned}
|\mu|^2 + m_{H_d}^2 &= b \tan \beta - (m_Z^2/2) \cos 2\beta \\
|\mu|^2 + m_{H_u}^2 &= b \cot \beta + (m_Z^2/2) \cos 2\beta
\end{aligned} \tag{3.53}$$

with the β parameter defined as:

$$\tan \beta = \frac{v_u}{v_d} \tag{3.54}$$

where $\langle H_u^0 \rangle = v_u$ and $\langle H_d^0 \rangle = v_d$ are the Higgs bosons VEVs at the minimum of the potential. Moreover, these quantities can be related to the known mass of the Z^0 boson and the electroweak gauge couplings:

$$v_u^2 + v_d^2 = v^2 = 2 \frac{m_Z^2}{g^2 + g'^2} \sim (174 \text{ GeV})^2 \tag{3.55}$$

⁴The Yukawa couplings are the same already measured in the SM

The value of $\tan \beta$ is not fixed by present experiments, but it can be computed starting from the parameters of the MSSM. It is possible to eliminate [38] two lagrangian parameters, b and $|\mu|$, in favor of $\tan \beta$ and the phase of μ .

Let us concentrate now on the one loop RG equation for the soft gaugino masses that appear in the first line of (3.37). From that equation it is simple to derive that the three ratios M_i/g_i^2 are RG invariant up to two loop corrections. In fact:

$$\begin{aligned} \frac{d}{dt} \left(\frac{M_i}{g_i^2} \right) &= g_i^{-2} \frac{dM_i}{dt} - 2M_i g_i^{-3} \frac{dg_i}{dt} \\ &= 2g_i^{-2} C_i g_i^2 - 2M_i g_i^{-3} C_i g_i^3 = 0 \end{aligned} \quad (3.56)$$

where $C_i = b_i^{MSSM}/(4\pi^2)$ and we have used the first lines of the equations (3.37) and (3.48).

Thus we can see that in mSUGRA models the following relations hold:

$$M_i(Q) = \frac{g_i^2(Q)}{g_i^2(Q_0)} m_{1/2} \quad i = 1, 2, 3 \quad (3.57)$$

at any RG energy scale $Q < Q_0$, where Q_0 is the high energy input scale which is presumably of the same order of M_{Pl} or of order of the unification scale $M_{GUT} \sim 10^{16}$ GeV. Since in the MSSM we observe the couplings unification, we put $Q_0 \equiv M_{GUT}$ and so:

$$g_1^2(Q_0) \sim g_2^2(Q_0) \sim g_3^2(Q_0) \quad (3.58)$$

Hence, substituting the previous relation into equation (3.57), allows us to obtain the following RG invariant relation:

$$\frac{M_1}{g_1^2} = \frac{M_2}{g_2^2} = \frac{M_3}{g_3^2} \quad (3.59)$$

modulo some small two loop effects and possibly larger threshold effects near the scale M_{GUT} and M_{Pl} . The common value of the previous equation can be put equal to:

$$\frac{m_{1/2}}{g_{GUT}^2}$$

where g_{GUT} is the unified gauge coupling at the input scale where $m_{1/2}$ is the common gaugino mass. If gaugino masses have, as in this case in which they satisfy the universality conditions, a common phase and are the dominant source of supersymmetry breaking, then μ can be taken real without loss of generality [82]. Moreover, if μ is not real, then there can be very bad CP violating effects in the low energy physics, including electric dipole moments

for both the electron and the neutron. Using the EWSB conditions (3.53) only the sign of μ , the function $sgn(\mu)$, remains as a free parameter. Thus to study the low energy phenomenology we can take as fundamental parameters:

$$m_0, m_{1/2}, A_0, \tan\beta, sgn(\mu) \quad (3.60)$$

that encode our ignorance about the mechanism of supersymmetry breaking and completely define the couplings and the mass spectrum of the MSSM, once they are RG evolved down to the weak scale.

3.7 Numerical RGE solutions for the MSSM

In section 3.5, we have seen that, not considering the gauge couplings and gaugino masses, even at one loop level, the RGE for the MSSM form a set of coupled differential equations. The situation is obviously more complicated when one consider the two loop equations. In the latter case it is not a simple task to find a closed form solution for these equations, but it is quite easy to solve them numerically using an appropriate algorithm.

In the following discussion we describe the ISASUGRA algorithm [65], that we have extensively used in order to compute the weak scale values of the MSSM parameters space⁵. The theoretical framework is the minimal supergravity (mSUGRA), that is also called constrained MSSM (cMSSM), without right handed neutrinos, that as been described in the previous section.

The input parameters specified at GUT scale are just those previously defined for a mSUGRA model (see equation (3.60)) and that we rewrite here:

$$m_0, m_{1/2}, A_0, \tan(\beta), sgn(\mu) \quad (3.61)$$

There is a fundamental distinction between free and constrained parameters. The former are identified with the input parameters, while the latter are constrained either by experiment, for example the quark masses and gauge couplings, or by relations among themselves such as $Y_b = Y_\tau$ calculated at M_{GUT} and minimization conditions at m_Z .

There are two types of boundary conditions, one at the weak scale and one at the GUT scale:

- At weak scale m_Z one imposes g_1, g_2, g_3 and Y_τ, Y_b to be equal to their experimental values.

⁵see the appendix for a brief description of the fortran code

- At GUT scale one imposes

$$\begin{aligned}
M_1 &= M_2 = M_3 = m_{1/2} \\
m_{scalar}^2 &= m_0^2 \\
A_\tau &= A_b = A_t = A_0
\end{aligned}$$

The first part of the algorithm is used in order to determine the right GUT scale, so it runs from the experimental value m_z to the M_{GUT} scale. Exact unification of all the gauge couplings is a theoretical simplification even in GUT theories, since one does not expect the gauge couplings to be exactly equal due to threshold effects at the GUT scale [66]. The threshold corrections are computed using the so called match-and-run technique [69], which is based on the successive decoupling of particles at the scale of their masses, following the description outlined in section 3.3. Let us consider a running mass \hat{m} in the \overline{DR} renormalization scheme, whose β -function depends on all the particles in the MSSM. Defining t by:

$$t = \log \left(\frac{Q}{M_{GUT}} \right) \quad (3.62)$$

where Q is the energy scale at which the equations are evaluated, the mass \hat{m} evolves according to its complete supersymmetric RGE. If we now start running \hat{m} towards the weak scale m_Z , along the way, we eventually encounter the scale of the squark masses. According to the match-and-run procedure, we must stop the evolution and construct a new effective theory in which the squarks are integrated out. We must then continue the evolution, using the new β -function, without the squark \tilde{q} contribution, subject to the matching condition:

$$\hat{m}(m_{\tilde{q}}^-) = \hat{m}(m_{\tilde{q}}^+) \quad (3.63)$$

where the superscript $+$ and $-$ refers to the two theories, respectively, with and without the squark \tilde{q} . This procedure must be repeated at each new threshold finally stopping at the scale:

$$t = \hat{m}(t) \quad (3.64)$$

The quantity $\hat{m}(\hat{m})$ is the approximation of the physical pole mass.

Let us compute the threshold correction to a particle of mass \hat{m} from a particle of mass M , with $M > m$. According to the match-and-run procedure, the decoupling of the heavy particle gives the correction:

$$\frac{\Delta m}{\hat{m}} = \frac{\Delta \beta}{16\pi^2} \log \left(\frac{\hat{M}^2}{\hat{m}^2} \right) \quad (3.65)$$

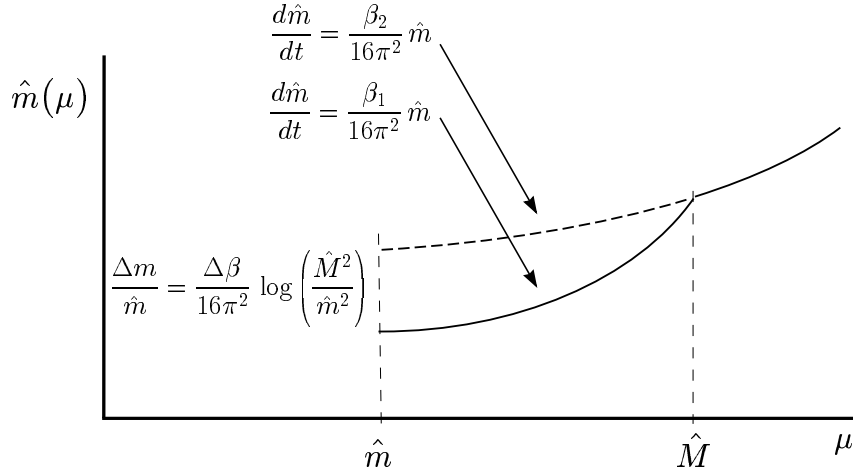


Figure 3.6: The running mass \hat{m} with and without the decoupling of a particle of running mass \hat{M} with $\mu \equiv t = \log(Q/M_{GUT})$ [69]

where in this expression, $\Delta\beta$ is the difference of the β -functions, before and after decoupling (see figure 3.6). The exact one loop result can be found computing the diagram shown in figure 3.7:

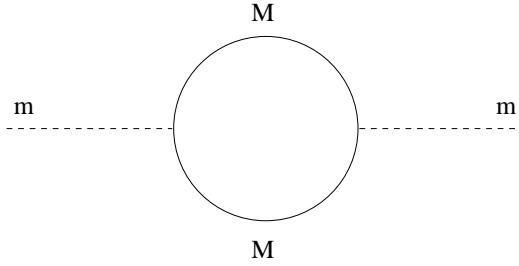


Figure 3.7: One loop diagram used to compute the threshold correction, due to an heavy particle of mass M , for a generic particle of mass m

The result is given by:

$$\frac{\Delta m}{\hat{m}} = \frac{\Delta\beta}{16\pi^2} \int_0^1 dx \log \left(\frac{|M^2 - x(1-x)m^2|}{t^2} \right) \quad (3.66)$$

that for $t = m$ reduces to:

$$\frac{\Delta m}{\hat{m}} = \frac{\Delta\beta}{16\pi^2} \left[\log \left(\frac{M^2}{m^2} \right) + (\text{finite terms}) \right] \quad (3.67)$$

where, as usual, the finite terms does not contain any logarithms. These results indicate that the match-and-run procedure gives a good approximation to the pole mass when $\hat{M} \gg \hat{m}$. In this case the large logarithm, proportional to $\log(\hat{M}^2/\hat{m}^2)$, dominates the threshold correction. But in the case $\hat{m} \sim \hat{M}$, the finite term is typically of the same order of the logarithm and so the finite corrections are completely missed by the match-and-run procedure.

From m_Z to M_{GUT}

The algorithm, RG evolves the 3 gauge couplings g_1, g_2, g_3 and the 3 Yukawa couplings Y_τ, Y_b, Y_t from the measured values at m_Z scale (Y_t starts from 0). It uses the Runge-Kutta method to integrate the two loop renormalization group equations (except for μ and B that are computed at one loop) with a common mass scale m_{SUSY} for all the sparticle. This scale is set equal to $m_{SUSY} = \left(m_0^2 + 4m_{1/2}^2\right)^{1/2}$. The RGE equations implemented are at the two loop level [60]. The equations at the one loop level are those written in (3.37). At this stage there is only one threshold correction implemented, following the procedure outlined in section 3.3:

$$\begin{aligned} Q < m_{SUSY} & \quad \text{SM RGE} \\ Q > m_{SUSY} & \quad \text{MSSM RGE} \end{aligned}$$

This means that the contribution of the superparticles to the β function is different from 0 only above the common scale m_{SUSY} . The running from m_Z to higher energy scales is taken on until it is reached a Q such that the condition

$$\alpha_1(Q) = \alpha_2(Q) \tag{3.68}$$

is satisfied. This is the condition that defines the gauge coupling unification, and hence the GUT scale and the α_{GUT} are determined as

$$M_{GUT} = Q, \quad \alpha_{GUT} = \alpha_1(Q) = \alpha_2(Q).$$

The value of the strong coupling constant $\alpha_3(M_{GUT}) = \alpha_3(Q)$ does not in general coincide with α_{GUT} ; so in order to get the unification of the strong and weak couplings, it is imposed that

$$\alpha_{GUT} = \alpha_1(Q) = \alpha_2(Q) = \alpha_3(Q). \tag{3.69}$$

During the running from m_Z to M_{GUT} , there is a check on the absolute values of the Yukawa couplings: if any of these absolute values becomes greater than 10, the RG procedure is terminated, because the perturbation theory breaks down [67]. If the algorithm is not able to find such Q , then the model is not a unified one.

From M_{GUT} to m_Z

We start with the following set of parameters defined at the GUT scale:

- the initial inputs defined in (3.61), that imply

$$M_1 = M_2 = M_3 = m_{1/2}$$

$$m_{scalar}^2 = m_0^2$$

$$A_\tau = A_b = A_t = A_0$$

- the 3 gauge couplings g_1, g_2, g_3 and the 3 Yukawa couplings Y_τ, Y_b, Y_t , that we have evolved in the previous step.

Now it is time to define the supersymmetric thresholds. In general each superparticle mass has associated with it a boundary between two effective theories. Above a particular mass threshold the associated particle is present in the effective theory, and contributes to the β functions, below the threshold the particle is absent. In the mSUGRA model that we are considering the superparticle spectrum is no longer degenerate as in a simple global supersymmetry model in which all the superparticles are given a common mass m_{SUSY} . The particular choice in the algorithm is:

$$m_{\tilde{g}} = m_{\tilde{u}} = m_{\tilde{d}_R} = m_{\tilde{\chi}_1^\pm} = m_{A^0} = m_{SUSY}$$

$$\mu = m_{SUSY}$$

Now we are ready to perform a second RG evolution, from the M_{GUT} scale to the weak scale m_Z , for all the parameters. The equations are computed at the two loop level [60], except for μ and B parameters that are still evaluated at one loop level. When the weak scale is reached the right constraints for the electroweak symmetry breaking are imposed [37]. The two conditions are obtained minimizing the tree level Higgs effective potential. It can be shown that the b and μ parameters must satisfy the following conditions [60]:

$$b = \left\{ m_{H_d}^2 + m_{H_u}^2 + 2 \left[\frac{m_{H_d}^2 - m_{H_u}^2 \tan^2 \beta}{\tan^2 \beta - 1} - \frac{1}{2} m_Z^2 \right] \right\} \frac{\sin 2\beta}{2\mu}$$

$$\mu = \left[\frac{m_{H_d}^2 - m_{H_u}^2 \tan^2 \beta}{\tan^2 \beta - 1} - \frac{1}{2} m_Z^2 \right]^{1/2} \cdot \text{sgn}(\mu) \quad (3.70)$$

The next step is a refinement of the EWSB conditions, and consists in determining the parameters appearing in the Higgs scalar potential at 1-loop level. If the quantity :

$$\frac{m_{H_d}^2 - m_{H_u}^2 \tan^2 \beta}{\tan^2 \beta - 1} - \frac{1}{2} m_Z^2 > 0 \quad (3.71)$$

is not satisfied, the electroweak symmetry breaking cannot be obtained, because the second equation in (3.70) is not well defined, and the procedure is stopped. If the condition (3.71) is satisfied the algorithm re-evaluate (3.70) with the m_{H_u} and m_{H_d} parameters evaluated at one loop level. At this stage are also introduced other one loop corrections to masses and couplings [68], and the entire particle spectrum is computed.

Iteration of the running from m_z to M_{GUT} and back

The next step consists of an iteration of the evolution procedure, running backward and forward from m_z to M_{GUT} .

- The initial conditions, at weak scale, are chosen so that:
 - the three coupling constants g_1, g_2, g_3 and two Yukawa couplings Y_τ, Y_b are equal to the experimental values.
 - the b and μ parameters are those that realize the radiative EWSB at one loop level, in equation (3.70).
 - all the other parameters are those computed in the previous RG running (in particular the Y_t). Yukawa coupling.

During these iterations, the particle spectrum is no more degenerate. This implies that the theory has many different thresholds, which can be identified with the particle masses. We now show how the threshold corrections are implemented in the RG flow. Let us suppose to have a particle with mass M_η , which contributes β_i^η to the β function of the gauge coupling α_i , which we denote as β_i , at a given loop order. If $\beta_i^{(0)}$ is the β function of the model for renormalization scale $Q < M_\eta$, then the algorithm is built in such a way that for $Q > M_\eta$, the same β function becomes

$$\beta_i = \beta_i^{(0)} + \beta_i^\eta.$$

In the algorithm, the following threshold scales are implemented:

1. $m_{\tilde{u}_L}$ for every squark
2. $m_{\tilde{e}_L}$ for every slepton
3. μ for the the two higgsino doublets
4. $m_{\chi_1^\pm}$ for charginos
5. $m_{\tilde{g}}$ for gluinos
6. m_{A^0} for the two Higgs doublets

7. M_1 for bino
8. M_2 for winos
9. m_t for third generation top quark

The RG running proceeds from the weak scale m_Z to higher values of the renormalization scale Q . The RG equations used in the process are at one-loop order, for Q lower than $m_{SUSY} = \left(m_0^2 + 4m_{1/2}^2\right)^{1/2}$, while are at two loop order for higher Q s, except for those of the parameters μ and b , that are always at one loop order. As before, the unification scale M_{GUT} is determined by the condition⁶

$$\alpha_1(Q) = \alpha_2(Q) \quad M_{GUT} = Q,$$

and the unification of α_3 at M_{GUT} is imposed. Once the GUT scale is reached, the mSUGRA boundary conditions (3.52) are imposed:

$$M_1 = M_2 = M_3 = m_{1/2}$$

$$m_{scalar}^2 = m_0^2$$

$$A_\tau = A_b = A_t = A_0,$$

and the RG running is performed back to m_Z , with the same prescriptions described above. Once the running reaches the weak scale, if a correct EWSB symmetry breaking can be achieved⁷, the entire physical spectrum is calculated. The whole procedure of running from m_Z to M_{GUT} and back is repeated, until the values that the running parameters take at the m_Z scale after each iteration, are stabilized at the level of 2%.

⁶If the condition cannot be satisfied for any $Q < 10^{16}$ GeV the algorithm stops.

⁷See the discussion above.

Chapter 4

Supersymmetric Dark Matter

4.1 Introduction

We have seen in the previous chapters how to build a suitable supersymmetric extension of the SM of fundamental interactions and how to connect an underlying high energy theory, that is able to explain the origin of the soft supersymmetry breaking terms, with the low energy physics, through the renormalization group equations. From chapter 1 we already know that we have to find a cold dark matter candidate in the particle spectrum of such supersymmetric theories. We will use the framework of the MSSM.

If we want to find a cold dark matter candidate, the key ingredient is the conservation of the peculiar R-parity that we have defined in the equation (2.61) in chapter 2. We recall that $R = +1$ for ordinary particles while $R = -1$ for supersymmetric particles (superpartners of the ordinary particles). If R-parity were broken there would be no special selection rules in order to prevent the decay of supersymmetric particles into lighter ordinary particles. This means also that there would be no stable supersymmetric particle, and so no natural candidate for cold dark matter. Therefore, we are led to consider only the MSSM with strict R-parity conservation. In this way the lightest supersymmetric particle (LSP) with $R = -1$ will be stable.

The LSP must be a superpartner of an ordinary particle. In the MSSM the possible choices are the gauge fermions (gluino, photino, wino, etc.), Higgs fermions (higgsinos), scalar quarks and leptons (squarks and sleptons) and the gravitino. In the early Universe, all these particles would be present in thermal equilibrium. As the temperature falls, the heavier supersymmetric particles decay into the lighter one, and so only the LSP will be left. In this case the dominant process becomes the pair annihilation. We must require that this process is efficient enough to reduce the present LSP number density

to an acceptable value from the cosmological point of view.

From the previous list of candidates it is possible to eliminate [77] the charged uncolored particles, such as a chargino or a slepton, due the failures in the search of anomalously heavy protons [78]. For the same reason and from consideration coming from GUT [77], it is possible to eliminate the colored particles such as squarks and gluinos. Finally the sneutrino is ruled out in most, but not all, regions of sneutrino parameter space from cosmological and WIMP direct detection experiments [79] and from indirect searches [80].

So the only remaining candidates, which are not colored and electrically neutral, are the gravitino, the spin 3/2 particles superpartner of the graviton, and the lightest neutralino, a linear combination of the gauge boson superpartners \widetilde{W}^0 and \widetilde{B} and of the Higgs boson superpartners \widetilde{H}_u^0 and \widetilde{H}_d^0 . We will concentrate on the neutralino. We will argue that, because it is stable and weak interacting, the neutralino is a good dark matter candidate.

4.2 Neutralino

As we have seen before the formal definition of the neutralino is a linear combination of the higgsinos and electroweak gauginos [37]. The neutral higgsinos, \widetilde{H}_u^0 and \widetilde{H}_d^0 , and the neutral gauginos \widetilde{W}^0 and \widetilde{B} combine to form four neutral mass eigenstates called neutralinos. We denote the neutralino mass eigenstates by

$$\widetilde{\chi}_i$$

with $i = 1, 2, 3, 4$. By convention the masses are labelled in ascending order:

$$m_{\widetilde{\chi}_1} < m_{\widetilde{\chi}_2} < m_{\widetilde{\chi}_3} < m_{\widetilde{\chi}_4}$$

so the lightest neutralino is the LSP (unless there is a lighter gravitino or if R-parity is not conserved). Introducing a gauge eigenstate basis it is possible to write the neutralino mass terms in the MSSM lagrangian as:

$$\mathcal{L} \supset -\frac{1}{2} (\psi^0)^T M_{\widetilde{\chi}} \psi^0 + c.c. \quad (4.1)$$

where:

$$\psi^0 = \left(\widetilde{B}, \widetilde{W}^0, \widetilde{H}_d^0, \widetilde{H}_u^0 \right) \quad (4.2)$$

and with the neutralino mass matrix given by:

$$M_{\widetilde{\chi}} = \begin{pmatrix} M_1 & 0 & -c_\beta s_W m_Z & s_\beta s_W m_Z \\ 0 & M_2 & c_\beta c_W m_Z & -s_\beta c_W m_Z \\ -c_\beta s_W m_Z & c_\beta c_W m_Z & 0 & -\mu \\ s_\beta s_W m_Z & -s_\beta c_W m_Z & -\mu & 0 \end{pmatrix} \quad (4.3)$$

where the θ_W parameter is the Weinberg angle and where we have introduced the following notation: $s_\beta = \sin \beta$, $c_\beta = \cos \beta$, $s_W = \sin \theta_W$ and $c_W = \cos \theta_W$. We remind that β is related to the Higgs bosons VEVs through the equation (3.54).

In the neutralino mass matrix (4.3) appear the two soft breaking parameters M_1 and M_2 that, recalling the expression for the soft terms MSSM lagrangian (2.84), are associated, respectively, to the bino and wino mass terms. The μ parameter, instead, is the supersymmetric higgsino parameter that appear in the lagrangian term (2.82).

The neutralino mass matrix (4.3) can be diagonalized by a unitary matrix N , in order to obtain the neutralino mass eigenstates:

$$\tilde{\chi}_i = N_{ij} \psi_j^0 \quad (4.4)$$

In this way the matrix:

$$M_{\tilde{\chi}}^{(diag)} = N^* M_{\tilde{\chi}} N^{-1} \quad (4.5)$$

possesses on the diagonal the eigenvalues, real and positive, $m_{\tilde{\chi}_1}$, $m_{\tilde{\chi}_2}$, $m_{\tilde{\chi}_3}$ and $m_{\tilde{\chi}_4}$. These are the absolute values of the eigenvalues of the matrix $M_{\tilde{\chi}}$, or equivalently the square roots of the eigenvalues of $M_{\tilde{\chi}}^\dagger M_{\tilde{\chi}}$. The indices (i, j) on the diagonalizing matrix N_{ij} are mass and gauge eigenstate labels. The mass eigenvalues and the matrix N_{ij} can be given in closed form in terms of the parameters M_1 , M_2 , μ and $\tan \beta$, although the results are not particularly illuminating [81].

In general M_1 , M_2 and μ can have arbitrary complex phase that depends on the form of the RGE used to evolve down the parameters of the high energy theory that must describe the origin of the soft supersymmetry breaking terms. If we assume an mSUGRA model for the origin of these terms, the relations (3.52) hold. Thus, we are able to redefine the phases of \tilde{B} and \tilde{W} in such a way that M_1 and M_2 are real and positive. It is possible to show that a redefinition of the phase of the fields \tilde{B} and \tilde{W}^0 allows us to make M_1 and M_2 real and positive, and, as we have previously seen, the other parameter is simply $sgn(\mu)$, that is still undetermined by the EWSB constraints.

In the mSUGRA models we have the amazing RG invariant relation (3.59). In particular the following relation holds for M_1 and M_2 , modulo two loop corrections:

$$M_1 = \frac{g_1^2}{g_2^2} M_2 \quad (4.6)$$

and recalling the conventions for the MSSM coupling constants (see sec-

tion 3.4):

$$\begin{aligned}
g_1 &= \sqrt{\frac{5}{3}} g' & g' &= e/\cos\theta_W \\
g_2 &= g & g &= e/\sin\theta_W
\end{aligned}
\tag{4.7}$$

where e is the usual electroweak coupling, we find the nice property:

$$M_1 = \frac{5}{3} \tan^2\theta_W M_2 \tag{4.8}$$

that holds at the electroweak scale. This implies that the neutralino masses and mixing angles depend on only three unknown parameters, that are related, through the RGE, to the parameters of the underlying high energy theory. In particular, we can study the neutralino mass dependence from the m_0 and $m_{1/2}$ mSUGRA parameters, and we find the results shown in figure 4.1, whose plots are obtained fixing the other three parameters A_0 , $\tan(\beta)$ and $\text{sgn}(\mu)$. We can observe that for $m_0 < 1$ TeV the neutralino mass heavily depends on $m_{1/2}$, as one could expect by taking into account that, for such values of m_0 , the lightest neutralino is nearly a pure gaugino [84]. In particular it is possible to show [85] that in the limit:

$$|M_1| + |\mu| \gg m_Z$$

the diagonalization of the neutralino mass matrix (4.3) can be carried out perturbatively and the result is that the LSP is an almost pure bino. Thus the eigenvalue of the lightest neutralino is, keeping terms up to $\mathcal{O}(m_Z)$:

$$m_{\tilde{\chi}_1} = M_1$$

while for the second lightest neutralino $\tilde{\chi}_2$ we have:

$$m_{\tilde{\chi}_2} = M_2$$

The phenomenology and the cosmological relic abundance of the lightest neutralino are determined essentially by its mass and its composition. Let us indicate, from now on, the mass of the lightest neutralino with:

$$m_{\tilde{\chi}} \equiv m_{\tilde{\chi}_1} \tag{4.9}$$

and we can express $\tilde{\chi}$ in terms of the mixing diagonalizing matrix N_{ij} (recalling the equation (4.4)) as:

$$\tilde{\chi} = N_{11}\tilde{B} + N_{12}\tilde{W}^0 + N_{13}\tilde{H}_u^0 + N_{14}\tilde{H}_d^0 \tag{4.10}$$

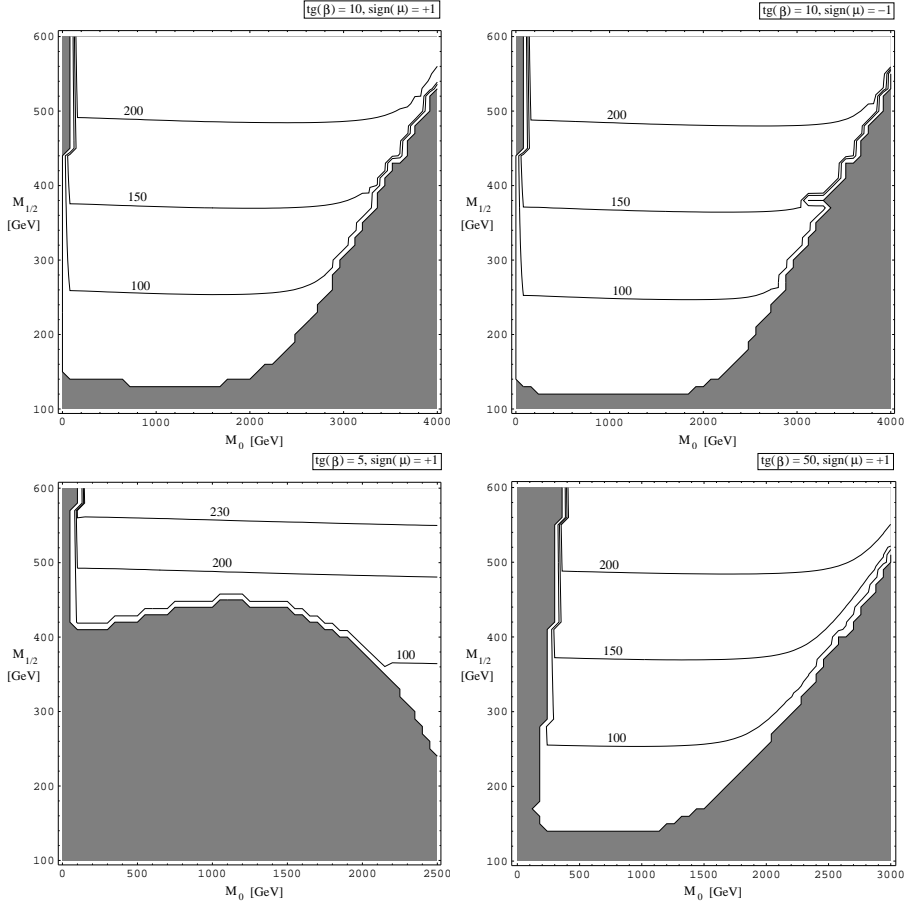


Figure 4.1: Neutralino mass contour plots in the $(m_0, m_{1/2})$ mSUGRA plane.

The neutralino composition can be described in terms of an other useful parameter, called gaugino fraction [83], that is defined in the following way:

$$Z_g = |N_{11}|^2 + |N_{12}|^2 \quad (4.11)$$

If $Z_g > 0.5$ then the neutralino is primarily a gaugino, while if $Z_g < 0.5$ then the neutralino is primarily an higgsino.

4.3 Chargino

There is another kind of supersymmetric particle that arise in the mass spectrum of the MSSM and that is important in order to study the possible neutralino interactions. If we consider the two charged higgsinos, \tilde{H}_u^+ and

\widetilde{H}_d^- , and the two charged winos, \widetilde{W}^+ and \widetilde{W}^- , we see that they generate two mass eigenstates with charge $C = \pm 1$ called charginos. We denote these two states as:

$$\widetilde{C}_i^\pm$$

where $i = 1, 2$. As in the neutralino case, the mass are labelled in ascending order:

$$m_{\widetilde{C}_1} < m_{\widetilde{C}_2}$$

and the mass eigenstates can be analyzed in an analogous way. Let us fix the gauge eigenstates basis:

$$\psi^\pm = \left(\widetilde{W}^+, \widetilde{H}_u^+, \widetilde{W}^-, \widetilde{H}_d^- \right) \quad (4.12)$$

in terms of which it is possible to write the chargino mass terms present in the MSSM lagrangian:

$$\mathcal{L} \supset -\frac{1}{2} (\psi^\pm)^T M_{\widetilde{C}} \psi^\pm \quad (4.13)$$

where we have introduced the chargino mass matrix $M_{\widetilde{C}}$ that can be written in a 2×2 block form, in the following way:

$$M_{\widetilde{C}} = \begin{pmatrix} 0 & X^T \\ X & 0 \end{pmatrix} \quad X = \begin{pmatrix} M_2 & \sqrt{2}s_\beta m_W \\ \sqrt{2}c_\beta m_W & \mu \end{pmatrix} \quad (4.14)$$

where m_W is the weak gauge boson mass. To find the corresponding mass eigenstates, we must introduce a 2×2 matrices U and V , that act on the gauge basis in the following way:

$$\begin{pmatrix} \widetilde{C}_1^+ \\ \widetilde{C}_2^+ \end{pmatrix} = V \begin{pmatrix} \widetilde{W}^+ \\ \widetilde{H}_u^+ \end{pmatrix} \quad \begin{pmatrix} \widetilde{C}_1^- \\ \widetilde{C}_2^- \end{pmatrix} = U \begin{pmatrix} \widetilde{W}^- \\ \widetilde{H}_d^- \end{pmatrix} \quad (4.15)$$

We see that there are two different mixing matrices for the positively charged states and for the negative ones. The mixing matrices satisfy:

$$U^* X V^{-1} = \begin{pmatrix} m_{\widetilde{C}_1} & 0 \\ 0 & m_{\widetilde{C}_2} \end{pmatrix} \quad (4.16)$$

and because these are 2×2 matrices, it is not hard to find an analytic solution:

$$\begin{aligned} m_{\widetilde{C}_1} &= \frac{1}{2} [(|M_2|^2 + |\mu|^2 + 2m_W^2) - \Delta_{\widetilde{C}}] \\ m_{\widetilde{C}_2} &= \frac{1}{2} [(|M_2|^2 + |\mu|^2 + 2m_W^2) + \Delta_{\widetilde{C}}] \end{aligned} \quad (4.17)$$

where we have introduced:

$$\Delta_{\tilde{C}} = \left[(|M_2|^2 + |\mu|^2 + 2m_W^2)^2 - 4|\mu M_2 - m_W^2 \sin 2\beta|^2 \right]^{1/2} \quad (4.18)$$

It is interesting to note that the chargino mass eigenvalues of equation (4.17) are the doubly degenerate eigenvalues of the 4×4 matrix $M_{\tilde{C}}^\dagger M_{\tilde{C}}$ or equivalently the eigenvalues of $X^\dagger X$, but they are not the squares of the eigenvalues of X . It is possible to show that in the same limit that we have seen in the neutralino discussion:

$$|M_1| + |\mu| \gg m_Z$$

the lightest chargino mass is, up to terms $\mathcal{O}(m_Z)$:

$$m_{\tilde{C}_1} = M_2$$

and so it is nearly degenerate in mass with the second lightest neutralino χ_2 .

4.4 Neutralino annihilations

We have derived in the section 1.4 of chapter 1 the cosmological abundance of a generic WIMP, without any particular assumption about the nature of this particle. The result, that we have obtained, is that the WIMP cosmological density is essentially determined, through the Boltzmann equation (1.37), by the thermal average of the annihilation cross section times the relative velocity of the WIMP pair, that is denoted as:

$$\langle \sigma_{ann} v \rangle$$

Moreover the calculation of the annihilation cross section is required in order to compute the expected flux of cosmic rays (in particular gamma rays) as we will see in the next chapter. There are some recent results [89] for a complete calculation of the annihilation cross section, but here we want to describe another approach, based on the expansion in helicity amplitudes, that allows us to obtain a more physical insight.

It is generally possible to expand the annihilation cross section into the non relativistic limit, because the relative velocity of the neutralino pair, being a CDM candidate (see chapter 1), is $v/c \sim 10^{-3}$ in the galactic halo. So, to the order $\mathcal{O}(v^2)$ we have:

$$\sigma_{ann} v = a + b v^2 \quad (4.19)$$

where the constants a and b are to be computed in the helicity amplitude formalism.

The annihilation process can be formally described as¹:

$$\chi\chi \rightarrow XY \quad (4.20)$$

There are various final states XY into which the neutralino can annihilate. The most important are those states that appear at tree level. Specifically, they are fermion-antifermion pairs ($f\bar{f}$ where f is a SM neutrino, lepton or quark) or state that involves gauge bosons and/or Higgs bosons, such as W^+W^- , Z^0Z^0 , W^+H^- , W^-H^+ , Z^0A^0 , Z^0H^0 , H^+H^- , and all six combinations of the Higgs bosons A^0 , h^0 and H^0 . We have performed a detailed numerical simulation, over the entire MSSM parameter space, of the branching ratio of different annihilation channels, defined as usual:

$$(BR)_i = \frac{A_i}{\sum_i A_i} \quad (4.21)$$

where A_i is the annihilation probability in the channel i . The result is that approximately 44% of the models annihilate in a quark-antiquark channel (we will see below which states are favored) and 36% of the models annihilate in a gauge boson final state.

In the expansion of the cross section in powers of v we have used the partial wave formalism, with the a and b associated to different partial waves contributions: a is the s-wave contribution at zero relative velocity, while b contains contribution coming from both the s and p-wave. In this formalism the helicity amplitude for the process (4.20), with h , \bar{h} , λ_X and λ_Y as the helicities of the corresponding particles, is written as:

$$T = \sum_{L=0}^{\infty} \sum_{S=0}^1 \sum_{J=|L-S|}^{L+S} A^{(2S+1)L_J} P^{(2S+1)L_J} d_{\lambda_i, \lambda_j}^J \quad (4.22)$$

where the reduced partial wave amplitude A describes annihilation from an initial state with definite spin S and orbital angular momentum L , and thus also with definite C and P quantum numbers. The spin projector P depend only on h and \bar{h} (the helicities of the $\chi\chi$ pair) while the angular dependence is contained in the functions $d_{\lambda_i, \lambda_j}^J$ where:

$$\begin{aligned} \lambda_i &= h - \bar{h} \\ \lambda_f &= \lambda_X - \lambda_Y \end{aligned} \quad (4.23)$$

are the differences of the helicities of the initial and final particles, respectively. Because our initial state involves two neutralinos, that are identical

¹from now on we will neglect the tilde over χ

Majorana fermions, we only need to consider initial states with $C = 1$. Moreover, since we want to expand the total annihilation only up to $\mathcal{O}(v^2)$, we find again that only annihilations from s and p-wave have to be included. At the end, we thus find that we need to include only the contributions from 1S_0 , 3P_0 , 3P_1 and 3P_2 initial states. Explicit expressions for the relevant spin projector can be found in [86].

In the following discussion we will derive the non relativistic limit $v \rightarrow 0$ for the annihilation cross section. In this limit only the a term of the expansion (4.19) is important. Thus we have to compute this term for the dominant annihilation channels.

Let us consider weak gauge bosons in the final state. The weak gauge boson annihilation channels are opened if they are kinematically allowed:

$$m_\chi > m_W$$

There is no s-wave suppression mechanism for these annihilations, and thus they can become very important for a neutralino heavy enough to make the final state available. These channels are usually important when $Z_g \lesssim 0.1$ and so when the neutralino is primarily an higgsino.

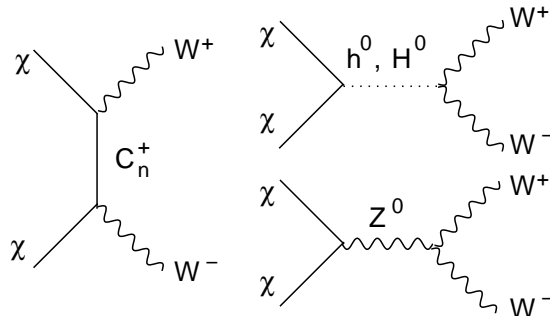


Figure 4.2: Diagrams that contribute to the amplitude of the neutralino annihilation into W^+W^- gauge bosons

The Feynman diagrams that contribute to the annihilation into W^+W^- gauge bosons are shown in the figure 4.2. The limit $v \rightarrow 0$ for the annihilation amplitude to a pair of W bosons is completely determined by a chargino exchange in the t and u-channel and is given by:

$$\mathcal{A}(\chi\chi \rightarrow W^+W^-)_{v \rightarrow 0} = 2\sqrt{2}\beta_W g^2 \sum_{n=1}^2 \left[(O_{0n}^L)^2 + (O_{0n}^R)^2 \right] \frac{1}{P_n} \quad (4.24)$$

where the kinematic factor β_W is given by:

$$\beta_W = \sqrt{1 - \frac{m_W^2}{m_\chi^2}} \quad (4.25)$$

and:

$$P_n = 1 + \left(\frac{m_{C_n^\pm}}{m_\chi}\right)^2 - \left(\frac{m_W}{m_\chi}\right)^2 \quad (4.26)$$

and the sum is extended over the two chargino states which can couple to the neutralino and the W boson. The functions O_{0n}^L and O_{0n}^R [31][85] can be expressed as:

$$\begin{aligned} O_{nm}^L &= -\frac{1}{\sqrt{2}}N_{4n}V_{2m}^* + N_{2n}V_{1m}^* \\ O_{nm}^R &= \frac{1}{\sqrt{2}}N_{3n}^*U_{2m}^* + N_{2n}^*U_{1m}^* \end{aligned} \quad (4.27)$$

where N is the neutralino diagonalizing matrix defined in the equation (4.4) and U and V are the chargino diagonalizing matrices defined in the equation (4.15). The indices are consistent with the basis, ψ^0 and ψ^\pm , definition.

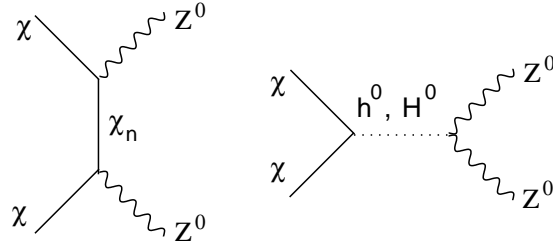


Figure 4.3: Diagrams that contribute to the amplitude of the neutralino annihilation into $Z^0 Z^0$ gauge bosons

The Feynman diagrams that contribute to the neutralino annihilation into $Z^0 Z^0$ gauge bosons are shown in figure 4.3. The $v \rightarrow 0$ amplitude for the neutralino annihilation into a Z boson pair is completely determined by the t and u-channel exchange of a neutralino χ_n , and is given by:

$$\mathcal{A}(\chi\chi \rightarrow Z^0 Z^0)_{v \rightarrow 0} = 4\sqrt{2}\beta_Z \frac{g^2}{\cos^2 \theta_W} \sum_{n=1}^4 \left(O_{0n}^L\right)^2 \frac{1}{P_n} \quad (4.28)$$

where now:

$$P_n = 1 + \left(\frac{m_{\chi_n}}{m_\chi}\right)^2 - \left(\frac{m_Z}{m_\chi}\right)^2 \quad (4.29)$$

and the kinematic factor is now given by:

$$\beta_Z = \sqrt{1 - \frac{m_Z^2}{m_\chi^2}} \quad (4.30)$$

The sum is now extended over the four neutralino states χ_n . In terms of the amplitude that we have computed, we can obtain the annihilation cross sections (times the relative velocity v) in the non relativistic limit as:

$$\sigma(\chi\chi \rightarrow VV)_{v \rightarrow 0} = \frac{1}{S_V} \frac{\beta_W}{128\pi m_\chi^2} |\mathcal{A}(\chi\chi \rightarrow VV)|^2 \quad (4.31)$$

where $V = W^\pm, Z^0$ and the coefficient S_V is a symmetry factor $S_W = 14$ and $S_Z = 2$, that take into account the fact that the Z boson final state contains two identical particles.

The annihilation channel of the neutralino into a fermion-antifermion pair is usually dominant because, given a neutralino mass $m_\chi \gtrsim 50$ GeV, this is an always open channel. However for the interesting range of neutralino masses, in particular from the cosmological point of view, *i.e.* $m_\chi \simeq 100$ GeV, the fermionic final states are not the only open channels. In this case the contribution of the gauge boson final states, that is no more closed or suppressed, becomes important.

When we study the non relativistic limit, we must consider that there are some helicity constraints for the fermionic final state [87]. In fact we know that the neutralino is a Majorana particle and so it coincides with its own antiparticle. This implies that two neutralinos that are in a relative s-wave, must have their spins oppositely directed, as a consequence of the Fermi-Dirac statistics. So also the final state, constituted by the fermion-antifermion pair, must have a total spin equal to zero, and so with opposite directed spins. The amplitude must have a factor of the fermion mass m_f in order to take into account the helicity flip. This result can be seen also by an other point of view: the initial state has $CP = -1$ and so the final state must have also $CP = -1$, because we are considering CP conserving interactions. The net resulting suppression factor for the s-wave amplitude is of order:

$$\frac{m_f^2}{m_\chi^2}$$

This suppression factor is important for the light fermionic final states. But, of course, there is no suppression factor for the t quark final state, unless the neutralino is much heavier than the t quark. For b and c quarks final states, the suppression factor is of the order of 10^{-4} for a neutralino with mass $m_\chi \simeq 100$ GeV.

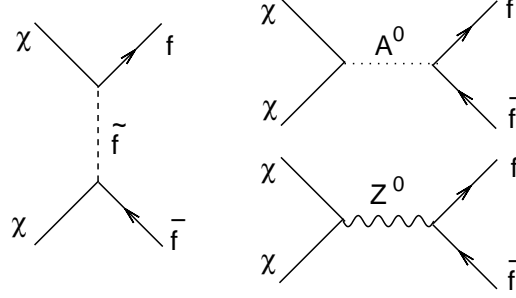


Figure 4.4: Diagrams that contribute to the amplitude of the neutralino annihilation into a $\bar{f}f$ pair

The Feynman diagrams for the neutralino annihilation into a $\bar{f}f$ pair are shown in figure 4.4. Let us compute the annihilation cross section for the fermion-antifermion production in the non relativistic limit. The s-wave amplitude has contributions coming from u and t-channel exchange of a sfermion state \tilde{f} , from an s-channel Z^0 boson and from an s-channel A^0 Higgs boson [77][88][85]. The amplitude can be written as:

$$\mathcal{A}(\chi\chi \rightarrow \bar{f}_i f_i)_{v \rightarrow 0} = \mathcal{A}_{\tilde{f}} + \mathcal{A}_{Z^0} + \mathcal{A}_{A^0} \quad (4.32)$$

Let us evaluate the different contributions. The sfermion \tilde{f} exchange is given by:

$$\mathcal{A}_{\tilde{f}} = \sqrt{2} \sum_{j=1}^6 \frac{1}{P_j} \left\{ \left[(X'_{f \ i j 0})^2 + (W'_{f \ i j 0})^2 \right] \frac{m_{f_i}}{m_\chi} + 2X'_{f \ i j 0} W'_{f \ i j 0} \right\} \quad (4.33)$$

where the sum is extended over the six sfermion states and the i and j are family indices. The functions $X'_{f \ i j n}$ and $W'_{f \ i j n}$ are the couplings that appear in the lagrangian terms that describe the interaction vertices of sfermions (included the sleptons $\tilde{\nu}_i$), fermions and neutralinos:

$$\begin{aligned} \mathcal{L}_{f\tilde{f}\chi} = & \sum_{f=u,d,e} \bar{f}_i (P_R X'_{f \ i j n} + P_L W'_{f \ i j n}) \chi_n^0 \tilde{f}_j \\ & + \bar{\nu}_i P_R X'_{\nu \ i j n} \chi_n^0 \tilde{\nu}_j + h.c. \end{aligned} \quad (4.34)$$

where P_L and P_R are the usual chiral projection operators:

$$\begin{aligned} P_L &= \frac{1}{2}(1 - \gamma_5) \\ P_R &= \frac{1}{2}(1 + \gamma_5) \end{aligned}$$

The couplings can be expressed as:

$$\begin{aligned} X'_{f\ ijn} &= X_{fn} (\Pi_L \Theta_f)_{ij} + Z_{fikn} (\Pi_R \Theta_f)_{kj} \\ W'_{f\ ijn} &= Y_{fn} (\Pi_R \Theta_f)_{ij} + Z_{fikn} (\Pi_L \Theta_f)_{kj} \end{aligned} \quad (4.35)$$

where we have introduced the sfermion mixing matrix Θ_f . These matrices can be defined in the diagonalization procedure for the sfermion mass matrix:

$$\left(M_{\tilde{f}}^{diag} \right)^2 = \Theta_f^\dagger M_{\tilde{f}}^2 \Theta_f \quad (4.36)$$

where we have introduced the sfermion projection operators Π_L and Π_R , which have the effect of projecting mass eigenstate sfermion fields onto subspaces corresponding to a particular handedness:

$$\begin{aligned} \tilde{u}_{Li} &= (\Pi_L)_{ik} \Theta_{kj}^u \tilde{u}_j \\ \tilde{u}_{Ri} &= (\Pi_R)_{ik} \Theta_{kj}^u \tilde{u}_j \end{aligned} \quad (4.37)$$

Analogous relations hold for the down type squarks and the charged sleptons. The other functions that appear in the definition of the couplings (4.35) are given by:

$$\begin{aligned} X_{fn} &= -g\sqrt{2} [T_{3f} N_{2n}^* - \tan \theta_W (T_{3f} - e_f) N_{1n}^*] \\ Y_{fn} &= g\sqrt{2} \tan \theta_W e_f N_{1n}^* \\ Z_{uijn} &= -\frac{g}{\sqrt{2} m_W \sin \beta} (M_{\tilde{u}})_{ij} N_{4n}^* \\ Z_{dijn} &= -\frac{g}{\sqrt{2} m_W \cos \beta} (M_{\tilde{d}})_{ij} N_{3n}^* \\ Z_{eijn} &= -\frac{g}{\sqrt{2} m_W \cos \beta} (M_{\tilde{e}})_{ij} N_{3n}^* \end{aligned} \quad (4.38)$$

where the neutralino mixing matrix N_{ij} is referred to the basis $\psi^0 = (\tilde{B}, \tilde{W}^0, \tilde{H}_d^0, \tilde{H}_u^0)$, and where T_{3f} is the T_3 quantum number of the fermion f and e_f is the charge of f in units of e [37].

The Z^0 exchange contribution to the total amplitude is given by:

$$\mathcal{A}_{Z^0} = 2\sqrt{2} \frac{g^2}{\cos^2 \theta_W} O_{00}''{}^L T_{3fi} \frac{m_{f_i} m_\chi}{m_Z^2} \quad (4.39)$$

where the coupling $O_{00}''{}^L$ is derived by the general formula:

$$O_{nm}''{}^L = -O_{nm}''{}^{R*} = \frac{1}{2} (-N_{3n} N_{3m}^* + N_{4n} N_{4m}^*) \quad (4.40)$$

We can immediately see that the Z-boson exchange amplitude (4.39) is proportional to the mass m_{f_i} of the final fermion state. Adding the amplitude \mathcal{A}^0 that is proportional to the mass m_{f_i} through the corresponding Yukawa coupling [31], we are able to obtain the total annihilation cross section in a fermion-antifermion pair in the non relativistic limit:

$$\sigma(\chi\chi \rightarrow \bar{f}f)_{v \rightarrow 0} = \frac{c_f \beta_f}{128\pi m_\chi^2} |\mathcal{A}(\chi\chi \rightarrow \bar{f}f)|^2 \quad (4.41)$$

where c_f is a color factor ($c_f = 3$ when the fermion in the final state is a quark), and the kinetic factor β_f is equal to:

$$\beta_f = \sqrt{1 - \frac{m_f^2}{m_\chi^2}}$$

In the limit $v \rightarrow 0$, the annihilation cross section in a fermion-antifermion pair is proportional to the mass m_f . Thus, the annihilation into lighter quarks and leptons is negligible respect to the annihilation into the heavy quarks c, b and t and into the heavier lepton τ . Moreover, when the neutralino mass is $m_\chi > m_t$ then the dominant annihilation channel is $\bar{t}t$.

Chapter 5

Indirect neutralino detection with cosmic γ -rays

5.1 Introduction

We have identified the neutralino as one of the best motivated WIMP cold dark matter candidate. We have seen that in the neutralino annihilation processes, ordinary SM particles are produced. Thus the study of neutralino properties is possible through indirect detection of these particles. In fact, if a dark halo, such as the Milky Way halo, is made of WIMPs, there is a small but finite probability for dark matter particles to annihilate in pairs into lighter SM particles (the annihilation strength is the quantity which fixes the WIMP relic abundance), giving rise to cosmic rays, as, for example, exotic γ -rays and antimatter fluxes. In particular, the distortion of the spectrum of the diffuse γ -ray flux in the Galaxy due to a WIMP induced component, extending up to an energy equal to the WIMP mass, is a possible signature to identify dark matter. In the following analysis we will focus on such a signal.

We might ask how it is possible to have a γ -ray flux coming from neutralino annihilations. We have seen in the previous chapter the possible tree level final state for neutralino annihilations. There are no final states that contains γ 's. This can be regarded as a consequence of the dark matter definition, *i.e.* matter that does not emit light. But, once SM particles are produced from annihilations, they can decay and/or interact to produce, at the end, a measurable γ -ray flux.

Our starting point will be the already available experimental data coming from EGRET γ -ray detector. We will concentrate ourselves on the data coming from our Galactic Center. In order to study the expected γ -rays flux and

to try a fit of the experimental data, we will build a simplified phenomenological toy model that describes the WIMP annihilations. This allows us to obtain some general results without worrying about the details of a more complex underlying theory. Then we will argue how the upcoming experiments, as the GLAST detector, will be able to constrain the parameter space of our WIMP theoretical models. In particular we specialize to mSUGRA models (introduced in section 3.6). Then we will see how this kind of analysis can tell us something about the detection possibilities of the upcoming GLAST experiment.

5.2 The EGRET data

The EGRET telescope on board of the Compton Gamma-Ray Observatory has mapped the γ -ray sky up to an energy of about 20 GeV. Moreover, EGRET has observed the Galactic center (GC) region, over a total period of 5 years. The collected data show high statistical evidence for a gamma-ray source, diffuse rather than point-like, located within 1.5° of the GC ($l = b = 0^\circ$) [90]. The detected flux largely exceeds the diffuse γ -ray component expected in the GC direction with a standard modeling of the interaction of primary cosmic rays with the interstellar medium (see, e.g., [91]); the latter fails also to reproduce the spectral shape of the GC source. Assuming the GC excess is indeed due to some form of diffuse gamma-ray emission, one might regard this issue as a particular aspect of a general problem concerning the diffuse Galactic γ -ray emission as measured by EGRET [95].

The generic feature emerging at all latitudes is that the measured diffuse flux shows a spectrum which is much harder than expected. As can be seen in figure 5.1, taken from [91], below 1 GeV the spectrum observed by EGRET can be modeled with fair accuracy as due to primary cosmic-ray protons and electrons propagating in the Galaxy, with spectra and normalizations as measured locally. On the other hand, under the same assumptions, one severely underestimates the flux above 1 GeV: the standard emission model predicts the flux in this energy range to be dominated by photons from the decay of π^0 's, but this component is sensibly softer than the measured flux, if the proton cosmic ray flux in the Galaxy is assumed to have the same spectral index as measured locally. Several solutions to this problem have been proposed: one option is, for example, to assume that the local cosmic ray electron spectrum is not representative for the entire Galaxy and it is on average harder than that measured locally. Another possibility is that there is some variability in the spectral indices of standard cosmic ray sources (for a discussion see, e.g., [96]).

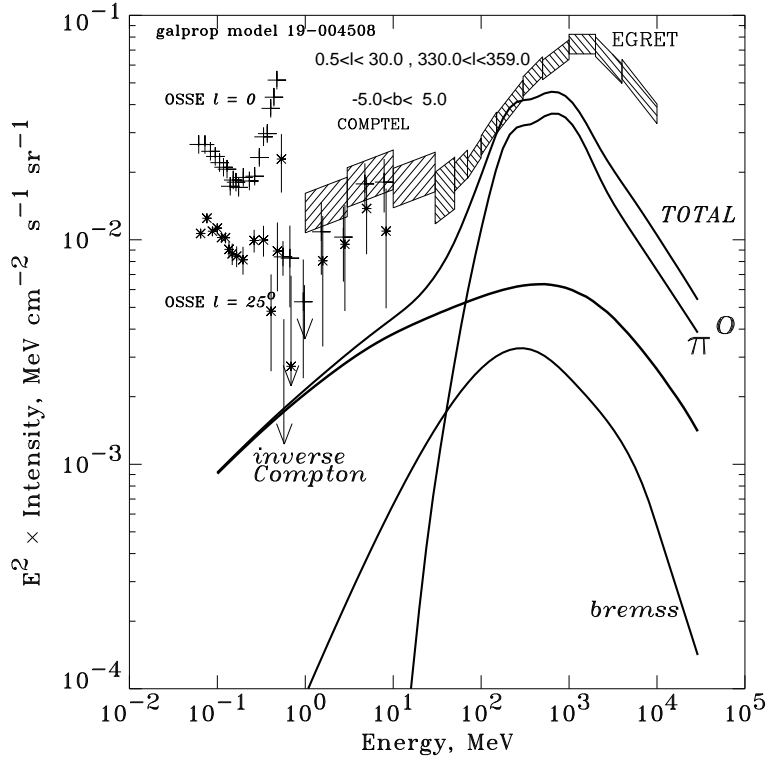


Figure 5.1: γ -ray energy spectrum of the inner galaxy ($300^\circ \geq l \leq 30^\circ$) compared with what is expected for standard propagation models [95].

The other interesting solution, is that the excess can be explained by the diffuse γ -ray flux expected from a WIMP induced component [92]. In fact, we will see that this component has just the right spectral feature to generate the kind of distortion in the diffuse γ -ray flux.

In Table 5.1 we report the flux per energy bin for the GC γ -ray source as measured by EGRET, together with the expected flux from cosmic ray interactions in a standard scenario [90].

5.3 The diffuse γ -ray background

To start with our analysis we must give a model that describes the production of γ -rays in the Galaxy. This is called the background diffuse component. There are three mechanisms which give rise to this diffuse γ -ray

Energy Bin (GeV)	Expected Diffuse γ -Ray Flux ($\text{cm}^{-2}\text{s}^{-1}\text{GeV}^{-1}\text{sr}^{-1}$)	Total γ -Ray Flux ($\text{cm}^{-2}\text{s}^{-1}\text{GeV}^{-1}\text{sr}^{-1}$)
0.03 – 0.05	$3.7 \cdot 10^{-3}$	$(5.0 \pm 0.8) \cdot 10^{-2}$
0.05 – 0.07	$1.8 \cdot 10^{-3}$	$(1.3 \pm 0.2) \cdot 10^{-2}$
0.07 – 0.1	$1.1 \cdot 10^{-3}$	$(6.1 \pm 0.5) \cdot 10^{-3}$
0.1 – 0.15	$6.2 \cdot 10^{-4}$	$(4.4 \pm 0.2) \cdot 10^{-3}$
0.15 – 0.3	$2.6 \cdot 10^{-4}$	$(2.03 \pm 0.06) \cdot 10^{-3}$
0.3 – 0.5	$1.0 \cdot 10^{-4}$	$(9.5 \pm 0.2) \cdot 10^{-4}$
0.5 – 1	$3.5 \cdot 10^{-5}$	$(3.9 \pm 0.1) \cdot 10^{-4}$
1 – 2	$9.1 \cdot 10^{-6}$	$(1.52 \pm 0.03) \cdot 10^{-4}$
2 – 4	$2.0 \cdot 10^{-6}$	$(3.2 \pm 0.1) \cdot 10^{-5}$
4 – 10	$2.3 \cdot 10^{-7}$	$(3.1 \pm 0.2) \cdot 10^{-6}$

Table 5.1: Estimated values for the Galactic diffuse γ -ray component component (second column) and EGRET data from a region of 1.5° around the GC (third column), extracted from [90].

radiation: production and decay of π^0 s, inverse Compton scattering and bremsstrahlung (see for example [91]). According to standard scenarios, in the energy range $E_\gamma > 1$ GeV we will mainly focus on, the dominant background source is through π^0 decays. The production of pions (and then of photons) is mainly due to primary cosmic-ray protons, with a small corrections from the primary helium component, through the interactions:

$$p + X \rightarrow \dots \rightarrow \pi^0 \rightarrow 2\gamma$$

$$He + X \rightarrow \dots \rightarrow \pi^0 \rightarrow 2\gamma,$$

where X is an interstellar atom, *i.e.* H and He .

The simulation of the induced γ -ray yield has been performed according to standard treatments implemented in the Galprop software package [91]. We assume that the p and He cosmic ray fluxes in the Galaxy have the same energy spectra and relative normalization as those measured in the local neighborhood, and that the He component in the interstellar medium is 24% in mass with respect to H . Then we write the background flux, splitting it into two factors:

$$\mathcal{S}_b(E_\gamma) = \frac{1}{(1 \text{ cm}^2\text{sr})} \cdot \mathcal{E}(E_\gamma) \quad (5.1)$$

and

$$N_b = \frac{1}{(1 \text{ cm}^{-2}\text{sr}^{-1})} \cdot \int_{l.o.s.} dl \frac{n_H(l)}{4\pi} \frac{\phi_p^{prim}(l)}{\phi_p^{prim}(l=0)}. \quad (5.2)$$

Here $\mathcal{E}(E_\gamma)$ [$\text{GeV}^{-1} \text{s}^{-1}$] is the local emissivity per hydrogen atom, i.e. the number of secondary photons with energy in the range $(E_\gamma, E_\gamma + dE_\gamma)$ emitted per unit time by one target hydrogen atom, for an incident flux of protons and helium nuclei equal to the locally measured primary proton and helium fluxes. The factor N_b is instead associated to the interstellar hydrogen column density $n_H(l)$, integrated along the line of sight and weighted over the proton primary flux at the location l , $\phi_p^{prim}(l)$, normalized to the local value $\phi_p^{prim}(l=0)$.

Above an energy of about 1 GeV the background spectrum (and therefore the function ϕ_b) recovers the same spectral index as the dominant primary component, i.e. the proton spectral index $\alpha = 2.7$. The relative normalization of the primary components in different places in the Galaxy can be estimated once a radial distribution of primary sources is chosen (following, for instance, the radial distribution of supernova) and then by propagating the injected fluxes with an appropriate transport equation (this is what is done in the Galprop code [91]). On the other hand, the hydrogen column density toward the Galactic center is very uncertain; we chose therefore to define the spectral shape of the background through the function \mathcal{S}_b and to keep N_b as a free normalization parameter.

5.4 γ -ray flux from WIMP annihilations

In order to explain the EGRET excess in the GC data, we assume that the bulk of the high energy γ -ray flux is due to WIMP annihilations. Let us introduce a generic framework in which the dark matter in the Galactic dark halo consists of non relativistic WIMPs of mass m_χ and total pair annihilation rate into lighter Standard Model particles $\sigma_{ann}v$ (in the non relativistic limit of vanishing relative velocity). The total γ -ray flux coming from the GC can be described as the superposition of two contributions:

- the background contribution due to interaction of primary cosmic rays with the interstellar medium, with spectral shape defined by the function (5.1)
- the signal contribution due to WIMP annihilations in the dark matter halo, whose energy spectrum is defined by $\mathcal{S}_\chi(E_\gamma)$

Hence we can write the flux as:

$$\phi_\gamma = \phi_b + \phi_\chi = N_b \mathcal{S}_b + N_\chi \mathcal{S}_\chi, \quad (5.3)$$

where N_b and N_χ are dimensionless normalization parameters. The N_b parameter is the normalization of the standard background contribution (5.2) while N_χ is the unknown normalization of the WIMP annihilation flux.

As we have seen in section 4.4, for a neutralino, among the kinematically allowed tree level final states, the leading channels are often:

$$b\bar{b}, c\bar{c}, t\bar{t}, \tau^+\tau^-, W^+W^-, Z^0Z^0$$

More generically this result holds for any Majorana fermion WIMP, as for such particles the s-wave annihilation rate into the light fermion species is suppressed by the factor m_f^2/m_χ^2 , where m_f is mass of the fermion in the final state.

Once the SM particles are produced, there are two processes that give rise to γ 's in the final state: the fragmentation and the decay process. The dominant intermediate step in these processes is the π^0 production. In this way we are able to compute the photon yield in the framework of the SM. The yield simulation has been performed with the Lund Monte Carlo program Pythia [118] implemented in the DarkSUSY¹ package [94].

In order to compute the γ -ray flux we must determine the dark matter distribution in the halo. Suppose that the dark matter halo is roughly spherical and consider the induced γ -ray flux in the direction that forms an angle ψ with the direction of the Galactic center. In this case the WIMP induced photon flux is the sum of the contributions along the line of sight (l.o.s):

$$\phi_\chi(E, \psi) = \frac{\sigma_{ann}v}{4\pi} \sum_f \frac{dN_f}{dE} B_f \int_{l.o.s} dl(\psi) \frac{1}{2} \frac{\rho(l)^2}{m_\chi^2} \quad (5.4)$$

where B_f is the branching ratio into the tree-level annihilation final state f , while dN_f/dE is the relative differential photon yield. The WIMP mass density along the line of sight $\rho(l)$ enters critically in the prediction for the flux, as the number of WIMP pairs scales with $\rho(l)^2$. It is then useful to factorize the flux in equation (5.4) into two pieces, one depending only by the underlying particle physics theory, *i.e.* on the cross section, the branching ratios and the WIMP mass, and the other depending on the WIMP distribution in the galactic halo. We rewrite equation (5.4) as:

$$\phi_\chi(E, \psi) = 3.74 \cdot 10^{-10} \left(\frac{\sigma_{ann}v}{10^{-26} \text{ cm}^3\text{s}^{-1}} \right) \left(\frac{50 \text{ GeV}}{m_\chi} \right)^2 \sum_f \frac{dN_f}{dE} B_f \cdot J(\psi) \quad (5.5)$$

¹see the appendix for a brief description of the fortran code

in units $\text{cm}^{-2}\text{s}^{-1}\text{GeV}^{-1}\text{sr}^{-1}$ and where we have defined the dimensionless function J , containing the dependence on the halo density profile, as

$$J(\psi) = \frac{1}{8.5 \text{ kpc}} \left(\frac{1}{0.3 \text{ GeVcm}^{-3}} \right) \int \rho^2(l) dl(\psi) \quad (5.6)$$

More precisely, given a detector with angular acceptance $\Delta\Omega$, we have to consider the average of $J(\psi)$ over the solid angle $\Delta\Omega$ around the direction ψ :

$$\langle J(\psi) \rangle_{\Delta\Omega} = \frac{1}{\Delta\Omega} \int J(\psi) d\Omega \quad (5.7)$$

To compare with the GC gamma-ray source, we will consider $\Delta\Omega \sim 10^{-3}$ sr, i.e. the same magnitude as the angular region probed by the EGRET experiment.

In an analogous way as for the background component, we have then splitted the signal into a term which fixes the spectral shape of the flux, plus a normalization factor. In the notation introduced in Equation (5.3), we have denoted $N_\chi \equiv \langle J(\psi) \rangle_{\Delta\Omega}$ and defined $\mathcal{S}_\chi \equiv \phi_\chi/N_\chi$. The WIMP density $\rho(l)$ is very poorly constrained towards the GC. Hence we will treat N_χ as a free parameter. Although there is a large span in the predictions for ϕ_χ when coming to specific WIMP models, the term \mathcal{S}_χ shows some generic trends. As most γ 's are produced in the hadronization and decay of π^0 s, the shape of the photon spectrum is always peaked, for kinematic reasons, at

$$m_{\pi^0}/2 \sim 70 \text{ MeV}$$

where m_{π^0} is the pion mass, The spectral shape is symmetric around it on a logarithmic scale. This feature is often called the “ π^0 bump”.

The same is true for the background, but still it may be possible to discriminate signal from background: the signal arises in processes which have all the same energy scale, *i.e.* $2m_\chi$, therefore the WIMP induced flux, contrary to the background, is spectral index free and shows a sharp cutoff when E_γ approaches the WIMP mass. This is shown in the right panel of Fig. 5.2, where we plot the differential photon yield per annihilation times the inverse of WIMP mass squared, for a few values of the WIMP mass, and assuming WIMPs have a single dominant decay channel ($b\bar{b}$ in the case displayed). In the same figure, for comparison, the spectral shape of the background is shown: as it can be clearly seen, one may hope to identify the WIMP induced component as a distortion of the background spectrum at relatively high energies.

For a given WIMP mass, the photon yields in the different annihilation channels are analogous, as shown in the left panel of Fig. 5.2: solid curves

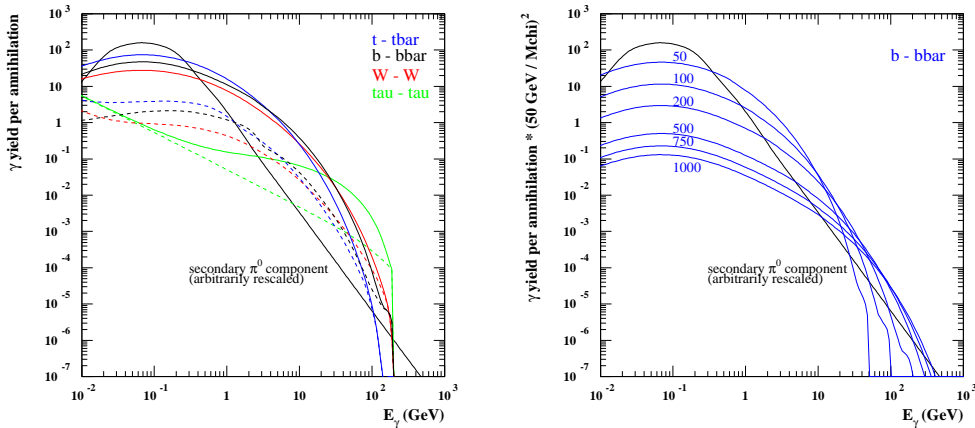


Figure 5.2: In the left panel: differential yield per annihilation for a few sample annihilation channels and a fixed WIMP mass (200 GeV). The solid lines are the total yields, while the dashed lines are components not due to π^0 decays. For comparison the emissivity, with normalization arbitrarily rescaled, from the interaction of primaries with the interstellar medium is shown. In the right panel: differential yields per annihilations for a fixed annihilation channel ($b\bar{b}$) and for a few sample values of WIMP mass, rescaled with the inverse of the WIMP mass squared.

indicate the total photon yield, while dashed curves indicate the photon yield in radiative processes, i.e. in all processes rather than π^0 decays. The spectrum for the $t\bar{t}$ and W^+W^- channels are very close to one for $b\bar{b}$ (differences are mainly given by prompt decays before hadronization); only in the $\tau^+\tau^-$ case, that we will not taken into account in this analysis, radiative photon emission is dominant, still with a large bump due to the hadronic decay modes of τ leptons.

5.5 Fit of EGRET data

We have seen that data in the EGRET measurement extend up to 10 GeV only, with few bins in the high energy region. Then, it is not likely that one can pin down many details on an eventual WIMP induced component. In particular, it is not possible to discriminate among the WIMP model by separating the photon components from single tree-level annihilation channels. It is convenient to keep the discussion as general as possible and consider a

simplified scenario (which we refer, from now on, to as a *toy model* [93]), in which only one intermediate annihilation channel is open ($B_f = 1$ in that channel), and we set the value of the total annihilation cross section according to the following general argument.

To start with, let us suppose that WIMPs in the halo are thermal relic particles: in the simplest scenario (i.e. when no resonances or thresholds appear near the kinematically released energy in the annihilation 2), we can fix the WIMP total annihilation rate through the approximate relation (see discussion in section 1.4 of chapter 1):

$$\sigma_{ann}v \sim \langle \sigma_{ann}v \rangle \sim \frac{3 \cdot 10^{-27} \text{cm}^3 \text{s}^{-1}}{\Omega_\chi h^2} \sim 3 \cdot 10^{-26} \text{cm}^3 \text{s}^{-1} , \quad (5.8)$$

where $\langle \sigma v \rangle$ is the thermally averaged annihilation cross section and Ω_χ the WIMP thermal relic abundance. We keep as the only free parameter the WIMP mass, as we have shown that the photon spectrum is rather sensitive to it.

The results shown below just depend on a mass scale and on a normalization parameter; they can be easily rescaled for any explicit model for which m_χ and $\sigma_{ann}v$ are defined. Note, in particular, that the scaling we have implemented between annihilation rate today, $\langle \sigma v \rangle$ and Ω_χ is only a rough approximation and that large deviations from it can appear, mainly due to resonances and thresholds, or, sometimes, coannihilation effects.

In section 5.7 below we will consider an explicit WIMP model, in the framework of mSUGRA models, and we will not use this approximate relation, but instead calculate the relic density including properly both coannihilations, resonances and thresholds.

For each WIMP mass m_χ and for each intermediate channel, we try to reproduce the EGRET data (third column of Table 5.1), with a flux of the form in equation (5.3) and varying the parameters N_b and N_χ . As in the fit we do not want to include cases in which the flux is underestimated, we implement the additional constraint on the normalization constants:

$$(N_b \mathcal{S}_b + N_\chi \mathcal{S}_\chi)_i \geq (\phi_{EGRET})_i , \quad (5.9)$$

where the index i runs over the energy bins for which we have experimental data; ϕ_{EGRET} is the diffuse γ -ray flux measured by EGRET in each bin, *i.e.* the third column in table 5.1 We do not use the first two energy bins in table 5.1, because they are in a region ($E \ll 1$ GeV) in which the background should be dominated by the inverse Compton and bremsstrahlung components instead of π^0 production as we are assuming.

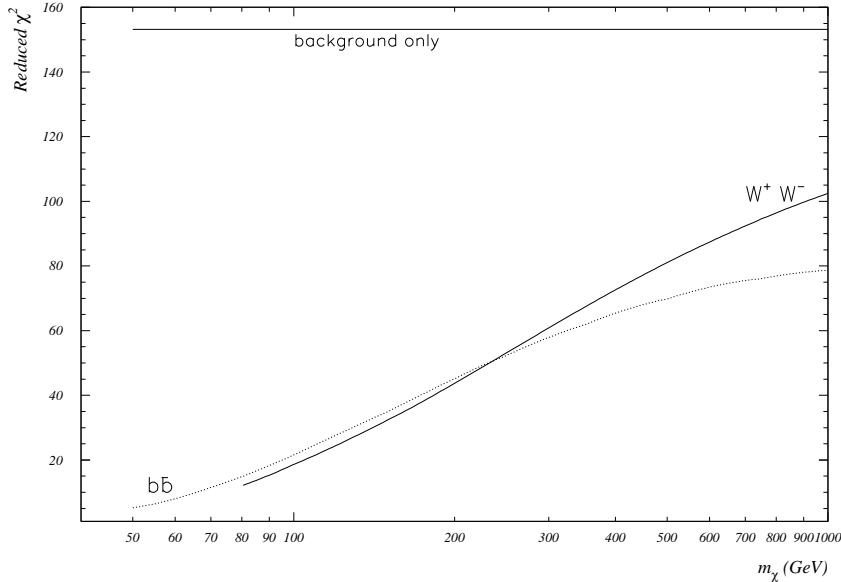


Figure 5.3: Reduced χ^2 for EGRET data fit vs m_χ for the two annihilation channels $b\bar{b}$ and W^+W^-

We find as allowed range of variation for the background normalization, N_b between $3.2 \cdot 10^{20}$ to $1.8 \cdot 10^{21}$, corresponding, respectively, to the case when the background is at the level estimated in a standard scenario (column 2 in Table 5.1) and to the best fit case with $N_\chi = 0$. In figure 5.3 we have plotted the value of the reduced χ^2 of such fits in two cases: one in which there is only the background contribution ($N_\chi = 0$), and the other in which we allow a WIMP contribution to the flux ($N_\chi > 0$). The number of degrees of freedom, for the reduced χ^2 , is 6, *i.e.* the number of EGRET experimental points above 100 MeV (which is 8) minus the number of free parameters, N_b and N_χ . Even in the case of small WIMP masses, which seems to be the favored ones, we have obtained that the reduced χ^2 values are of the order of 5.

In figure 5.4 we show two fits of the EGRET data, obtained for the intermediate channels $b\bar{b}$ and W^+W^- , for values of the WIMP mass close to the respective production thresholds. This two plots are shown just to give a qualitative idea of the 'goodness' of the fits of EGRET data, in relation to the reduced χ^2 value. As it can be seen from the figure, the fit to the data greatly improves when a neutralino component is added.

Next we have studied the reduced χ^2 in fitting EGRET data with our

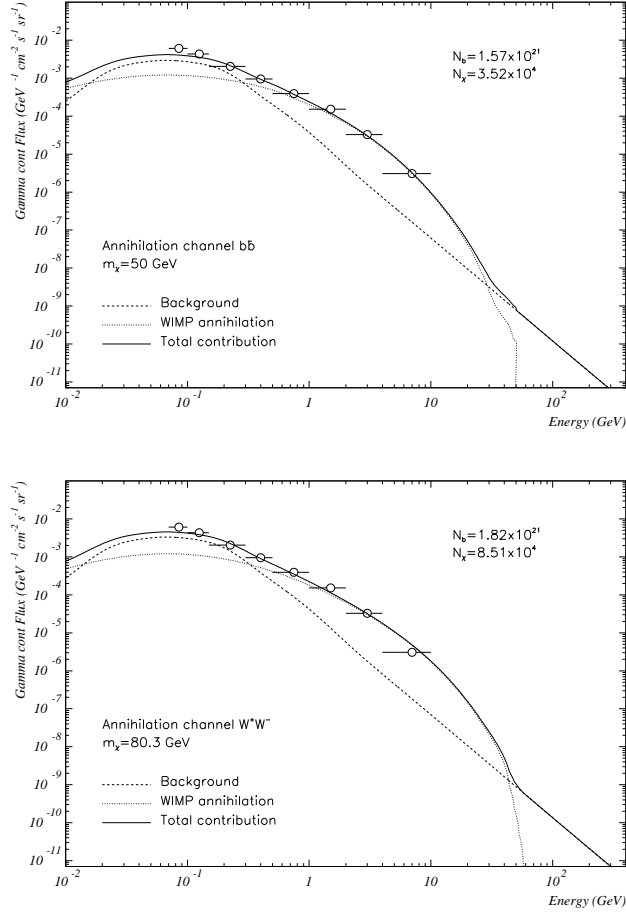


Figure 5.4: Fits of EGRET data for two different models with $\chi_r^2 \sim 5$, with the corresponding values for N_b and N_χ .

signal plus background theoretical curve, in function of the parameters m_χ and N_χ , for the intermediate annihilation channel bb . Figure 5.5 contains lines of constant values of such reduced χ^2 in the (N_χ, m_χ) plane. We find again the same result that we have inferred from figure 5.3, namely that the EGRET data are best fitted for low neutralino masses.

5.6 WIMP signal detection with GLAST

The Gamma-ray Large Area Space Telescope (GLAST) (see [107] for an exhaustive description of the experiment and of the scientific organizations

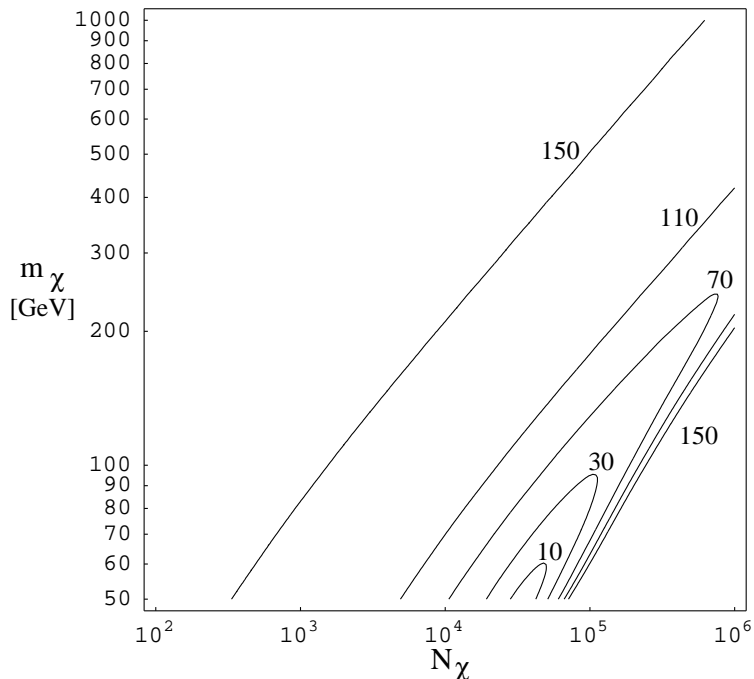


Figure 5.5: Lines of constant reduced χ^2 for the fit of Galactic center EGRET data with $\phi_\gamma = N_b\phi_b + N_\chi\phi_\chi$, in the (N_χ, m_χ) plane.

involved) is a new generation satellite with greatly improved features with respect to EGRET. Besides studying dark matter, the main scientific objectives are the study of all γ -ray sources such as blazars, γ -ray bursts, supernova remnants, pulsars, diffuse radiation, and unidentified high-energy sources. It is worth noting that the experimental techniques for the detection of γ -rays in the energy range in which there is pair production are very different from the techniques used for X-ray detection. In fact, in the detection of X-rays it is possible to optically focus the incoming beam: this allows for a large effective area, excellent energy resolution, very low background. For γ -rays no such focusing is possible and this means limited effective area, moderate energy resolution and an high background. With respect to EGRET, GLAST allows for a better space resolution. This could be revealed as a very important feature in order to study WIMP annihilations.

In the following analysis we will use in a crucial way GLAST technical features. The most important features, from the point of view of WIMP detection, shown in figure 5.6, are:

- an energy range between 20 MeV and 300 GeV

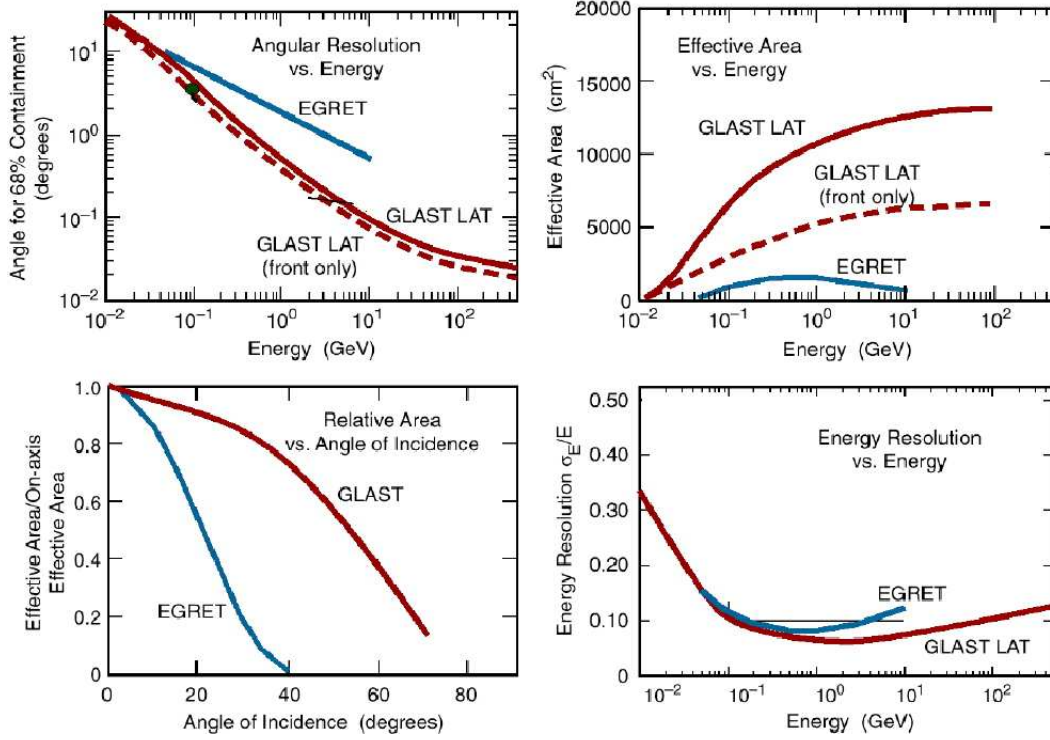


Figure 5.6: *Expected GLAST performances*

- a field of view of ~ 3 sr
- an energy resolution of $\sim 5\%$ at 1 GeV
- a point source sensitivity of 2×10^{-9} (ph cm⁻² s⁻¹) at 0.1 GeV
- an event deadtime of 20 μ s
- a peak effective area of 10⁴ cm²

A more detailed description of the apparatus can be found in [108] and of its main physics items in [109].

In the context of a simplified toy model, in section 5.5 we have explored the possibility of fitting the EGRET data from the GC with a neutralino induced continuum γ -ray component. This exercise was performed for a given intermediate WIMP annihilation channel. The satisfactory outcome of this trial urges a more detailed analysis. We thus examine the possibility to detect the continuum γ signal from $\chi\chi$ annihilations in the GC, with the upcoming experiment GLAST. For each intermediate channel and WIMP mass, we look for the minimum ratio between the two normalization factors

Profile	$\langle J(0) \rangle_{\Delta\Omega} \Delta\Omega = 10^{-5} \text{ sr}$
Modified isothermal	$3.03 \cdot 10^1$
Navarro, Frenk, White	$1.26 \cdot 10^4$
Moore <i>et al.</i>	$9.46 \cdot 10^7$

Table 5.2: Halo profiles.

N_χ/N_b , that is needed in order to detect with GLAST the WIMP annihilation signal among the background one. As we have seen in section 5.5, the factor N_χ is exactly $J(\psi)$, while N_b is related to the density of the interstellar medium. The best fits in section 5.5 give a typical value of N_b of the order of $10^{20} \div 10^{21}$. Given also a typical halo profile (see table 5.2) we expect N_χ/N_b to be of the order of

$$\frac{N_\chi}{N_b} \sim \frac{10 \div 10^7}{10^{20} \div 10^{21}} \Rightarrow 10^{-20} < \frac{N_\chi}{N_b} < 10^{-13} \quad (5.10)$$

In figure 5.8 we plot, for one intermediate channel (the other channels look very similar) and for each WIMP mass, the minimum ratio of N_χ/N_b to be able to discriminate the WIMP signal with GLAST at a 3σ confidence level. For such an analysis, we have considered a region around the GC of an angular extension of the order of the GLAST angular resolution at 10 GeV , that, as can be seen from figure 5.6, is $\sim 10^{-5} \text{ sr}$. We have made this choice in order to exploit the GLAST capability to sharply focus on the GC, that is very advantageous to consider in an indirect dark matter search, since around it the dark matter density could very likely be strongly enhanced. We will return on this point below.

The discrimination criterion we have used is based on the usual χ^2 test statistic. Our choice can be easily understood referring to figure 5.7, that shows an example of a supersymmetric continuum γ ray flux, together with the background only component and the sum of the two. The points represent the expected flux measurements of the GLAST detector, with the associated statistical error for the chosen energy binning. We have computed the reduced χ^2 between the number of counts expected in each energy bin for the two hypothesis: supersymmetric signal plus background and background only. Taking into account the number of degrees of freedom, which in our case is equal to the number of energy bins, the signal plus background curve is distinguishable from the background only curve, for a reduced $\chi^2 > cost..$ This constant is uniquely determined by the number of degrees of freedom and by the confidence level we want to reach. We have also checked our results against those obtained with the likelihood ratio method [110, 111],

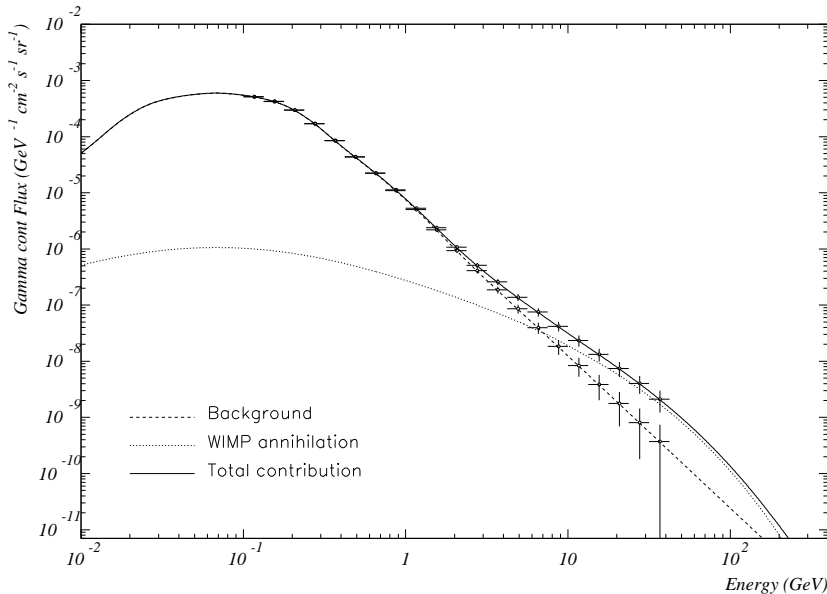


Figure 5.7: The figure shows an example of a supersymmetric continuum γ ray flux, together with the background only component and the sum of the two. The points represents the expected GLAST flux measurements with the associated statistical error for the chosen energy binning.

obtaining no discrepancies². This latter method is especially suited for the case we have at hand: deciding if a certain event belongs to the background only hypothesis (H_0) or to signal plus background hypothesis (H_1), one starts by constructing two probability distributions, P_0 and P_1 , for an estimator $F = \mathcal{L}(H_1)/\mathcal{L}(H_0)$, which is the ratio between the likelihoods \mathcal{L} of the two hypotheses. In our case, since we are interested in counting, we can choose the Poisson distribution to obtain the likelihood. Comparing the two distributions one can decide, at a certain confidence level, if they will result distinguishable or not, once it is fixed the accuracy of the experimental data that will be used for the discrimination. The likelihood ratio method is in general more powerful than the χ^2 one, since, in addition to giving the probability of a certain set of data to belong to the signal plus background probability distribution, it allows to compute the probability to be wrong when accepting such hypothesis, the so called *power of the test*, considering the background only hypothesis as the *true* one.

²I thank G.Ganis for the computer code that allows to perform this analysis.

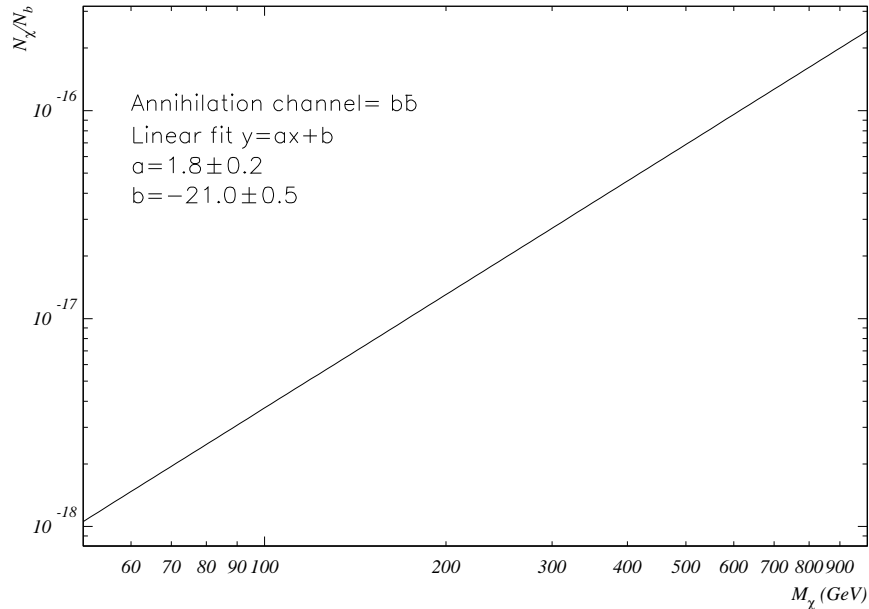


Figure 5.8: Fit of the normalization ratio vs m_χ for the $b\bar{b}$ intermediate channel: $y = \log_{10} \left(\frac{N_\chi}{N_b} \right)$, $x = \log_{10} M_\chi$

From figure 5.8 we can see that, given an annihilation channel, the minimum value of N_χ/N_b to distinguish the WIMP signal raise as a quadratic power law with the WIMP mass m_χ . Such a behavior could be expected because in equation (5.5) for the flux ϕ_χ , there is a suppression factor m_χ^{-2} (it is useful to see also figure 5.8). Let us further observe, again from figure 5.8, that the minimum values of N_χ/N_b needed to discriminate a signal with GLAST, ranges inside the interval of equation (5.10) that has been computed from the values of $N_\chi = \langle J(0) \rangle$ of table 5.2 and from the typical values of N_b needed to best fit the GC EGRET data.

5.7 mSUGRA Neutralino detection with GLAST

All the results that we have obtained in previous sections hold for a generic WIMP in the framework of our toy model. At the end we want to identify this WIMP with a neutralino. We know that in the MSSM there is a huge number of independent parameters, so to perform phenomenological analysis we must reduce this number. Let us consider the mSUGRA theories (de-

Ann. Channel	$(\sigma v)_{min}$ [$cm^3 s^{-1}$]	$(\sigma v)_{max}$ [$cm^3 s^{-1}$]
$b\bar{b}$	10^{-36}	10^{-20}
$c\bar{c}$	10^{-40}	10^{-26}
$t\bar{t}$	10^{-33}	10^{-25}
W^+W^-	10^{-35}	10^{-28}
Z^0Z^0	10^{-35}	10^{-29}

Table 5.3: mSUGRA cross sections for the relevant annihilation channels.

scribed in section 3.6) as the underlying high energy theory. The theory is then completely defined in terms of five input parameters, that we rewrite here for convenience:

$$m_0, m_{1/2}, A_0, \tan\beta, \text{sgn}(\mu)$$

These parameters are defined at the GUT scale. In this way the MSSM can be regarded as an effective low energy theory and so the weak scale parameters can be obtained, from the high energy theory, solving the appropriate RG equations described in section 3.5 and 3.6. The numerical procedure that we have followed is described in section 3.7. Moreover we have performed a phenomenological study of the neutralino, obtaining the neutralino isomass curve of figure 4.1 in section 4.2.

Let us concentrate on the annihilation cross sections of a neutralino pair. In our toy model we have assumed that the neutralino annihilation cross section was essentially fixed, for a given annihilation channel, by the inverse of the relic density. Now, in the context of mSUGRA models, we can relax this assumption. We have computed in table 5.7, the range of variation, among the entire mSUGRA parameter space, of the cross sections of the 5 processes:

$$\chi\chi \rightarrow \{b\bar{b}, c\bar{c}, t\bar{t}, W^+W^-, Z^0Z^0\}.$$

Calling σ_{tot} the total annihilation cross section, the partial ones and the corresponding branching ratios are defined by the following equations:

$$\sigma_{tot} = \sum_i \sigma_i, \quad \Gamma_i = \frac{\sigma_i}{\sigma_{tot}}, \quad (5.11)$$

where the index i runs over every annihilation channel. We remind that the neutralino pair could decay through a lot of other intermediate states but the five considered above are just the dominant ones (see section 4.4).

After this phenomenological study of the properties of a mSUGRA neutralino, we have tried to determine the region of the mSUGRA parameter space that, for a given dark matter halo normalization factor, could give a detectable continuum γ -ray neutralino induced flux, using GLAST. Fixing $\tan\beta$, A_0 and $\text{sgn}(\mu)$, we have performed an accurate scan in the $(m_0, m_{1/2})$ plane, searching for the minimum $\langle J(\psi) \rangle_{\Delta\Omega}$ needed to be able to distinguish the neutralino annihilation signal with GLAST, using the same discrimination criteria described in section 5.6. In figure 5.9 we show the iso-contour regions for the minimum allowed value of $\langle J(\psi) \rangle_{\Delta\Omega}$ for the signal detection, in the $(m_0, m_{\frac{1}{2}})$ plane, where we have taken into account the latest bounds coming from the current accelerator limits [114]. Among these we have considered lower bounds for the chargino, the gluino and squarks masses besides the bounds for $b \rightarrow s\gamma$ process. We have also implemented a lower bound for the neutralino mass:

$$m_\chi \gtrsim 50 \text{ GeV} \quad (5.12)$$

For this analysis, we have used for $\Delta\Omega$ the GLAST angular resolution, for the same reason explained in section 5.6, where we have also seen that it is $\sim 10^{-5} \text{ sr}$. We can observe that the regions where the neutralino signal can be detected by GLAST cover almost the entire allowed portion of the $(m_0, m_{\frac{1}{2}})$ plane, for values of the halo normalization factor $\langle J(\psi) \rangle_{\Delta\Omega}$, that are of the same order of magnitude of the “typical” ones, reported in table 5.2.

As an aside, we compare our results with those of [115], which assume a certain rough estimation for the GLAST sensitivity for the integrated continuum γ -ray flux from a region around the GC, of an extension equal to the GLAST angular resolution, and consider the neutralino signal detectable if its integrated flux is not lower than such sensitivity. Their figures 18 and 19 for the visible regions in the $(m_0, m_{\frac{1}{2}})$ plane for a value of $\langle J(\psi) \rangle_{\Delta\Omega}$ equal to 500 are in qualitative agreement with our corresponding predictions: first and fourth panels of figure 5.9.

In addition to this study of the GLAST sensitivity, we have tried to single out the regions of the mSUGRA parameter space $((m_0, m_{\frac{1}{2}})$ for fixed $\tan(\beta)$, A_0 and $\text{sign}(\mu)$), which are already experimentally excluded, due to a supersymmetric component of the γ -ray flux exceeding the GC EGRET data of table 5.1. The excluded regions, at 5σ level, are shown using $\langle J(0) \rangle$ contour plots in figure 5.10. This result implies that no significant constraints on the mSUGRA parameter space can actually be imposed, on the basis of the GC γ -ray data taken by EGRET. In figures 5.9 and 5.10, we have shaded the regions of the $(m_0, m_{\frac{1}{2}})$ plane, for which the neutralino relic abundance

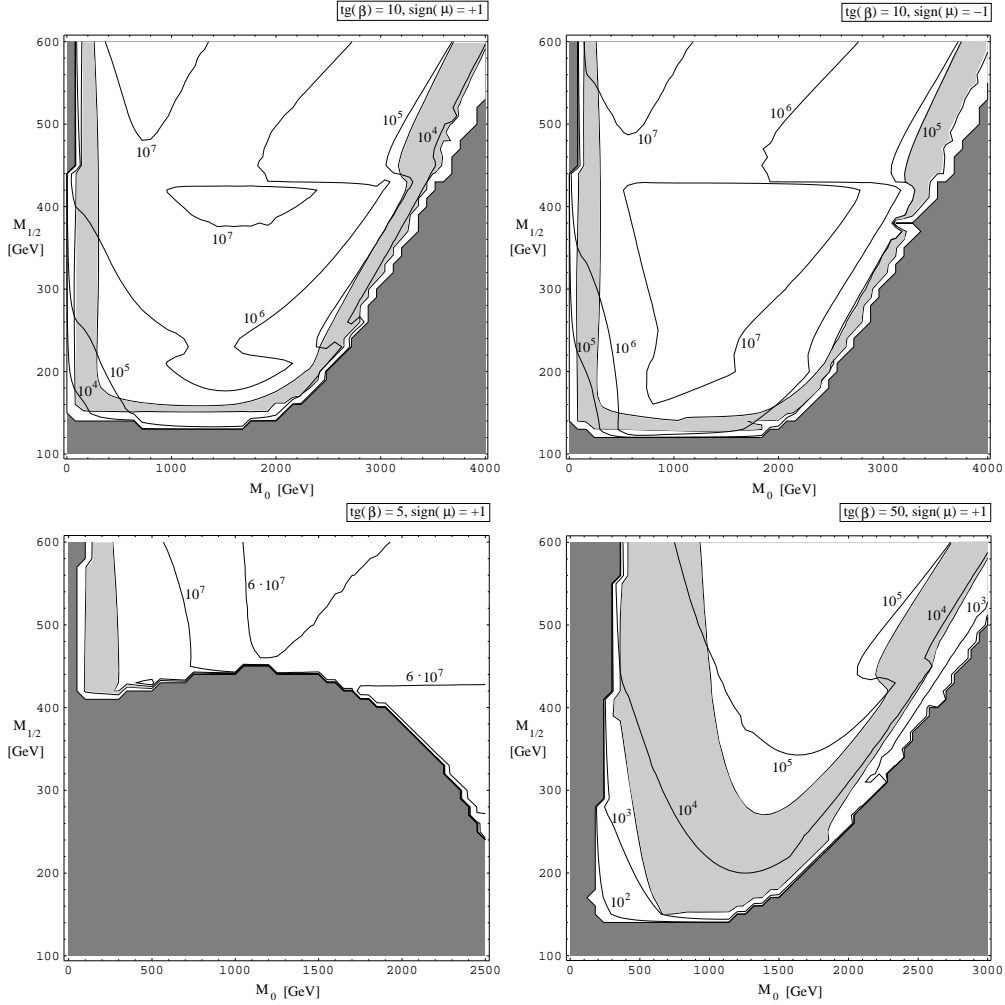


Figure 5.9: Contour plots in the mSUGRA $(m_0, m_{1/2})$ plane, for the value of the normalization factor N_χ , that allows the detection of the neutralino γ ray signal, with GLAST. The light shaded region corresponds to $0.1 \leq \Omega_\chi h^2 \leq 1$, while the dark shaded one corresponds to models that are excluded either by incorrect EWSB, LEP bounds violations or because the neutralino is not the LSP.

lies inside the cosmologically preferred interval [99]:

$$0.1 \leq \Omega_\chi h^2 \leq 1$$

We can observe that this last request strongly constraints the acceptable portion of the mSUGRA parameter space. As a consequence, fixing a value

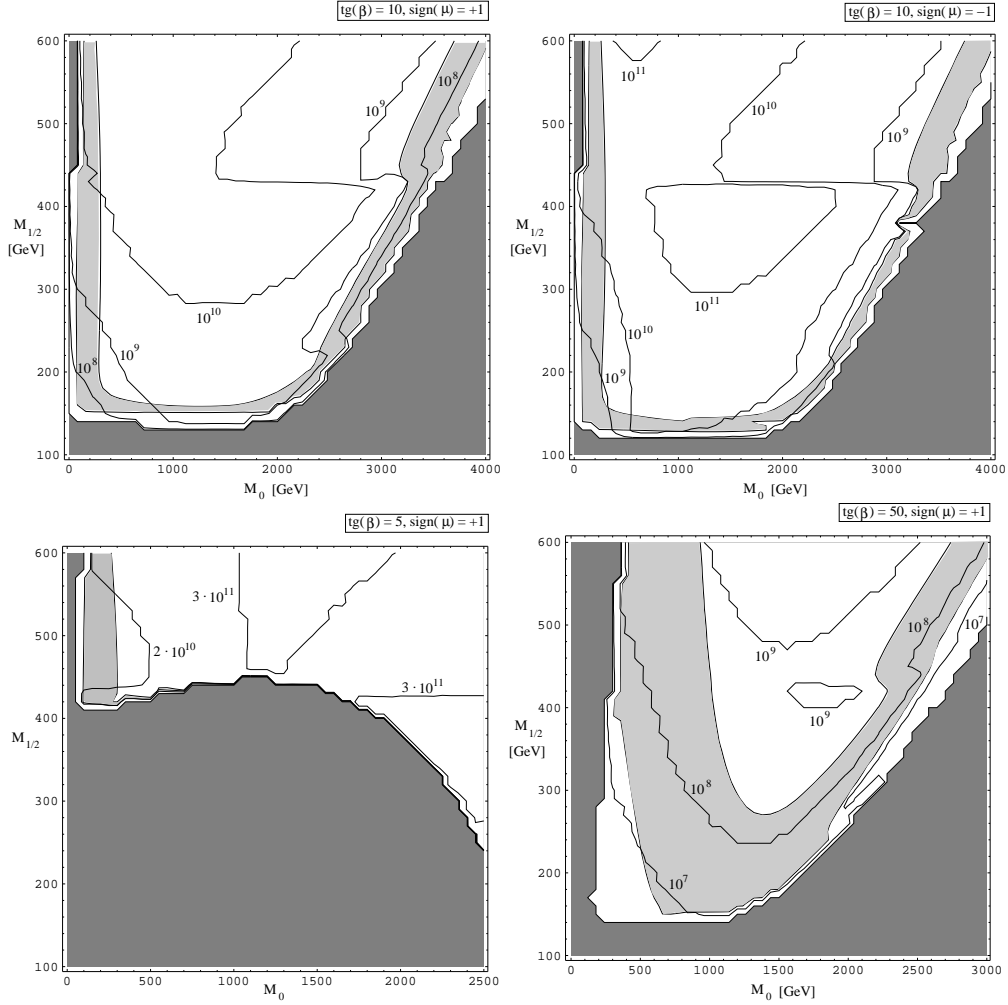


Figure 5.10: Contour plots in the mSUGRA $(m_0, m_{1/2})$ plane, for values of N_χ that are already excluded by EGRET data at 5σ confidence level. The light shaded region corresponds to $0.1 \leq \Omega_\chi h^2 \leq 1$, while the dark shaded one corresponds to models that are excluded either by incorrect EWSB, LEP bounds violations or because the neutralino is not the LSP.

for $\langle J(\psi) \rangle_{\Delta\Omega}$, gives extremely small regions of parameter space in which the neutralino signal is detectable using GLAST.

5.8 GC Angular Extension as seen by GLAST

Given that a γ -ray signal coming from WIMP annihilations could be detected by the experiment GLAST, we want to study if the apparatus is able to resolve its spatial position. This is an interesting problem related to the hypothesis that the GC be a point-like or an extended source.

In order to discriminate between the two assumptions we assume a simple dark matter halo profile whose overall normalization has been obtained by constraining the flux ϕ_γ to fit the GC EGRET data. Then we estimate the minimum value of the normalization of the WIMP flux, $(N_\chi)_{min}$, needed to detect the signal with GLAST.

Next, with the normalized dark matter halo profile, we compute the angle ψ_{max} beyond which the value of $\langle J(\psi) \rangle_{\Delta\Omega}$ becomes lower than $(N_\chi)_{min}$, and consequently the neutralino signal gets undetectable by GLAST. Finally we compare the value of ψ_{max} with the GLAST angular resolution ω (see fig 5.6). If $\psi_{max} > \omega$ we say that GLAST sees the GC as an extended source of γ -rays generated by neutralino annihilations.

Let us now explain in detail each step of the above strategy. The estimated angular resolution at $E = 10 \text{ GeV}$ of the GLAST telescope is approximately 10^{-5} sr (corresponding to $\omega \sim 0.1^\circ$ as in fig 5.6). Focusing on a region of such angular extent around the GC, we can find a *typical value* of the normalization of the neutralino flux, $(N_\chi)_{fit}$, averaging among those values that give the best fit of the EGRET data. From figure 5.3 we see that for a given annihilation channel the EGRET data are best fitted by models that have a WIMP mass near the energy threshold of the channel.

We hence find $(N_\chi)_{fit} = 1.2 \cdot 10^5$ averaging over all the dominant WIMP annihilations channels: $b\bar{b}, c\bar{c}, t\bar{t}, W^+W^-, Z^0Z^0$ and for all the WIMP masses between threshold and twice threshold. For these same annihilation channels and masses, we can also easily compute the average value of the normalization needed to detect the WIMP signal with GLAST (see the discussion in section 5.6). Let us call this other average $(N_\chi)_{min} = 4.5 \cdot 10^3$. The dark matter halo profile that we have considered is a simple isothermal profile:

$$\rho(r) = \begin{cases} \rho_0 \left(\frac{r}{r_0}\right)^{-\gamma}, & r > r_{min} \\ \rho_0 \left(\frac{r_{min}}{r_0}\right)^{-\gamma}, & r \leq r_{min} \end{cases} \quad (5.13)$$

with $\rho_0 = 0.3 \text{ GeV/cm}^3$ the local halo density, $r_0 = 8.5 \text{ Kpc}$ the distance of the sun from the GC. To avoid the singularity in $r = 0$ we have introduced a lower cut-off $r_{min} = 10^{-5} \text{ Kpc}$, corresponding to a distance from the GC below which one cannot trust a smooth dark matter halo distribution [116].

We can now identify $\langle J(0) \rangle_{\Delta\Omega}$ (see equation 5.7 with $\Delta\Omega$ of order $\sim 10^{-5} sr$) with $(N_\chi)_{fit}$. From equation (5.13) we infer the value of the parameter γ compatible with the above identification: $\gamma = 1.54$.

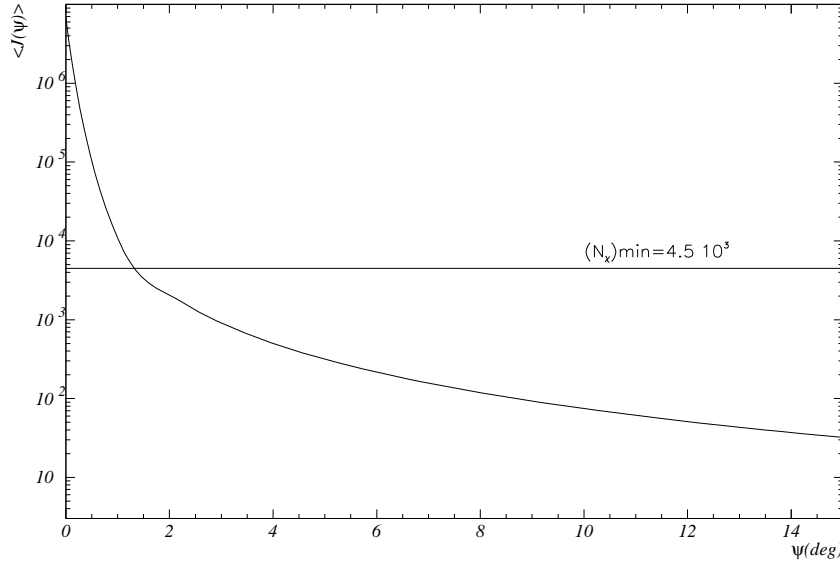


Figure 5.11: $\langle J(\psi) \rangle_{\Delta\Omega}$ with $\Delta\Omega = 10^{-5} sr$ computed using the halo profile in equation 5.13

We now compute the function $\langle J(\psi) \rangle_{\Delta\Omega}$ for every angle ψ , according to its definition equation (5.7), obtaining the shape shown in figure 5.11. The function $\langle J(\psi) \rangle_{\Delta\Omega}$ decreases with increasing ψ , and hence we can find a value (ψ_{max}) such that $\langle J(\psi) \rangle_{\Delta\Omega}$ is lower than $(N_\chi)_{min}$ for every $\psi > \psi_{max}$. ψ_{max} could then be interpreted as the angular extension of the GC as seen by the GLAST telescope; in fact the WIMP signal will be detectable only if the GLAST telescope is focused in a region within a ψ_{max} angular distance from the GC. Comparing $\psi_{max} \simeq 1.5^\circ$ with the estimated angular resolution of the GLAST detector ($\omega \simeq 0.1^\circ$ at $E = 10 GeV$ as in figure 5.6) we can argue that the GC can be considered as an extended source if observed with the GLAST telescope. We have to stress that this result must be considered only as a qualitative indication, because it has been obtained averaging over the WIMP annihilation channels and masses. Moreover it depends in a crucial way by the dark matter halo profiles choice. A more detailed analysis must keep into account the details of both the supersymmetric model and of the neutralino dark matter halo.

5.9 Optimal $\Delta\Omega$ for WIMP Signal Detection

We have shown in the previous section that the GC can be considered as an extended source, from the GLAST detection point of view. Now we want to try to determine the optimal value of the angular acceptance $\Delta\Omega$ in equation (5.7) to maximize the chance to detect the γ -ray signal from WIMP annihilations with GLAST. For various values of $\Delta\Omega$ we have computed the average minimum WIMP normalization factor needed to discriminate the WIMP signal from the background. As in the previous section, the average has been calculated over the five annihilation channels and for every WIMP mass between the threshold and twice the threshold.

For each value of $\Delta\Omega$ we have compared $(N_\chi)_{min}$ with the value of the function $\langle J(0) \rangle_{\Delta\Omega}$ obtained using the halo profile of equation (5.13) with $\gamma = 1.54$. Given $\Delta\Omega$, the WIMP signal is detectable if the following condition is satisfied:

$$\langle J(0) \rangle_{\Delta\Omega} > (N_\chi)_{min}$$

In figure 5.12 we show the plot of the ratio of these two quantities, with respect to $\Delta\Omega$, starting from a value of $\Delta\Omega$ equal to the angular resolution of the GLAST detector. It can be seen that for lower values of $\Delta\Omega$ one has higher ratios between $\langle J(0) \rangle_{\Delta\Omega}$ and $(N_\chi)_{min}$ and hence a more favorable situation for the WIMP signal detection. Our conclusion is that the optimal $\Delta\Omega$ to use in a search for continuum γ -ray signals from WIMP annihilations with the GLAST detector is its minimum value *i.e.* the GLAST angular resolution.

We stress that such result depends on the particular choice of the halo profile function (see equation (5.13)): it is valid only if the actual halo density profile could be approximated by the power law of equation (5.13) within an angular extent around the GC of at least $\omega \sim 0.1^\circ$ which is the value of the GLAST angular resolution.

5.10 Results

The result of our analysis on the EGRET data from the Galactic Center (GC) suggests there is room for a supersymmetric dark matter component that is suitable to explain the excess with respect to standard continuum γ -ray production expectation.

A general feature, independent on the particular nature of the WIMP, that has emerged, is that the best fit of the EGRET data is obtained for small WIMP masses without the need to assume highly singular dark matter halo profiles.

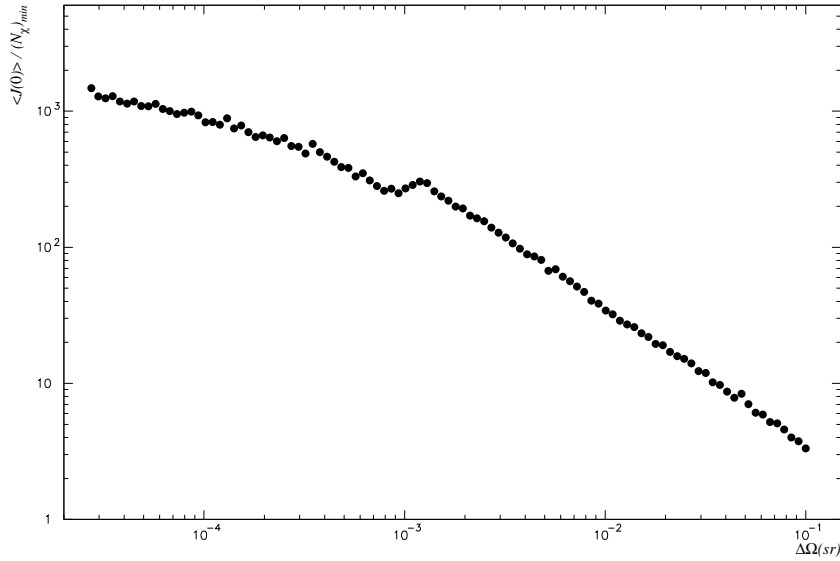


Figure 5.12: Ratio between $\langle J(0) \rangle_{\Delta\Omega}$ and $(N_\chi)_{min}$ vs $\Delta\Omega$.

We have also found that a convincing signal, in a statistical sense, of the continuum γ -ray flux from WIMP annihilation in the GC will be possible with the upcoming experiment GLAST, without the need to assume highly singular dark matter halo profiles. This result has also been obtained in the particular case in which the WIMP is the lightest neutralino of the minimal supergravity model. In such case, we have also argued that the EGRET data already impose some weak constraints on the particle physics model, and we have determined, for certain halo profile choices, some regions of the minimal supergravity parameter space that could already be ruled out.

Another result that we have obtained is that, from the point of view of the GLAST detector, the GC region is an extended source for γ -rays coming from WIMP annihilation. Furthermore, we have found that the optimal angular extension of the region around the GC center to consider, in order to maximize the chance to detect the WIMP signal with GLAST, is the lowest possible, *i.e.* the GLAST angular resolution.

Chapter 6

Conclusions

In this work we have performed a detailed analysis of the possibilities to discover supersymmetric dark matter through continuum γ -ray flux from the GC. In particular, we have presented what can be already learned from satellite experiments like EGRET and what we can expect from GLAST upcoming experiment. This task has been achieved using a toy model to obtain results for a generic WIMP without worrying about the particle physics model. Then we have specialized to a particular underlying theory, mSUGRA, that gives rise to supersymmetry breaking terms in the MSSM. We have shown, in chapter 2, what are the important ingredients in building such supersymmetric extension of the SM and in chapter 3 we have seen how to obtain low energy predictions, through RGE, starting from a high energy theory. There are interesting issues in the numerical procedure to solve RGE. They must be carefully taken into account in order to compare our analysis of the expected γ -ray flux with other similar studies (for example [84]).

The problem of the excess of EGRET data coming from the GC has been analyzed with explicit calculation of the expected neutralino component induced flux. We have left the two normalization, associated to the continuum background and to the WIMP components, as free parameters, because of the high uncertainty in their determination. The result is that there is indeed room for a WIMP induced component. We expect for the WIMP mass:

$$m_\chi \lesssim 100 \text{ GeV}$$

in reasons of the best fit of EGRET data. The analysis can be improved when further data in the region $E > 10 \text{ GeV}$ will be available with GLAST. Moreover we have to wait for a more precise determination of the interstellar hydrogen column density associated to the N_b parameter, and of the actual dark matter density profile, which is very poorly known towards the GC.

We have shown that, in order to obtain a statistical evidence for a WIMP induced components in the continuum γ -ray flux, we have to assume $\langle J(\Psi) \rangle$ of the order of 10^4 . This is a higher value than the prediction of a more naive analysis. The statistical evidence relies on our discrimination method, based on the equivalent procedure, *i.e.* χ^2 statistics and likelihood ratio. Thus our method put more constraints on the discover of a WIMP induced component.

One important result is that an improved WIMP signal detection will indeed be possible with the GLAST experiment, that has a better angular resolution with respect to EGRET.

This work can be extended in several ways. One of these, from the pure phenomenological side, is to implement a more precise description of GLAST features coming from improved simulations of the apparatus. Another possibility is to consider constraints on the parameter space of the theory coming from other cosmic rays measurements, like that of cosmic antiproton flux. In fact, we have seen that these are allowed final states for neutralino annihilations. It also possible to study the one loop annihilation processes with γ 's in the final state. These would be a very convincing signal for the existence of supersymmetric dark matter.

To complete the analysis is then possible to consider other mechanism of supersymmetry breaking, that give rise to different underlying theory for the MSSM. One example is given by the so called anomaly mediated models that implies a different phenomenology for the neutralino.

Acknowledgments

I would like to thank my mother, for all the support she gives to me in all these years, and my endless love Posi. I also thank all the people of the Physics Department in Roma Tor Vergata that has been involved in this fascinating research. In particular I want to thank Francesco Fucito, Aldo Morselli and Alessandro Cesarini with which I have shared many ideas and I have had many useful and interesting discussions. I would also like to thank Piero Ullio of SISSA in Trieste for all the important helps he gives to me.

Appendix A

Spinorial notation

In defining supersymmetric theories it is very useful to work with two components Weyl spinors. In this appendix we will define the opportune formalism.

Let us start by defining the usual Minkowski space-time metric tensor in $D = 4$ dimensions:

$$\eta_{mn} = \text{diag}(-1, +1, +1, +1) \quad (\text{A.1})$$

where we use the latin indices m, n, \dots to denote the space-time coordinates, to better distinguish them from the spinorial indices. Then we introduce the Van der Waerden notation to work with the Weyl spinors. The Lorentz group in $D = 4$ is:

$$SO(1, 3) \sim SL(2, \mathbb{C}) \quad (\text{A.2})$$

Let us consider a 2×2 matrix with unit determinant $M \in SL(2, \mathbb{C})$. This matrix allows us to build representations of the Lorentz group that acts over two components Weyl spinors, and we obtain the following transformation properties:

$$\begin{aligned} \psi'_\alpha &= M_\alpha{}^\beta \psi_\beta & \bar{\psi}'_{\dot{\alpha}} &= (M^*)_{\dot{\alpha}}{}^{\dot{\beta}} \bar{\psi}_{\dot{\beta}} \\ \psi'^\alpha &= (M^{-1})^\alpha{}_\beta \psi^\beta & \bar{\psi}'^{\dot{\alpha}} &= [(M^*)^{-1}]^{\dot{\alpha}}{}_{\dot{\beta}} \bar{\psi}^{\dot{\beta}} \end{aligned} \quad (\text{A.3})$$

where we have used the dotted-undotted notation to distinguish between different representations of $SL(2, \mathbb{C})$. The greek indices $\alpha, \beta = 1, 2$ are used to denote the spinorial indices. In particular the undotted indices α, β, \dots transform as the right handed representation $(1/2, 0)$ while the dotted indices $\dot{\alpha}, \dot{\beta}, \dots$ transform as the left handed representation $(0, 1/2)$ of the Lorentz

group. We can assume the Pauli matrices as a basis for $SL(2, \mathbb{C})$:

$$\begin{aligned}\sigma^0 &= \begin{pmatrix} -1 & 0 \\ 0 & -1 \end{pmatrix} & \sigma^1 &= \begin{pmatrix} 0 & 1 \\ 1 & 0 \end{pmatrix} \\ \sigma^2 &= \begin{pmatrix} 0 & -i \\ i & 0 \end{pmatrix} & \sigma^3 &= \begin{pmatrix} 1 & 0 \\ 0 & -1 \end{pmatrix}\end{aligned}\tag{A.4}$$

so that an arbitrary $SL(2, \mathbb{C})$ matrix can be written in terms of this basis as:

$$\begin{aligned}P &= P_m \sigma^m = P_0 \sigma^0 + P_1 \sigma^1 + P_2 \sigma^2 + P_3 \sigma^3 \\ &= \begin{pmatrix} -P_0 + P_3 & P_1 - iP_2 \\ P_1 - iP_2 & -P_0 + P_3 \end{pmatrix}\end{aligned}\tag{A.5}$$

Every hermitian matrix $P = P^\dagger$ can thus be written in terms of real P_m . This property can be seen, recalling the hermiticity of the Pauli matrices:

$$(\sigma^i)^\dagger = \sigma^i \quad i = 0, 1, 2, 3$$

so that:

$$\begin{aligned}P &= P^\dagger = \left(\sum_i P_i \sigma^i \right)^\dagger \\ &= \sum_i P_i^* \sigma^i\end{aligned}\tag{A.6}$$

obtaining at the end the reality condition:

$$\sum_i P_i \sigma^i = \sum_i P_i^* \sigma^i \Rightarrow P_i^* = P_i \Rightarrow P_i \in \mathbb{R}\tag{A.7}$$

From every hermitian matrix P , it is possible to obtain another hermitian matrix by applying the following transformation:

$$P' = M P M^\dagger\tag{A.8}$$

where both P and P' admit an expansion in terms of the σ^m basis:

$$P' = P'_m \sigma^m = M P_m \sigma^m M^\dagger\tag{A.9}$$

Since M is unimodular, *i.e.* $\det M = 1$, we can show that the coefficients P_m and P'_m are connected by a Lorentz transformation:

$$\det(P'_m \sigma^m) = \det(P_m \sigma^m) = P_0'^2 - \vec{P}' \cdot \vec{P}' = P_0^2 - \vec{P} \cdot \vec{P}\tag{A.10}$$

The Pauli matrices have the following index structure:

$$\sigma_{\alpha\dot{\alpha}}^m \quad (\text{A.11})$$

that allows us to write some Lorentz scalar quantities:

$$\psi^\alpha \psi_\alpha \quad \bar{\psi}_{\dot{\alpha}} \bar{\psi}^{\dot{\alpha}} \quad \psi^\alpha \sigma_{\alpha\dot{\alpha}}^m \partial_m \bar{\psi}^{\dot{\alpha}}$$

It is possible to define the $SL(2, \mathbb{C})$ metric tensor $\epsilon_{\alpha\beta}$, that is a totally anti-symmetric tensor defined with the following conventions:

$$\begin{aligned} \epsilon_{21} &= \epsilon^{21} = 1 \\ \epsilon_{12} &= \epsilon^{21} = -1 \\ \epsilon_{11} &= \epsilon_{22} = \epsilon^{11} = \epsilon^{22} = 0 \end{aligned} \quad (\text{A.12})$$

It is obviously invariant under Lorentz transformations:

$$\begin{aligned} \epsilon_{\alpha\beta} &= M_\alpha^\gamma M_\beta^\delta \epsilon_{\gamma\delta} \\ \epsilon^{\alpha\beta} &= \epsilon^{\gamma\delta} M_\gamma^\alpha M_\delta^\beta \end{aligned} \quad (\text{A.13})$$

Using the metric tensor $\epsilon_{\alpha\beta}$ we can raise and lower spinorial indices:

$$\begin{aligned} \psi^\alpha &= \epsilon^{\alpha\beta} \psi_\beta \\ \psi_\alpha &= \epsilon_{\alpha\beta} \psi^\beta \end{aligned} \quad (\text{A.14})$$

where it is important to note that we have defined $\epsilon_{\alpha\beta}$ and $\epsilon^{\alpha\beta}$ in such a way to satisfy:

$$\epsilon_{\alpha\beta} \epsilon^{\beta\gamma} = \delta_\alpha^\gamma \quad (\text{A.15})$$

Analogous relations hold for the undotted indices.

The $\epsilon_{\alpha\beta}$ can also be used to raise and lower indices of the Pauli matrices:

$$\bar{\sigma}^{m\alpha\dot{\alpha}} = \epsilon^{\alpha\beta} \epsilon^{\dot{\alpha}\dot{\beta}} \sigma_{\alpha\dot{\alpha}}^m \quad (\text{A.16})$$

that can be explicitly written in matrix form, as:

$$\begin{aligned} \sigma_0 = \bar{\sigma}_0 &= \begin{pmatrix} -1 & 0 \\ 0 & -1 \end{pmatrix} & \sigma_1 = -\bar{\sigma}_1 &= \begin{pmatrix} 0 & 1 \\ 1 & 0 \end{pmatrix} \\ \sigma_2 = -\bar{\sigma}_2 &= \begin{pmatrix} 0 & -i \\ i & 0 \end{pmatrix} & \sigma_3 = -\bar{\sigma}_3 &= \begin{pmatrix} 1 & 0 \\ 0 & -1 \end{pmatrix} \end{aligned} \quad (\text{A.17})$$

Moreover the following relations hold:

$$\begin{aligned} (\sigma^m \bar{\sigma}^n + \sigma^n \bar{\sigma}^m)_\alpha^\beta &= -2\eta^{mn} \delta_\alpha^\beta \\ (\bar{\sigma}^m \sigma^n + \bar{\sigma}^n \sigma^m)^{\dot{\alpha}}_{\dot{\beta}} &= -2\eta^{mn} \delta^{\dot{\alpha}}_{\dot{\beta}} \end{aligned} \quad (\text{A.18})$$

with the following completeness relations:

$$\begin{aligned} \text{Tr}(\sigma^m \bar{\sigma}^n) &= -2\eta^{mn} \\ \sigma_{\alpha\dot{\alpha}}^m \bar{\sigma}_m^{\dot{\beta}\beta} &= -2\delta_{\alpha}^{\beta} \delta_{\dot{\beta}}^{\dot{\alpha}} \end{aligned} \quad (\text{A.19})$$

where the trace is over the spinorial indices. These relations can be used to relate a spinor product representations to a vector representation:

$$\left(\frac{1}{2}, 0\right) \otimes \left(0, \frac{1}{2}\right) = \left(\frac{1}{2}, \frac{1}{2}\right)$$

and so we can use the σ matrices to write:

$$\begin{aligned} v_{\alpha\dot{\alpha}} &= \sigma_{\alpha\dot{\alpha}}^m v_m \\ v^m &= -\frac{1}{2} \bar{\sigma}^{m\dot{\alpha}\alpha} v_{\alpha\dot{\alpha}} \end{aligned} \quad (\text{A.20})$$

It is also possible to give the Lorentz generators in the spinorial representation:

$$\begin{aligned} \sigma^{nm}{}_{\alpha}{}^{\beta} &= \frac{1}{4} (\sigma_{\alpha\dot{\alpha}}^n \bar{\sigma}^{m\dot{\alpha}\beta} - \sigma_{\alpha\dot{\alpha}}^m \bar{\sigma}^{n\dot{\alpha}\beta}) \\ \bar{\sigma}^{nm\dot{\alpha}}{}_{\dot{\beta}} &= \frac{1}{4} (\bar{\sigma}^{n\dot{\alpha}\alpha} \sigma_{\alpha\dot{\beta}}^m - \bar{\sigma}^{m\dot{\alpha}\alpha} \sigma_{\alpha\dot{\beta}}^n) \end{aligned} \quad (\text{A.21})$$

It is possible to relate two component Weyl spinors to the usual four component Dirac spinor, using the relations (A.18). Thus in the Weyl basis the 4×4 Dirac matrices are written as:

$$\gamma^m = \begin{pmatrix} 0 & \sigma^m \\ \bar{\sigma}^m & 0 \end{pmatrix} \quad \gamma^5 = \begin{pmatrix} 1 & 0 \\ 0 & 1 \end{pmatrix} \quad (\text{A.22})$$

where the matrices are in 2×2 blocks form. In this basis a Dirac spinor contains two Weyl spinors:

$$\psi_D = \begin{pmatrix} \chi_{\alpha} \\ \bar{\psi}^{\dot{\alpha}} \end{pmatrix} \quad (\text{A.23})$$

while a Majorana spinor contains only one Weyl spinor (the other component is simply the complex conjugate):

$$\psi_M = \begin{pmatrix} \chi_{\alpha} \\ \bar{\chi}^{\dot{\alpha}} \end{pmatrix} \quad (\text{A.24})$$

To finish we write down the conventions for the sum of spinorial indices, with the so called “upper left” notation. We can derive the following relations for a product of two spinors:

$$\begin{aligned}\psi\chi &= \psi^\alpha\chi_\alpha = -\psi_\alpha\chi^\alpha = \chi^\alpha\psi_\alpha = \chi\psi \\ \bar{\psi}\bar{\chi} &= \bar{\psi}_{\dot{\alpha}}\bar{\chi}^{\dot{\alpha}} = -\bar{\psi}^{\dot{\alpha}}\bar{\chi}_{\dot{\alpha}} = \bar{\chi}_{\dot{\alpha}}\bar{\psi}^{\dot{\alpha}} = \bar{\chi}\bar{\psi}\end{aligned}\tag{A.25}$$

where we have used the anticommuting property of the spinors. The definition of the product $\bar{\psi}\bar{\chi}$ is chosen in a such a way that:

$$(\chi\psi)^\dagger = (\chi^\alpha\psi_\alpha)^\dagger = \bar{\psi}_{\dot{\alpha}}\bar{\chi}^{\dot{\alpha}} = \bar{\psi}\bar{\chi} = \bar{\chi}\bar{\psi}\tag{A.26}$$

where we can see that the conjugation change the order of the spinors.

Appendix B

Description of the algorithms

In this appendix we give a description of the algorithms used to compute the renormalization group equations of the MSSM parameters, the gamma ray flux coming from neutralino annihilations and its relic abundance.

B.1 ISASUGRA

The ISASUGRA algorithm is able to compute, using the renormalization group equations (at two loop level), the weak scale parameters of the minimal supersymmetric extension of the Standard Model from those at the GUT scale. ISASUGRA is written in standard FORTRAN77 and it is a part of the ISAJET package. This is a Monte Carlo event generator which simulates pp , $\bar{p}p$ and e^+e^- interactions at high energies. The latest source, contained in the file `isajet.car`, is available at `ftp://ftp.phy.bnl.gov/pub/isajet`. From now on we will refer to the version 7.63¹.

The main program is SUGRUN and starts from line 34555 of the file `isajet.car` (this is a raw text file). This program requires as input the high scale parameters of the underlying fundamental theory. In general this theory is minimal supergravity but also other supersymmetry breaking scenario can be considered. In the mSUGRA case (defined in section 3.6) the input real single precision variables are:

`M0, MHF, A0, TANB, SGNMU, MT`

They denote respectively the high energy parameters:

$$m_0, m_{1/2}, A_0, \tan \beta, \text{sgn}(\mu)$$

¹available at <http://www.fis.uniroma3.it/~lionetto/>

while MT denote the “pole” top quark mass m_t . We set, as usual

$$m_t = 173.8 \text{ GeV}$$

that is the LEP value coming from direct observation of top events. The integer variable IMODEL=IMODIN determines the supersymmetry breaking scenario. It can assume the following values:

IMODEL	Scenario
1	mSUGRA
2	mGMSB
3	non-universal SUGRA
4	SUGRA with truly unified gauge couplings
5	non-minimal GMSB
6	SUGRA+right-handed neutrino
7	anomaly-mediated SUSY breaking

The renormalization group evolution is achieved with a call to the subroutine SUGRA in line 34699:

```
15 CALL SUGRA(M0,MHF,A0,TANB,SGNMU,MT,IMODEL)
```

The routine output is saved in the common block SUGMG at line 790. It contains the values of all the couplings that have been RG evolved down to weak scale. The couplings are stored in a real vector variable GSS(29):

```
C          Frozen couplings from RG equations:
C      GSS( 1) = g_1          GSS( 2) = g_2          GSS( 3) = g_3
C      GSS( 4) = y_tau       GSS( 5) = y_b          GSS( 6) = y_t
C      GSS( 7) = M_1         GSS( 8) = M_2         GSS( 9) = M_3
C      GSS(10) = A_tau       GSS(11) = A_b         GSS(12) = A_t
C      GSS(13) = M_h1^2     GSS(14) = M_h2^2     GSS(15) = M_er^2
C      GSS(16) = M_el^2     GSS(17) = M_dnr^2    GSS(18) = M_upr^2
C      GSS(19) = M_upl^2    GSS(20) = M_taur^2   GSS(21) = M_taul^2
C      GSS(22) = M_btr^2    GSS(23) = M_tpr^2    GSS(24) = M_tpl^2
C      GSS(25) = mu         GSS(26) = B           GSS(27) = Y_N
C      GSS(28) = M_nr       GSS(29) = A_n
```

where, GSS(1)...GSS(3) are, respectively, the MSSM couplings g_1 , g_2 and g_3 defined in section 3.4, GSS(4)...GSS(6) are the Yukawa couplings and GSS(7)...GSS(9) are the soft breaking mass parameters M_1 , M_2 and M_3 defined in section 2.9.

Another output variable of the SUGRA routine is NOGOOD. Its value is the result of a consistency check performed by the SUGRA subroutine on

the supersymmetric model defined by M0, MHF, A0, TANB, SGNMU. The model is accepted if NOGOOD=0 and it is rejected if NOGOOD assumes the following values:

NOGOOD	Excluded by
1	BAD POINT: TACHYONIC PARTICLES
2	BAD POINT: NO EW SYMMETRY BREAKING
3	BAD POINT: $M(H_P)^2 < 0$
4	BAD POINT: YUKAWA > 10
5	SUGRA BAD POINT: Z1SS NOT LSP
6	BAD POINT: XT EWSB BAD
7	BAD POINT: $M_{HL}^2 < 0$

The value 1 implies that some tachyonic particle appears in the low energy spectrum. Hence the model is inconsistent. The values 2,3,6,7 refer to an incorrect electroweak symmetry breaking as explained in section 3.6. The value 4 implies that the absolute value of some of the Yukawa couplings has become greater than 10. Finally, the value 5 implies that the neutralino is not the lightest supersymmetric particle.

The next step after the consistency check for the supersymmetric model, is to calculate all masses and decay modes. This is performed by a call to the subroutine SSMSSM in line 34761. The definitions of the masses are also contained in the SUGMG common block at line 790. The vector MSS(32) contains all the MSSM masses:

```

C           Masses:
C     MSS( 1) = glss      MSS( 2) = upl      MSS( 3) = upr
C     MSS( 4) = dnl      MSS( 5) = dnr      MSS( 6) = stl
C     MSS( 7) = str      MSS( 8) = chl      MSS( 9) = chr
C     MSS(10) = b1       MSS(11) = b2       MSS(12) = t1
C     MSS(13) = t2       MSS(14) = nue1     MSS(15) = num1
C     MSS(16) = nut1     MSS(17) = e1-     MSS(18) = er-
C     MSS(19) = mul-     MSS(20) = mur-    MSS(21) = tau1
C     MSS(22) = tau2     MSS(23) = z1ss    MSS(24) = z2ss
C     MSS(25) = z3ss     MSS(26) = z4ss    MSS(27) = w1ss
C     MSS(28) = w2ss     MSS(29) = h10     MSS(30) = hh0
C     MSS(31) = ha0      MSS(32) = h+

```

where, MSS(1) is the gluino mass, MSS(2)...MSS(13) are the (left and right) squark masses, MSS(23)...MSS(26) are the neutralino masses, MSS(27) and MSS(28) are the chargino masses and MSS(29)...MSS(32) are the higgs masses.

Then it is possible to do a further check on low energy parameters. If we want to test if they satisfy the LEP and SLC bounds² we can call the subroutine SSTEEST in line 34755. This subroutine (whose code starts from line 44841) gives as output the variable IALLOW. These are the possible values that it can take:

IALLOW	Bounds on SUSY particles
1	Z1 is not LSP
2	$\Gamma(Z \rightarrow Z1SS Z1SS) < \text{GAMINV}$
4	Z \rightarrow charginos allowed
8	$\text{BF}(Z \rightarrow Z1SS Z2SS) > 10^5$
16	Z \rightarrow squarks, sleptons
32	$\text{BR}(Z \rightarrow Z^* HLO) < \text{B}(Z \rightarrow Z^* H(M=\text{MHSM}))$
64	$\text{BR}(Z \rightarrow HLO HAO) > 0$
128	$M(H^+) > M(Z)/2$

We have already seen that the most important subroutine called by the main program is SUGRA. Its source code starts from line 49442. It uses a Runge-Kutta algorithm to integrate the renormalization group equations from the weak energy scale M_Z to the GUT scale M_{GUT} and back. The iteration method is explained in section 3.7. The maximum number of iterations is determined by the integer variable MXITER. Its value is set in line 49501:

```
C          This choice is a compromise between precision and speed:
DATA MXITER/20/,NSTEPO/1000/ ,DELLIM/2.E-3/
```

In the same line there is the NSTEPO variable that determines the number of intervals in the energy range from M_Z to the GUT scale M_{GUT} . The variable DELLIM controls the precision of the iterative procedure (see section 3.7).

Here we rewrite the complete inputs for the SUGRA routine:

```
C      Calculate supergravity spectra for ISAJET using as inputs
C      M0      = M_0          = common scalar mass at GUT scale
C      MHF     = M_(1/2)     = common gaugino mass at GUT scale
C      A0      = A_0          = trilinear soft breaking parameter at GUT scale
C      TANB    = tan(beta)   = ratio of vacuum expectation values v_1/v_2
C      SGNMU   = sgn(mu)     = +-1 = sign of Higgsino mass term
C      MT      = M_t          = mass of t quark
C      MO      = Lambda      = ratio of vevs <F>/<S>
C      MHF     = M_Mes        = messenger scale
C      A0      = n_5          = number of messenger fields
```

²caveat: the latest version is updated to 5/25/95

C	IMODEL	= 1 for SUGRA model
C		= 2 for GMSB model
C		= 7 for AMSB model

All the inputs has to be thought as the high energy parameters specified at M_{GUT} . For the first iteration only the first six couplings are included and a common threshold for all the supersymmetric masses is used.

The first run of the three gauge and three Yukawa couplings in order to find M_{GUT} , A_{GUT} and Y_{GUT} starts from line 49619. The inverse evolution from M_{GUT} to M_Z starts from line 49799. For the successive runs the subroutine used is SUGRGE whose code starts from line 49988. The fortran code can also be found in appendix C. This routine makes one complete iteration of the renormalization group equations from M_Z to M_{GUT} and back, setting the boundary conditions on each end. The integration routine, that encodes the Runge-Kutta method, is called RKSTP and it starts from line 34920.

The complete set of two loop β -functions for the MSSM (see [60]) is written in the two subroutines SURG06 (located at line 50286) and SURG26 (located at line 50442). The difference between the two routines is in the SUSY mass threshold. The former assumes a single common scale MSUSY, while the latter uses different thresholds, contained in the vector MSS, for each mass calculated with the couplings G0 frozen by using the routine SUGFRZ. This routine is located at line 49076.

B.2 DarkSUSY

DarkSUSY [94] implements the general structure of the MSSM, with R-parity and CP conservation (except in the quarks CKM matrix). The supersymmetric mass spectrum and the particle mixing matrices are computed from seven input parameters at the electroweak scale. The values of these weak scale parameters have been obtained by the high energy ones by using ISASUGRA. In this way we have computed the γ -ray flux coming from neutralino annihilations and the neutralino relic abundance. We have also exploited the feature that permits to check that a given supersymmetric model does not violate the current accelerator bounds³.

The latest version can be found at <http://www.physto.se/~edsjo/darksusy/>. From now on we will refer to the version ds-3.14.05-beta11⁴.

The sources of each different DarkSUSY packages can be found in the src directory. The following is the description of all the subdirectories of src:

³updated to 2002 limits by the Particle Data Group

⁴available at <http://www.fis.uniroma3.it/~lionetto/>

Subdirectory	Description
ac	Accelerator limits
an	Neutralino/Chargino annihilation - driver routines for an1l and anstu
an1l	
anstu	Annihilation at 1-loop
dd	Helicity amplitudes for annihilation
ep	Direct detection
ge	Positron routines
ha	General routines, like integration routines, etc.
hm	Halo annihilation yield, like antiprotons, gamma rays, etc.
hr	Halo models
ini	Halo rates, driver routines for ep, pb and ha routines
mu	Initialization routines
nt	Muon yields.
pb	Neutrino telescope rates, driver routines for mu.
rd	Antiproton routines.
rn	Relic density routines.
su	Relic density for neutralinos, driver routines for rd.
xcern	SUSY routines, vertices, couplings, masses, etc.
xcmlib	Some required CERNLIB routines.
	Some required CMLIB routines.

The main program that can be used to test all the DarkSUSY computational features is called DSTEST.F and is contained in the test/ directory. Here we briefly describe only the subroutine and the functions that we have actually used. The interface between ISASUGRA and DarkSUSY is realized by the subroutine DSISASUGRA.DARKSUSY located in the src/rge subdirectory. It performs the translation from the ISASUGRA common block SUGMG, that contains all the couplings and masses, into the corresponding DarkSUSY variables. For example, the following is the MSSM gauge couplings translation:

```
m1=gss(7)
m2=gss(8)
m3=gss(9)
```

where m1, m2 and m3 are the DarkSUSY variables. The squark masses are translated as:

```
c===== Sfermion Masses "1" = "L", "2" = "R" =====
mass(ksu1)=mss(2)
mass(ksu2)=mss(3)
```

```

mass(ksd1)=mss(4)
mass(ksd2)=mss(5)
mass(kss1)=mss(6)
mass(kss2)=mss(7)
mass(ksc1)=mss(8)
mass(ksc2)=mss(9)
mass(ksb1)=mss(10)
mass(ksb2)=mss(11)
mass(kst1)=mss(12)
mass(kst2)=mss(13)

```

where, again, the DarkSUSY variables are defined in the left hand side. The neutralino and chargino masses correspondence is:

```

c===== Neutralino and Chargino Masses
c===== ISASUGRA orders the neutralino and chargino mass eigenvalues
mass(kn1)=abs(amz1ss)
mass(kn2)=abs(amz2ss)
mass(kn3)=abs(amz3ss)
mass(kn4)=abs(amz4ss)

```

The fortran function that computes the continuum γ -ray flux coming from neutralino annihilations is DSHRGACONTDIFF. Its source is located in the subdirectory src/hr (see previous table). Given the supersymmetric model parameters, the energy EGAM and the integral of the halo profile JPSI (see chapter 5 to see the equations that are implemented), this function gives the corresponding continuum γ -ray flux in unit of $\text{cm}^{-2} \text{s}^{-1} \text{sr}^{-1} \text{GeV}^{-1}$. The following is a sample code that show the usage of DSHRGACONTDIFF:

```
fluxgacdiff=dshrgacontdiff(egam,jpsi,istat)
```

where ISTAT is a dummy variable.

The relic density computation is performed by using the function DSR-DOMEGA located in the subdirectory src/rn. The function usage is:

```
oh2=dsrdomega(1,1,xf,ierr,iwar,nfc)
```

The first argument determines if coannihilations between the lightest neutralino and the heavier neutralinos and charginos should be included (1=yes, 0=no). The second argument determines the accuracy. If it is 1 a faster calculation (*e.g.* only including coannihilations if the mass difference is less then 30%) is performed while if it is 0 a more accurate calculation is performed. In practice, the fast option is more than adequate (better than 5% accuracy).

The function returns the relic density, Ωh^2 , the freeze-out temperature, x_f ($x=m/T$), one error flag, IERR and one warning flag, IWAR, both of which are 0 if everything is OK. NFC is the number points in momentum where the cross section had to be calculated. Note that the omega calculation can be very time consuming, needing up to several minutes for tricky models (with many resonances, thresholds, coannihilations etc).

Appendix C

Fortran codes

C.1 SUGRGE subroutine

```
      SUBROUTINE SUGRGE(MO,MHF,AO,TANB,SGNMU,MT,G,GO,IG,W2
$,NSTEP,IMODEL)
C
C      Make one complete iteration of the renormalization group
C      equations from MZ to MGUT and back, setting the boundary
C      conditions on each end.
C
+SELF,IF=IMPNONE
      IMPLICIT NONE
+SELF
+CDE,SSLUN
+CDE,SSSM
+CDE,SUGPAS
+CDE,SUGNU
+CDE,SUGXIN
+CDE,SUGMG
C
      EXTERNAL SURG26
      DOUBLE PRECISION DDILOG,XLM
      REAL MO,MHF,AO,TANB,SGNMU,MT,G(29),GO(29),W2(87)
      INTEGER IG(29),NSTEP,IMODEL
      REAL PI,TZ,A1I,A2I,A3I,GGUT,AGUTI,SIG1,SIG2,
$MH1S,MH2S,MUS,T,MZ,TGUT,DT,AGUT,Q,ASMT,MTMT,SINB,
$BETA,QOLD,XLAMGM,XMESGM,XN5GM,XC,G3GUT,THRF,THRG,DY,
$BLHAT,BBHAT,BTHAT
      INTEGER I,II
      DATA MZ/91.187/
```

```

C
C           Re-initialize weak scale parameters
C
XLAMGM=MO
XMESGM=MHF
XN5GM=AO
PI=4.*ATAN(1.)
BETA=ATAN(XTANB)
SINB=SIN(BETA)
ASMZ=0.118
C   ASMT=G3MT**2/4./PI
C   MTMT=MT/(1.+4*ASMT/3./PI+(16.11-1.04*(5.-6.63/MT))*(ASMT/PI)**2)
C   FTMT=MTMT/SINB/VEV
G(1)=SQRT(4*PI*A1MZ)
G(2)=SQRT(4*PI*A2MZ)
G(3)=SQRT(4*PI*ASMZ)
G(4)=FTAMZ
G(5)=FBMZ
G(6)=G(6)
G(25)=MU
G(26)=B
G(27)=0.
G(28)=0.
G(29)=0.
C           Compute gauge mediated threshold functions
IF (IMODEL.EQ.2) THEN
  XLM=XLAMGM/XMESGM
  THRF=((1.DO+XLM)*(LOG(1.DO+XLM)-2*DDILOG(XLM/(1.DO+XLM)))+
,      .5*DDILOG(2*XLM/(1.DO+XLM)))+
,      (1.DO-XLM)*(LOG(1.DO-XLM)-2*DDILOG(-XLM/(1.DO-XLM)))+
,      .5*DDILOG(-2*XLM/(1.DO-XLM)))/XLM**2
  THRG=((1.DO+XLM)*LOG(1.DO+XLM)+(1.DO-XLM)*LOG(1.DO-XLM))/XLM**2
END IF
C
C           Run back up to mgut with approximate susy spectra
C
IF (IMODEL.EQ.1) THEN
  IF (XSUGIN(7).EQ.0.) THEN
    MGUT=1.E19
  ELSE
    MGUT=XSUGIN(7)
  END IF
ELSE IF (IMODEL.EQ.2) THEN

```

```

    MGUT=XMESGM
END IF
TZ=LOG(MZ/MGUT)
TGUT=0.
DT=(TGUT-TZ)/FLOAT(NSTEP)
DO 250 II=1,NSTEP
    T=TZ+(TGUT-TZ)*FLOAT(II-1)/FLOAT(NSTEP)
    QOLD=Q
    Q=MGUT*EXP(T)
    IF (QOLD.LE.MT.AND.Q.GT.MT) G(6)=FTMT
    IF (QOLD.LE.XNRIN(2).AND.Q.GT.XNRIN(2)) THEN
        G(27)=FNMZ
        G(28)=G0(28)
        G(29)=G0(29)
    END IF
    CALL RKSTP(29,DT,T,G,SURG26,W2)
    A1I=4*PI/G(1)**2
    A2I=4*PI/G(2)**2
    A3I=4*PI/G(3)**2
C    TEST YUKAWA DIVERGENCE
    IF (G(4).GT.10..OR.G(5).GT.10..OR.
G(6).GT.10..OR.G(27).GT.10.) THEN
        NOGOOD=4
        GO TO 100
    END IF
    IF (A1I.LT.A2I.AND.XSUGIN(7).EQ.0.) GO TO 30
250 CONTINUE
    IF (IMODEL.EQ.1.AND.XSUGIN(7).EQ.0.) THEN
        WRITE(LOUT,*) 'SUGRGE ERROR: NO UNIFICATION FOUND'
        NOGOOD=1
        GO TO 100
    END IF
30    IF (XSUGIN(7).EQ.0.) THEN
        MGUT=Q
    ELSE
        MGUT=XSUGIN(7)
    END IF
    AGUT=(G(1)**2/4./PI+G(2)**2/4./PI)/2.
    GGUT=SQRT(4*PI*AGUT)
    AGUTI=1./AGUT
    FTAGUT=G(4)
    FBGUT=G(5)
    FTGUT=G(6)

```

```

IF (XNRIN(2).LT.1.E19.AND.XNRIN(1).EQ.0.) THEN
C   IMPOSE FN-FT UNIFICATION
      FNGUT=G(6)
ELSE
      FNGUT=G(27)
END IF
G3GUT=G(3)
MGUTSS=MGUT
AGUTSS=AGUT
GGUTSS=GGUT

C
C       Set GUT boundary condition
C
DO 260 I=1,3
  IF (IMODEL.EQ.1) THEN
    G(I)=G(I)
    G(I+6)=MHF
    G(I+9)=A0
  ELSE IF (IMODEL.EQ.2) THEN
    G(I)=G(I)
    G(I+6)=XGMIN(11+I)*XGMIN(8)*THRG*(G(I)/4./PI)**2*XLAMGM
    G(I+9)=0.
  END IF
  IF (XNRIN(2).LT.1.E19) THEN
    G(27)=FNGUT
    G(28)=XNRIN(4)**2
    G(29)=XNRIN(3)
  ELSE
    G(27)=0.
    G(28)=0.
    G(29)=0.
  END IF
260 CONTINUE
C   OVERWRITE ALFA_3 UNIFICATION TO GET ALFA_3(MZ) RIGHT
  IF (IMODEL.EQ.1.AND.IAL3UN.NE.0) G(3)=GGUT
  IF (IMODEL.EQ.1) THEN
    DO 270 I=13,24
      G(I)=M0**2
270 CONTINUE
C       Set possible non-universal GUT scale boundary conditions
DO 280 I=1,6
  IF (XNUSUG(I).LT.1.E19) THEN
    G(I+6)=XNUSUG(I)

```

```

      END IF
280  CONTINUE
      DO 281 I=7,18
          IF (XNUSUG(I).LT.1.E19) THEN
              G(I+6)=XNUSUG(I)**2
          END IF
281  CONTINUE
      ELSE IF (IMODEL.EQ.2) THEN
          XC=2*THRF*XLAMGM**2
          DY=SQRT(3./5.)*G(1)*XGMIN(11)
          G(13)=XC*(.75*XGMIN(13)*(G(2)/4./PI)**4+.6*.25*
, XGMIN(12)*(G(1)/4./PI)**4)+XGMIN(9)-DY
          G(14)=XC*(.75*XGMIN(13)*(G(2)/4./PI)**4+.6*.25*
, XGMIN(12)*(G(1)/4./PI)**4)+XGMIN(10)+DY
          G(15)=XC*(.6*XGMIN(12)*(G(1)/4./PI)**4)+2*DY
          G(16)=XC*(.75*XGMIN(13)*(G(2)/4./PI)**4+.6*.25*
, XGMIN(12)*(G(1)/4./PI)**4)-DY
          G(17)=XC*(4*XGMIN(14)*(G(3)/4./PI)**4/3.+.6*XGMIN(12)*
, (G(1)/4./PI)**4/9.)+2*DY/3.
          G(18)=XC*(4*XGMIN(14)*(G(3)/4./PI)**4/3.+.6*4*XGMIN(12)*
, (G(1)/4./PI)**4/9.)-4*DY/3.
          G(19)=XC*(4*XGMIN(14)*(G(3)/4./PI)**4/3.+.75*XGMIN(13)*
, (G(2)/4./PI)**4+.6*XGMIN(12)*(G(1)/4./PI)**4/36.)+DY/3.
          G(20)=G(15)
          G(21)=G(16)
          G(22)=G(17)
          G(23)=G(18)
          G(24)=G(19)
      ELSE IF (IMODEL.EQ.7) THEN
          G(1)=G(1)
          G(2)=G(2)
          G(3)=G(3)
          BLHAT=G(4)*(-9*G(1)**2/5.-3*G(2)**2+3*G(5)**2+4*G(4)**2)
          BBHAT=G(5)*(-7*G(1)**2/15.-3*G(2)**2-16*G(3)**2/3.+
, G(6)**2+6*G(5)**2+G(4)**2)
          BTHAT=G(6)*(-13*G(1)**2/15.-3*G(2)**2-16*G(3)**2/3.+
, 6*G(6)**2+G(5)**2)
          G(7)=-33*MHF*G(1)**2/5./16./PI**2
          G(8)=-MHF*G(2)**2/16./PI**2
          G(9)=3*MHF*G(3)**2/16./PI**2
          G(10)=-BLHAT*MHF/G(4)/16./PI**2
          G(11)=-BBHAT*MHF/G(5)/16./PI**2
          G(12)=-BTHAT*MHF/G(6)/16./PI**2

```

```

      G(13)=(-99*G(1)**4/50.-3*G(2)**4/2.+3*G(5)*BBHAT+G(4)*BLHAT)*
,      MHF**2/(16*PI**2)**2
      G(14)=(-99*G(1)**4/50.-3*G(2)**4/2.+3*G(6)*BTHAT)*
,      MHF**2/(16*PI**2)**2
      G(15)=(-198*G(1)**4/25.)*MHF**2/(16*PI**2)**2
      G(16)=(-99*G(1)**4/50.-3*G(2)**4/2.)*MHF**2/(16*PI**2)**2
      G(17)=(-22*G(1)**4/25.+8*G(3)**4)*MHF**2/(16*PI**2)**2
      G(18)=(-88*G(1)**4/25.+8*G(3)**4)*MHF**2/(16*PI**2)**2
      G(19)=(-11*G(1)**4/50.-3*G(2)**4/2.+8*G(3)**4)*
,      MHF**2/(16*PI**2)**2
      G(20)=(-198*G(1)**4/25.+2*G(4)*BLHAT)*MHF**2/(16*PI**2)**2
      G(21)=(-99*G(1)**4/50.-3*G(2)**4/2.+G(4)*BLHAT)*
,      MHF**2/(16*PI**2)**2
      G(22)=(-22*G(1)**4/25.+8*G(3)**4+2*G(5)*BBHAT)*
, MHF**2/(16*PI**2)**2
      G(23)=(-88*G(1)**4/25.+8*G(3)**4+2*G(6)*BTHAT)*
, MHF**2/(16*PI**2)**2
      G(24)=(-11*G(1)**4/50.-3*G(2)**4/2.+8*G(3)**4+G(5)*BBHAT+
,      G(6)*BTHAT)*MHF**2/(16*PI**2)**2
      DO 284 I=13,24
284      G(I)=G(I)+M0**2
      END IF
      DO 285 I=1,29
      IG(I)=0
285 CONTINUE
C      Check for tachyonic sleptons at GUT scale
      IF (G(15).LT.0..OR.G(16).LT.0.) THEN
      ITACHY=2
      ELSE
      ITACHY=0
      END IF
C
C      Run back down to weak scale
C
      TZ=LOG(MZ/MGUT)
      TGUT=0.
      DT=(TZ-TGUT)/FLOAT(NSTEP)
      DO 290 II=1,NSTEP+2
      T=TGUT+(TZ-TGUT)*FLOAT(II-1)/FLOAT(NSTEP)
      QOLD=Q
      Q=MGUT*EXP(T)
      CALL RKSTP(29,DT,T,G,SURG26,W2)
      CALL SUGFRZ(Q,G,G0,IG)

```

```

      IF (QOLD.GE.AMNRMJ.AND.Q.LT.AMNRMJ.AND.XNRIN(1).EQ.0.) THEN
        FNMZ=G(27)
      END IF
      IF (Q.LT.AMNRMJ) THEN
        G(27)=0.
        G(28)=0.
        G(29)=0.
      END IF
      IF (NOGOOD.NE.0) GO TO 100
      IF (Q.LT.MZ) GO TO 40
290  CONTINUE
40   CONTINUE
C
C       Electroweak breaking constraints; tree level
C
      MUS=(GO(13)-GO(14)*TANB**2)/(TANB**2-1.)-MZ**2/2.
      IF (MUS.LT.0.) THEN
        MUS=AMZ**2
      END IF
      MU=SQRT(MUS)*SIGN(1.,SGNMU)
      B=(GO(13)+GO(14)+2*MUS)*SIN2B/MU/2.
      CALL SUGMAS(GO,0,IMODEL)
      IF (NOGOOD.NE.0) GO TO 100
C
C       Electroweak breaking constraints; loop level
C
      CALL SUGEFF(GO,SIG1,SIG2)
      MH1S=GO(13)+SIG1
      MH2S=GO(14)+SIG2
      MUS=(MH1S-MH2S*TANB**2)/(TANB**2-1.)-MZ**2/2.
      IF (MUS.LT.0.) THEN
        NOGOOD=2
        GO TO 100
      END IF
      MU=SQRT(MUS)*SIGN(1.,SGNMU)
      B=(MH1S+MH2S+2*MUS)*SIN2B/MU/2.
C
C       Once more, with feeling!
C
      CALL SUGEFF(GO,SIG1,SIG2)
      MH1S=GO(13)+SIG1
      MH2S=GO(14)+SIG2
      MUS=(MH1S-MH2S*TANB**2)/(TANB**2-1.)-MZ**2/2.

```

```
IF (MUS.LT.0.) THEN
  NOGOOD=2
  GO TO 100
END IF
MU=SQRT(MUS)*SIGN(1.,SGNMU)
B=(MH1S+MH2S+2*MUS)*SIN2B/MU/2.
CALL SUGMAS(GO,1,IMODEL)
C
100 RETURN
END
```

Bibliography

- [1] F. Zwicky, *Helv. Phys. Acta.* **6** (1933) 110.
- [2] Blanton, M. R. et al. 2001, *Astronomy J.* 121, 2358
- [3] S. M. Faber and J. J. Gallagher, *Ann. Rev. Astron. Astrophysics.* **17** (1979) 135
- [4] D. J. Hegyi and K. A. Olive, *Phys. Lett. B* **126** (1983) 28.
- [5] S. D. White, C. S. Frenk and M. Davis, *Astrophys. J.* **274** (1983) L1.
- [6] K. G. Begeman, A. H. Broeils, R. H. Sanders, *MNRAS* **249**, 523 (1991)
- [7] G. Golse, J. P. Kneib and G. Soucail, [arXiv:astro-ph/0103500](https://arxiv.org/abs/astro-ph/0103500).
- [8] M. J. White, *Astrophys. J.* **506** (1998) 495 [[arXiv:astro-ph/9802295](https://arxiv.org/abs/astro-ph/9802295)].
- [9] J. A. Willick, M. A. Strauss, A. Dekel and T. Kolatt, [arXiv:astro-ph/9612240](https://arxiv.org/abs/astro-ph/9612240).
- [10] H. V. Klapdor-Kleingrothaus, H. Pas and A. Y. Smirnov, *Phys. Rev. D* **63** (2001) 073005 [[arXiv:hep-ph/0003219](https://arxiv.org/abs/hep-ph/0003219)].
- [11] S. F. King, [arXiv:hep-ph/0210089](https://arxiv.org/abs/hep-ph/0210089).
- [12] E. Masso, *Nucl. Phys. Proc. Suppl.* **114** (2003) 67 [[arXiv:hep-ph/0209132](https://arxiv.org/abs/hep-ph/0209132)].
- [13] S. Weinberg, *Phys. Rev. Lett.* **40** (1978) 223.
- [14] S. J. Asztalos *et al.*, *Astrophys. J.* **571** (2002) L27 [[arXiv:astro-ph/0104200](https://arxiv.org/abs/astro-ph/0104200)].
- [15] G. F. Ellis, *Chaos Solitons Fractals* **16** (2003) 505.
- [16] J. M. Bardeen, P. J. Steinhardt and M. S. Turner, *Phys. Rev. D* **28** (1983) 679.
- [17] D. Blais, C. Kiefer and D. Polarski, *Phys. Lett. B* **535** (2002) 11 [[arXiv:astro-ph/0203520](https://arxiv.org/abs/astro-ph/0203520)].

- [18] M. Gell-Mann, P. Ramond and R. Slansky, “Complex Spinors And Unified Theories,” Print-80-0576 (CERN)
R. N. Mohapatra and G. Senjanovic, Phys. Rev. Lett. **44** (1980) 912.
- [19] S. H. Hansen, J. Lesgourgues, S. Pastor and J. Silk, Mon. Not. Roy. Astron. Soc. **333** (2002) 544 [arXiv:astro-ph/0106108].
- [20] W. L. Freedman *et al.*, Astrophys. J. **553** (2001) 47 [arXiv:astro-ph/0012376].
- [21] P. de Bernardis *et al.*, Astrophys. J. **564** (2002) 559 [arXiv:astro-ph/0105296].
- [22] R. Stompor *et al.*, Astrophys. J. **561** (2001) L7 [arXiv:astro-ph/0105062].
- [23] C. Pryke, N. W. Halverson, E. M. Leitch, J. Kovac, J. E. Carlstrom, W. L. Holzapfel and M. Dragovan, Astrophys. J. **568** (2002) 46 [arXiv:astro-ph/0104490].
- [24] C. L. Bennett *et al.*, arXiv:astro-ph/0302207.
D. N. Spergel *et al.*, arXiv:astro-ph/0302209.
- [25] G. S. Watson, arXiv:astro-ph/0005003.
A. Riotto, arXiv:hep-ph/0210162.
- [26] A. D. Linde, Phys. Lett. B **108** (1982) 389.
- [27] D. H. Lyth and A. Riotto, Phys. Rept. **314** (1999) 1 [arXiv:hep-ph/9807278].
- [28] K. Griest and D. Seckel, Nucl. Phys. B **283** (1987) 681 [Erratum-ibid. B **296** (1988) 1034].
- [29] [EROS Collaboration], arXiv:astro-ph/0212176.
- [30] E. W. Kolb and M. S. Turner, “The Early Universe,”
- [31] G. Jungman, M. Kamionkowski and K. Griest, Phys. Rept. **267** (1996) 195 [arXiv:hep-ph/9506380].
- [32] S. R. Coleman and J. Mandula, Phys. Rev. **159** (1967) 1251.
- [33] M. F. Sohnius, Phys. Rept. **128** (1985) 39.
- [34] R. Haag, J. T. Lopuszanski and M. Sohnius, Nucl. Phys. B **88** (1975) 257.
- [35] J. Wess and J. Bagger, “Supersymmetry And Supergravity,”
S. J. Gates, M. T. Grisaru, M. Rocek and W. Siegel, “Superspace, Or One Thousand And One Lessons In Supersymmetry,” Front. Phys. **58** (1983) 1 [arXiv:hep-th/0108200].

- [36] H. P. Nilles, Phys. Rept. **110** (1984) 1.
- [37] H. E. Haber and G. L. Kane, Phys. Rept. **117** (1985) 75.
- [38] S. P. Martin, arXiv:hep-ph/9709356.
- [39] J. Wess and B. Zumino, Nucl. Phys. B **78** (1974) 1.
- [40] A. Salam and J. Strathdee, Phys. Rev. D **11** (1975) 1521.
J. Wess and B. Zumino, Nucl. Phys. B **70** (1974) 39.
- [41] A. Salam and J. Strathdee, Nucl. Phys. B **76** (1974) 477.
- [42] S. Ferrara and B. Zumino, Nucl. Phys. B **79** (1974) 413.
- [43] P. Fayet, Nucl. Phys. B **90** (1975) 104.
- [44] A. Salam and J. Strathdee, Nucl. Phys. B **87** (1975) 85.
- [45] G. G. Ross, “Grand Unified Theories,”
- [46] L. O’Raifeartaigh, Nucl. Phys. B **96** (1975) 331.
- [47] P. Fayet and J. Iliopoulos, Phys. Lett. B **51** (1974) 461.
- [48] L. Randall, arXiv:hep-ph/9706474.
A. E. Nelson, Nucl. Phys. Proc. Suppl. **62** (1998) 261 [arXiv:hep-ph/9707442].
- [49] G. F. Giudice and R. Rattazzi, Phys. Rept. **322** (1999) 419 [arXiv:hep-ph/9801271].
- [50] L. Girardello and M. T. Grisaru, Nucl. Phys. B **194** (1982) 65.
- [51] J. F. Gunion and H. E. Haber, Nucl. Phys. B **272** (1986) 1 [Erratum-ibid. B **402** (1993) 567].
- [52] S. Dimopoulos and D. W. Sutter, Nucl. Phys. B **452** (1995) 496 [arXiv:hep-ph/9504415].
- [53] F. Gabbiani, E. Gabrielli, A. Masiero and L. Silvestrini, Nucl. Phys. B **477** (1996) 321 [arXiv:hep-ph/9604387].
- [54] G. F. Giudice and A. Masiero, Phys. Lett. B **206** (1988) 480.
- [55] J. A. Casas and C. Munoz, Phys. Lett. B **306** (1993) 288 [arXiv:hep-ph/9302227].
- [56] G. R. Dvali, G. F. Giudice and A. Pomarol, Nucl. Phys. B **478** (1996) 31 [arXiv:hep-ph/9603238].

- [57] P. Van Nieuwenhuizen, Phys. Rept. **68** (1981) 189.
- [58] T. Appelquist and J. Carazzone, Phys. Rev. D **11** (1975) 2856.
- [59] W. Siegel, Phys. Lett. B **84** (1979) 193.
D. M. Capper, D. R. Jones and P. van Nieuwenhuizen, Nucl. Phys. B **167** (1980) 479.
- [60] S. P. Martin and M. T. Vaughn, Phys. Rev. D **50** (1994) 2282 [arXiv:hep-ph/9311340].
- [61] M. E. Peskin and D. V. Schroeder, “An Introduction To Quantum Field Theory”
C. Itzykson and J. B. Zuber, “Quantum Field Theory”
- [62] Y. Yamada, Phys. Rev. D **50** (1994) 3537 [arXiv:hep-ph/9401241].
I. Jack and D. R. Jones, Phys. Lett. B **415** (1997) 383 [arXiv:hep-ph/9709364].
- [63] G. F. Giudice and R. Rattazzi, Nucl. Phys. B **511** (1998) 25 [arXiv:hep-ph/9706540].
- [64] L. V. Avdeev, D. I. Kazakov and I. N. Kondrashuk, Nucl. Phys. B **510** (1998) 289 [arXiv:hep-ph/9709397].
- [65] H. Baer, F. E. Paige, S. D. Protopopescu and X. Tata, arXiv:hep-ph/0001086.
- [66] D. J. Castano, E. J. Piard and P. Ramond, Phys. Rev. D **49** (1994) 4882 [arXiv:hep-ph/9308335].
- [67] M. Carena, S. Pokorski and C. E. Wagner, Nucl. Phys. B **406** (1993) 59 [arXiv:hep-ph/9303202].
- [68] D. M. Pierce, J. A. Bagger, K. T. Matchev and R. j. Zhang, Nucl. Phys. B **491** (1997) 3 [arXiv:hep-ph/9606211].
- [69] J. Bagger, K. T. Matchev and D. Pierce, arXiv:hep-ph/9501378.
- [70] D. Z. Freedman, P. van Nieuwenhuizen and S. Ferrara, Phys. Rev. D **13** (1976) 3214.
- [71] S. Deser and B. Zumino, Phys. Lett. B **62** (1976) 335.
- [72] E. Cremmer, S. Ferrara, L. Girardello and A. Van Proeyen, Nucl. Phys. B **212** (1983) 413.

- [73] L. E. Ibanez and G. G. Ross, Phys. Lett. B **110** (1982) 215.
J. R. Ellis, D. V. Nanopoulos and K. Tamvakis, Phys. Lett. B **121** (1983) 123.
L. Alvarez-Gaume, J. Polchinski and M. B. Wise, Nucl. Phys. B **221** (1983) 495.
- [74] G. 't Hooft and M. J. Veltman, Nucl. Phys. B **44** (1972) 189.
- [75] J. A. Helayel-Neto, Phys. Lett. B **135** (1984) 78.
- [76] F. Feruglio, J. A. Helayel-Neto and F. Legovini, Nucl. Phys. B **249** (1985) 533.
- [77] J. R. Ellis, J. S. Hagelin, D. V. Nanopoulos, K. A. Olive and M. Srednicki, Nucl. Phys. B **238** (1984) 453.
- [78] P. F. Smith and J. R. Bennett, Nucl. Phys. B **149** (1979) 525.
- [79] T. Falk, K. A. Olive and M. Srednicki, Phys. Lett. B **339** (1994) 248 [arXiv:hep-ph/9409270].
- [80] K. A. Olive and M. Srednicki, Phys. Lett. B **205** (1988) 553.
- [81] A. Bartl, H. Fraas, W. Majerotto and N. Oshimo, Phys. Rev. D **40** (1989) 1594.
- [82] S. P. Martin, Phys. Rev. D **65** (2002) 035003 [arXiv:hep-ph/0106280].
- [83] K. Griest, M. Kamionkowski and M. S. Turner, Phys. Rev. D **41** (1990) 3565.
- [84] J. L. Feng, K. T. Matchev and F. Wilczek, Phys. Lett. B **482** (2000) 388 [arXiv:hep-ph/0004043].
- [85] M. Drees and M. M. Nojiri, Phys. Rev. D **47**, 376 (1993) [arXiv:hep-ph/9207234].
- [86] V. D. Barger, E. W. Glover, K. Hikasa, W. Y. Keung, M. G. Olsson, C. J. Suchyta and X. R. Tata, Phys. Rev. D **35** (1987) 3366 [Erratum-ibid. D **38** (1988) 1632].
- [87] H. Goldberg, Phys. Rev. Lett. **50** (1983) 1419.
- [88] K. Griest, Phys. Rev. D **38** (1988) 2357 [Erratum-ibid. D **39** (1989) 3802].
- [89] T. Nihei, L. Roszkowski and R. Ruiz de Austri, JHEP **0203** (2002) 031 [arXiv:hep-ph/0202009].
- [90] H. Mayer-Hasselwander *et al.*, Astron. Astrophys. **335**, 161 (1998).

- [91] A. W. Strong, I. V. Moskalenko and O. Reimer, *Astrophys. J.* **537** (2000) 763 [Erratum-ibid. **541** (2000) 1109] [arXiv:astro-ph/9811296].
- [92] A. Morselli, A. Lionetto, A. Cesarini, F. Fucito and P. Ullio, *Nucl. Phys. Proc. Suppl.* **113** (2002) 213 [arXiv:astro-ph/0211327].
- [93] A. Cesarini, F. Fucito, A. Lionetto, A. Morselli and P. Ullio, [arXiv:astro-ph/0305075].
- [94] P. Gondolo, J. Edsjo, P. Ullio, L. Bergstrom, M. Schelke and E. A. Baltz, [arXiv:astro-ph/0211238].
- [95] S. Hunter *et al.*, *Astrophys. J.* **481** (1997) 205
- [96] M. Pohl, "Gamma-ray astronomy," [arXiv:astro-ph/0111552].
- [97] P. de Bernardis *et al.*, *Frascati Physics Series Vol. XXIV*, 399, (2002), <http://www.roma2.infn.it/inf/aldo/ISSS01.html>.
- [98] A. G. Riess *et al.*, *Astrophys. J.* **560** (2001) 49 [arXiv:astro-ph/0104455].
- [99] J. Primack, *Frascati Physics Series Vol. XXIV*, 449, (2002), [astro-ph/0112255].
- [100] H. E. Haber and G. L. Kane, *Phys. Rept.* **117** (1985) 75.
- [101] L. Maiani, *Proc. Summer School on Particle Physics*, Gif-sur-Yvette, 1979 (IN2P3, Paris, 1980), 3.
G 't Hoof in G 't Hoof *et al.*, eds., *Recent Developments in Field Theories* (Plenum Press, New York, 1980).
- [102] J. Ellis, *Frascati Physics Series Vol. XXIV*, 49, (2002), (<http://www.roma2.infn.it/inf/aldo/ISSS01.html>).
- [103] P. Smith, *Contemp. Phys.* **29**, 159, (1998).
- [104] H. V. Klapdor-Kleingrothaus and Y. Ramachers, *Eur. Phys. J. A* **3** (1998) 85.
- [105] J. R. Ellis, T. Falk, G. Ganis and K. A. Olive, *Phys. Rev. D* **62** (2000) 075010 [arXiv:hep-ph/0004169].
- [106] V. S. Berezinsky, *Phys. Lett. B* **261** (1991) 71.
G. Jungman and M. Kamionkowski, *Phys. Rev. D* **51** (1995) 3121 [arXiv:hep-ph/9501365].
- [107] W. Atwood *et al.*, *NIM*, **A342**, 302, (1994). Proposal for the Gamma-ray Large Area Space Telescope, SLAC-R-522 (1998). B. Dingus *et al.*, 25th ICRC, OG 10.2.17, **5**, p.69, Durban.

- [108] R. Bellazzini, Frascati Physics Series Vol.XXIV, 353, (2002), (<http://www.roma2.infn.it/inf/aldo/ISSS01.html>).
- [109] A.Morselli, Frascati Physics Series Vol.XXIV, 363, (2002), (<http://www.roma2.infn.it/inf/aldo/ISSS01.html>).
- [110] Hongbo Hu, J. Nielsen, Wisc-Ex-99-352, 1999
- [111] A. L. Read, DELPHI 97-158 PHYS 737, 1997
- [112] L. J. Hall, J. Lykken and S. Weinberg, Phys. Rev. D **27** (1983) 2359.
- [113] H. Baer, F. E. Paige, S. D. Protopopescu and X. Tata, [arXiv:hep-ph/0001086].
The source code is available at <ftp://ftp.phy.bnl.gov/pub/isajet>
- [114] Joint LEP2 supersymmetry working group,
<http://lepsusy.web.cern.ch/lepsusy/Welcome.html>
- [115] J. L. Feng, K. T. Matchev and F. Wilczek, Phys.Rev. D **63** (2001) 045024, [astro-ph/0008115]
- [116] P. Ullio, H. Zhao and M. Kamionkowski, Phys. Rev. D **64** (2001) 043504 [arXiv:astro-ph/0101481].
- [117] L. Bergstrom, J. Edsjo, P. Gondolo and P. Ullio, Phys. Rev. D **59** (1999) 043506 [arXiv:astro-ph/9806072].
- [118] T. Sjostrand, L. Lonnblad and S. Mrenna, [arXiv:hep-ph/0108264].